

DESIGN OF A SECONDARY PACKAGING ROBOTIC SYSTEM

A THESIS SUBMITTED TO  
THE GRADUATE SCHOOL OF NATURAL AND APPLIED SCIENCES  
OF  
MIDDLE EAST TECHNICAL UNIVERSITY

BY

HAKAN ŞAHİN

IN PARTIAL FULFILLMENT OF THE REQUIREMENTS  
FOR  
THE DEGREE OF MASTER OF SCIENCE  
IN  
MECHANICAL ENGINEERING

DECEMBER 2005

Approval of the Graduate School of Natural and Applied Sciences

---

Prof. Dr. Canan ÖZGEN  
Director

I certify that this thesis satisfies all the requirements as a thesis for the degree of Master of Science.

---

Prof. Dr. S. Kemal İDER  
Head of Department

This is to certify that we have read this thesis and that in our opinion it is fully adequate, in scope and quality, as a thesis for the degree of Master of Science.

---

Prof. Dr. Tuna BALKAN  
Supervisor

---

Prof. Dr. M. A. Sahir ARIKAN  
Co-Supervisor

**Examining Committee Members:**

Asst. Prof. Dr. E. İlhan KONUKSEVEN (METU, ME) \_\_\_\_\_

Prof. Dr. Tuna BALKAN (METU, ME) \_\_\_\_\_

Prof. Dr. M. A. Sahir ARIKAN (METU, ME) \_\_\_\_\_

Asst. Prof. Dr. Buğra KOKU (METU, ME) \_\_\_\_\_

Dr. Hakan POLATOĞLU (ETİ Group of Companies) \_\_\_\_\_

**I hereby declare that all information in this document has been obtained and presented in accordance with academic rules and ethical conduct. I also declare that, as required by these rules and conduct, I have fully cited and referenced all material and results that are not original to this work.**

Name, Last name: Hakan ŞAHİN

Signature:

## **ABSTRACT**

### **DESIGN OF A SECONDARY PACKAGING ROBOTIC SYSTEM**

ŞAHİN, Hakan

M.Sc., Department of Mechanical Engineering

Supervisor : Prof. Dr. Tuna BALKAN

Co-Supervisor: Prof. Dr. M. A. Sahir ARIKAN

December 2005, 182 pages

The use of robotic systems in consumer goods industry has increased over recent years. However, food industry has not taken to the robotics technology with the same desire as in other industries due to technical and commercial reasons. Difficulties in matching human speed and flexibility, variable nature of food products, high production volume rates, lack of appropriate end-effectors, high initial investment rate of the so-called systems and low margins in food products are still blocking the range of use of robotics in food industry.

In this thesis study, as a contribution to the use of robotic systems in food industry, a secondary packaging robotic system is designed. The system is composed of two basic subsystems: a dual-axis controlled robotic arm and a special-purpose gripper. Mechanical and control systems design of basic subsystems are performed within the scope of the study. During the designing process, instead of using classical design methods, modern computer-aided design and engineering tools are utilized.

**Keywords:** Secondary Packaging, System Simulation, Mechanical Modeling, Gripper Design

## ÖZ

### BİR İKİNCİL PAKETLEME ROBOTİK SİSTEMİ TASARIMI

ŞAHİN, Hakan

Yüksek Lisans, Makina Mühendisliği Bölümü

Tez Yöneticisi : Prof. Dr. Tuna BALKAN

Ortak Tez Yöneticisi: Prof. Dr. M. A. Sahir ARIKAN

Aralık 2005, 182 sayfa

Tüketici malları endüstrisinde robotik sistemlerin kullanımı son yıllarda artış göstermiştir. Ancak, teknik ve ticari nedenlerden dolayı gıda endüstrisi robot teknolojisini diğer endüstri dallarının gösterdiği istekle benimsememiştir. İnsan hızı ve esnekliğini karşılamadaki zorluk, gıda ürünlerinin değişken doğası, yüksek üretim kapasiteleri, uç eyleyicilerin yetersizliği, adı geçen sistemlerin ilk yatırım maliyetlerinin yüksekliği ve gıda ürünlerindeki düşük kar oranları robotik sistemlerin bu endüstrideki kullanımını kısıtlamaktadır.

Bu tez çalışmasında, robotik sistemlerin gıda endüstrisinde kullanımına bir katkı olarak, bir ikinci paketleme robotik sistemi tasarımı yapılmıştır. Sistem iki eksen kontrollü bir robot kol ve özel amaçlı bir tutucu olmak üzere iki ana alt sistemden oluşmaktadır. Tez kapsamı dahilinde, alt sistemlerin mekanik ve denetim sistemleri tasarımı gerçekleştirilmiştir. Tasarım sürecinde alışılmadık yöntemlerin aksine, günümüz bilgisayar destekli tasarım ve mühendislik araçlarından faydalanılmıştır.

Anahtar Kelimeler: İkinci Paketleme, Sistem Benzetimi, Mekanik Modelleme, Tutucu Tasarımı

To my darling, Yıldız,  
for ten wonderful years of our love...

## ACKNOWLEDGMENTS

Starting from my primary school teacher, it would be impossible to thank all of individuals who made, in one way or another, contributions in making this thesis possible. My special thanks go to Dr. Hakan Polatođlu, Prof. Dr. Tuna Balkan and Prof. Dr. M. Sahir Arıkan for providing me this research opportunity, their confidence and continuous support throughout the study.

I would like to express my deep sincere gratitude to ETİ Machinery Industry and Trade Co. Inc. and its laborers: Hüseyin Sezer, İremet Karaca, Ünal Dikmen, Metin Yurdaer, Zeki Güler, Ünal Pamuksuz, Özgür Şen, Haydar Kılınç, Metin Şen, Mustafa Sezer, Baki Kılınç, Fethi Metin, Uđur Özdamar, Cüneyt Artam, Murat Özöğüt, Şahin Eker. You are real heroes of manufacturing.

I am especially thankful to Hüseyin Sezer and İremet Karaca in that they thought me that learning is not a place like a big university but rather a personal desire and discipline.

I would like to thank my dear friends Serhan Yıldız, Mehmet Selçuk Arslan, Necati Omurtak, Nida Tokgöz, Şenol Genç, Mehmet Ünlü, İbrahim Dönmez, Sadık Behlül Kuran, Yasin Şahin, Halit Şahin, Öner Bilgin, Erbay Özmen, Ekrem Özmen, and Sertan Köybaşı for their support and presence in my life.

I also owe many thanks to my high school teacher Arslan Cingiz who has influenced my professional career as much as my family.

Finally, many thanks to my altruistic family, especially to my parents Mihriban and Mehmet Şahin. I feel the pride of being your son in every second of my life. I love you very much.

## TABLE OF CONTENTS

PLAGIARISM .....	iii
ABSTRACT .....	iv
ÖZ .....	v
ACKNOWLEDGMENTS .....	vii
TABLE OF CONTENTS .....	viii

### CHAPTERS

1. INTRODUCTION .....	1
1.1 Introduction .....	1
1.2 Robotics in Food Industry .....	3
1.2.1 Technical Difficulties in Handling Food Products.....	6
1.2.2 Commercial Difficulties.....	8
1.3 Objective of the Study.....	8
1.4 Scope of the Thesis .....	10
1.5 Outline of the Thesis .....	13
1.6 Conclusion .....	13
2. INTRODUCTION TO SECONDARY PACKAGING ROBOTIC SYSTEM.....	15
2.1 Introduction .....	15
2.2 Current State of the Art in Secondary Packaging Automation .....	17
2.2.1 OPM's Secondary Packaging Automation Solution.....	17
2.2.2 Schubert's Secondary Packaging Automation Solution .....	18
2.2.3 SIG's Secondary Packaging Automation Solution .....	20
2.3 Secondary Packaging Robotic System.....	21
2.4 Control System Architecture.....	28
2.5 SPRS Operational State Model .....	29
2.5.1 SPRS Operational State Descriptions .....	30

2.6 Conclusion .....	32
<b>3. MANIPULATOR MECHANICAL DESIGN .....</b>	<b>34</b>
3.1 Introduction .....	34
3.2 Manipulator Mechanical Design Procedure .....	35
3.3 Design Condition Inputs .....	36
3.4 Fundamental Mechanism Design .....	38
3.4.1 Selection of Manipulator Structure .....	39
3.4.2 Kinematic Synthesis .....	46
3.4.3 Kinematic Analysis .....	48
3.4.4 Kinematics Evaluation .....	52
3.5 Drive System Design .....	54
3.5.1 Motor Allocations and Transmission Systems .....	54
3.5.2 Design of Link Structures .....	58
3.5.4 Bearings and Bearing Arrangements .....	69
3.5.5 Dynamic Analysis .....	81
3.5.6 Selection of Motors and Speed Reducers .....	87
3.6 Detailed Structural Design .....	100
3.6.1 Stress and Deflection Analysis .....	100
3.6.2 Natural Frequency Analysis .....	102
<b>4. CONTROL SYSTEM DESIGN .....</b>	<b>103</b>
4.1 Introduction .....	103
4.2 Modeling of the Transmission System .....	103
4.3 Electro-Mechanical Modeling .....	105
4.4 Control System Hardware .....	108
4.4.1 Tuning of Current Loop Controller Parameters .....	110
4.4.2 Tuning of Velocity Loop Controller Parameters .....	114
4.4.3 Tuning of Position Loop Controller Parameters .....	117
<b>5. SYSTEM SIMULATION .....</b>	<b>120</b>
5.1 Introduction .....	120

5.2 System Simulation Techniques .....	122
5.2.1 Simulation without Time Limitation.....	124
5.2.2 Real-Time Simulation .....	125
5.2.3 System Simulation Software Tools .....	128
5.3 System Simulation of the Robotic Arm .....	131
5.3.1 Simulation in Non-real-time .....	131
5.3.2 Simulation in Real-time .....	138
6. DESIGN OF THE GRIPPER SYSTEM.....	144
6.1 Introduction .....	144
6.2 The SPRS Gripper Benchmark Goals .....	145
6.3 Design of the Pick-up Mechanism .....	147
6.3.1 Selection of Suction Cups .....	150
6.3.2 Force Analysis.....	151
6.3.3 Design of the Suction Cups Mounting Element.....	155
6.3.4 Design of the Vacuum Distributor .....	157
6.3.5 Selection of the Type and Size of The Vacuum Generator.....	157
6.3.6 Selection of the Solenoid Valves .....	161
6.4 Design of the Grouping Mechanism .....	162
7. SUMMARY AND CONCLUSION.....	165
7.1 Summary .....	165
7.2 Conclusion .....	166
REFERENCES.....	167
APPENDIX A .....	172
APPENDIX B .....	181

## **CHAPTER 1**

### **INTRODUCTION**

#### **1.1 Introduction**

Food manufacturing, one of the main divisions of fast moving consumer goods (so called FMCG) industry, are becoming more and more attractive field for robotic system developers and integrators. During the past ten years, the use of robotics in food manufacturing environment increased and new, exciting applications come up frequently. Automatic inspection, handling, packaging, cutting and general processing of products are main areas of interest for automation involving robots.

The most apparent reasons associated with the installation of robotic systems in food industry are:

- Labor savings
- Improved efficiency
- Improved quality
- The ability to work in cold and hostile environments
- Increased yields and reduced wastage
- Increased consistency
- Increased flexibility

Before going into the discussion of robotics applications in food industry, it is useful to comprehend the fundamental processes in food manufacturing. Bearing in mind that the manufacturing of some food products does not involve baking process, a

generic food manufacturing process can be divided into 6 fundamental processes including baking process as shown in the figure 1.1:

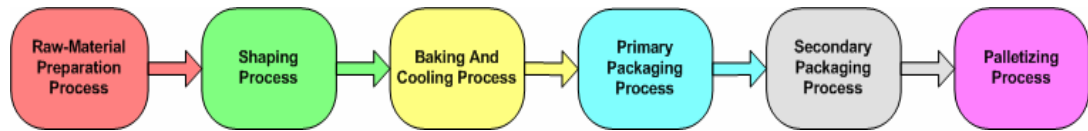


Figure 1.1 Basic processes in a generic food manufacturing line

Although names reveal the meaning of processes, it is necessary to give extra information about fundamental processes for solid understanding of the following discussion. Since the primary, secondary packaging and palletizing are all areas of high automation, special attention will be given to these processes.

The first three processes in a generic food manufacturing line are raw material preparation, shaping, baking and cooling. Raw material preparation process involves the pre-treatment of raw materials and preparation of necessary mixes for manufacturing. Generally, automatic raw materials feeding systems and mixers are utilized in this stage. Following the preparation of raw materials, special purpose extruder and/or decorating machines are used to give a desired form to raw materials. Formed articles are cooked in ovens and cooled on long conveyor belts before the primary packaging process takes place.

Primary packaging refers to packaging that immediately envelops a product. Figure 1.2 shows the state of a product after primary packaging process. It provides most of the strength and the moisture, vapor or any contaminating material barrier needed to safeguard a product's purity and integrity. This protection starts when the product leaves the manufacturing line and continues until it's consumed by the customer.

Generally, two types of primary packaging machines are utilized in a typical primary packaging process. First type of these machines, filling machine, measures a predetermined weight or number of the product and fill it into a bag type of package. The second type, wrapping machine, wrap a flexible material around the product. These machines can be used interchangeably in order to produce products having different package types.



Figure 1.2 State of a product after primary packaging

Secondary packaging is the process of taking products coming from primary packaging process and placing them into cardboard boxes. Figure 1.3 shows resulting cardboard box involving finished products. Secondary packaging not only gives extra strength to products, but also it protects them during transportation. Finally, Palletizing is the last process. Cartoons or cardboard boxes coming from the secondary packaging process are palletized and taken to the depot in this phase of the production.

## **1.2 Robotics in Food Industry**

Before going into details, a brief description and definition of robot is essential to ensure a solid understanding because there are different approaches to define robots. According to British Robot Association [1]:

“An industrial robot is a reprogrammable device designed both to manipulate and/or transport parts, tools, or specified manufacturing implements through variable programmed motions for the performance of specific manufacturing tasks.”



Figure 1.3 State of products after secondary packaging

The international Standards Organization (ISO) defines a robot as [2]:

“An automatically controlled, re-programmable, multi-purpose, manipulative machine with several degrees of freedom, which may be either, fixed in place or mobile for use in industrial automation applications.”

Although other countries and their national organizations have different definitions, robots can be generally defined as [3] “things which have a flexible capability for movement resembling the capabilities of moving parts of living creatures and with intelligent functions which move in response to human requirements.”

Some of the earliest food industry applications of robotic systems evolved in 1980s for the packaging of assorted chocolates into trays. These systems were more experimental than commercial, and used by very few confectionary and equipment

companies. Because the technology was expensive at that time, most of food manufacturers decided not to invest in robotics.

Looking to the manufacturing industry now, robotic applications have gained common acceptance in specific production systems, predominantly in the areas of materials handling, primary and secondary packaging and palletizing operations. The primary packaging operation is typically one of the highest speed operations in the whole process. For example 2000 distinct food items can be packaged per minute. The speed of production is at a maximum because the product is its simplest unit form. Because, in most cases, the product is unwrapped at this stage of the process, it is often sensitive microbiologically and needs to be treated utmost care. The application of robotic systems in primary packaging of food is therefore difficult because the speeds are higher and the product is probably at its most vulnerable with regard to quality and safety. For self-stable products such as biscuits and chocolates, the situation is less important, but for cooked pies, pastries and meats, primary packaging is most important from the point of view of product safety.

In a typical food manufacturing line, it is likely to find cases that contain typically 12, 18, 24 or 36 individual or multipack wrapped products in secondary packaging process. These cases are normally filled at a rate of 10-20/min. The case filling operation can be carried out by several different means: manually, using fixed automation or using robotic systems. The application of robotic systems to secondary packaging process is reasonable because of the following reasons:

- The material to be handled can be presented in an ordered format.
- The material is of a relatively regular shape.
- The material is relatively rigid.
- There are few hygiene-related problems.
- Throughputs are achievable.

In palletizing process, pallets are produced from the end of the production line typically every few minutes in a medium to large factory. Thus, it is not too difficult

to handle this number of units per minutes automatically, and if a problem arises, it can be recovered without causing major problems. The systems in use include robotics or fixed palletizers and automated guided vehicles which are used to load goods or transfer them to the depot. A system's complexity and level of automation depend on factors such as investment issues and flexibility required.

Parallel to the rapid developments in digital computers and control systems technology, more intelligent and lower in cost robotic applications have become both possible and affordable. However, food manufacturers still hesitate to adapt this new technology unlike the other industries like automotive and electronics. There are still considerable amount of tasks currently performed by both skilled and unskilled labors in food industry. Reasons behind this fact can be analyzed in two categories: technical and commercial difficulties. Following two sections discuss these difficulties.

### **1.2.1 Technical Difficulties in Handling Food Products**

Despite the recent advances in the application of robotics technology in food manufacturing, there are considerable amount of tasks currently performed by both skilled and unskilled labors in the industry because food manufacturing presents important challenges in robotic handling of food products. The major technical problem to be overcome is still reliably picking and placing of flexible and irregularly shaped discrete food items into their primary and secondary packages. Difficulties in matching human speed, dexterity, and flexibility, variable nature and number of products, high production volume rates, and lack of appropriate robot tools or end-effectors are still blocking the range of use of robotics in food manufacturing environments.

Non-rigid or fragile materials like food products present additional problems to rigid materials from the handling point of view. One of the main differences between a rigid material and a food product is the delicacy of the food product. They inherently

deform significantly because of the forces during handling. In addition, food products are easily bruised and marked when they come into contact with hard and rough surfaces. Bruised, deformed or marked products reduce the attraction of customers and shorten the shelf life in the market. Besides price, consumers look at the shape, color, and appearance before checking the taste and flavor. Even a small mark and color variation on the food may cause rejection by the customer although such marks and slight color variation do not violate the hygiene and food safety regulations.

Human laborers easily deal with handling and manipulation of non-rigid or fragile materials. This is actually a complex operation and it is achieved by human's built-in hand-eye coordination ability. The reason behind this complexity is that the personnel who are currently used to pick and place products are performing a multi-task operation. These are:

- Inspecting for color, shape, texture, size type, etc.
- Stopping the line if there is an important problem.
- Adapting to new products.
- Making decisions based on previous events.

The technologies required to carry out these tasks are possible but quite complex. Rapid developments in vision technology make it possible to inspect the manufacturing line at high speeds and with a good degree of accuracy. On the other hand, lighting is still a major problem for some products and processes.

Humans can be extremely rapid in decision making, whereas a machine has to be given a set of standards for the same operation. If these standards or thresholds are too low, the system might reject nearly all of the products, and if it is too high, product quality might decrease. Therefore, there is a need for a fuzzy type of decision making system with the ability of perception such as neural network or fuzzy logic devices.

### **1.2.2 Commercial Difficulties**

Despite the potential benefits from robotic applications, commercial difficulties are still continued to be a problematic issue for these systems. Historically, cost justification, which has always been a strong driver for investment, has been based on labor savings. Low price of individual food items and generally low margins in food industry also complicate the cost justification. At present, most robotic systems are far too expensive; therefore, do not meet the general commercial requirements of food producers. This is especially true for Turkish food industry.

Another drawback is the necessity of a shift in the technical skills within the factory. The maintenance and operation of robotic systems will require technical skills that did not previously exist. The food industry has generally invested less in production technical support than have other industry sectors.

Lack of expertise in commercialization is another problem restricting the use of robotic systems in food industry. There is a need for more specialist companies to work on the commercialization of robotic systems for food industry.

As a summary, main commercial difficulties are:

- Robot builders are not willing to invest in developing new technology without food companies providing financial support.
- Financial justification has not given short-enough pay-back times.
- There is lack of expertise in commercialization.
- Low margins in food products.

### **1.3 Objective of the Study**

The use of robotics in food industry is becoming more popular in recent years. The trend seems to continue as long as the robotics technology meets diverse and challenging needs of the food producers. Rapid developments in digital computers

and control systems technologies have significant impact in robotics like any other engineering fields. By utilizing new hardware and software tools, design of these complex systems that need strong integration of distinct disciplines is no longer difficult compared to the past. While most of companies in food industry still meet these technology requirements from more specialized suppliers, ETİ Group of Companies, a leading group in confectionary industry in TURKEY, opt to develop their own know-how in robotics in order to keep the persistency in the market. As a first step, ETİ Group of Companies has started a project called “Design of a Secondary Packaging Robotic System (SPRS)” project.

The project has aimed the automation of secondary packaging process of the ETİ TUTKU production line. The reason behind selecting this line was unsystematic distribution of the labor force along the manufacturing line shown in figure 1.4. It is clear from the figure that the concentration of labor force on secondary packaging makes this process most urgent stage of the production for automation.

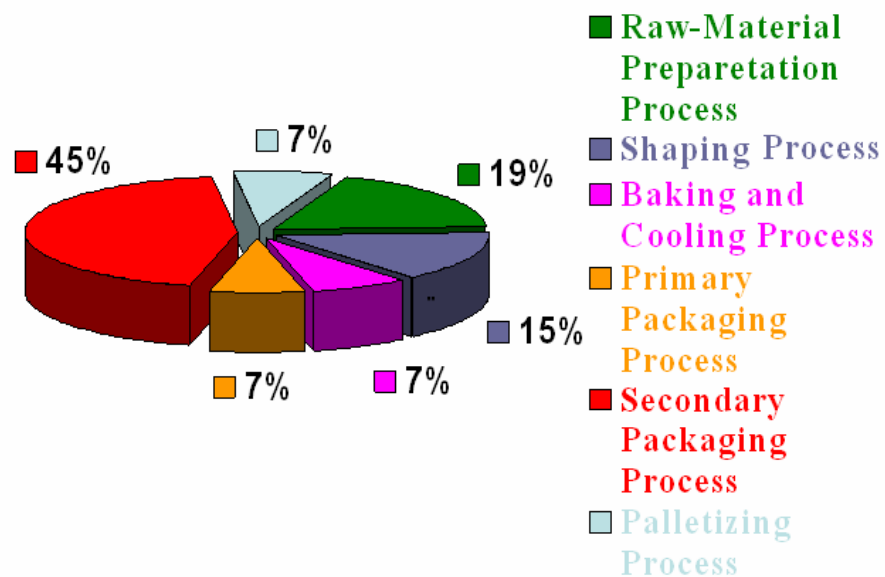


Figure 1.4 Labor distributions along ETİ TUTKU manufacturing line

Therefore, the purpose of this thesis study was to design and implement a reliable and high performance secondary packaging robotic system for ETİ TUTKU manufacturing line.

As stated in section 1.2.1, robotic handling of food products presents sophisticated problems compared to rigid materials because they can be very fragile and deformable. They can be also easily bruised and marked when they come into contact with hard and/or rough surfaces. Taking into account the technical requirements of the process, the most important design constraint was to perform the secondary packaging operation of ETİ TUTKU product automatically at a rate of 200 products/minute without causing any distortion to product. This rate is the throughput of the manufacturing line at present. Objectives of the study were:

- Increasing the manufacturing capacity,
- Increasing the labor productivity by the redistribution of laborers,
- Reducing the product cost and manufacturing time,
- Eliminating the manual and boring tasks.

#### **1.4 Scope of the Thesis**

The SPRS, shown in figure 1.5 can be represented by three basic subsystems as follows:

- A dynamic sorter machine,
- A pick and place robotic arm,
- A special purpose gripper unit.

Within the context of this study, mechanical and control systems design of the robotic arm and the gripper unit were performed. Design procedure, shown in figure 1.6, adopted for the robotic arm differs from classical design methods in a way that it enables feedbacks between mechanical design of the manipulator and its control system software. System performance was precisely predicted by detailed system

simulation and inevitable design modifications were performed before expensive system realization.

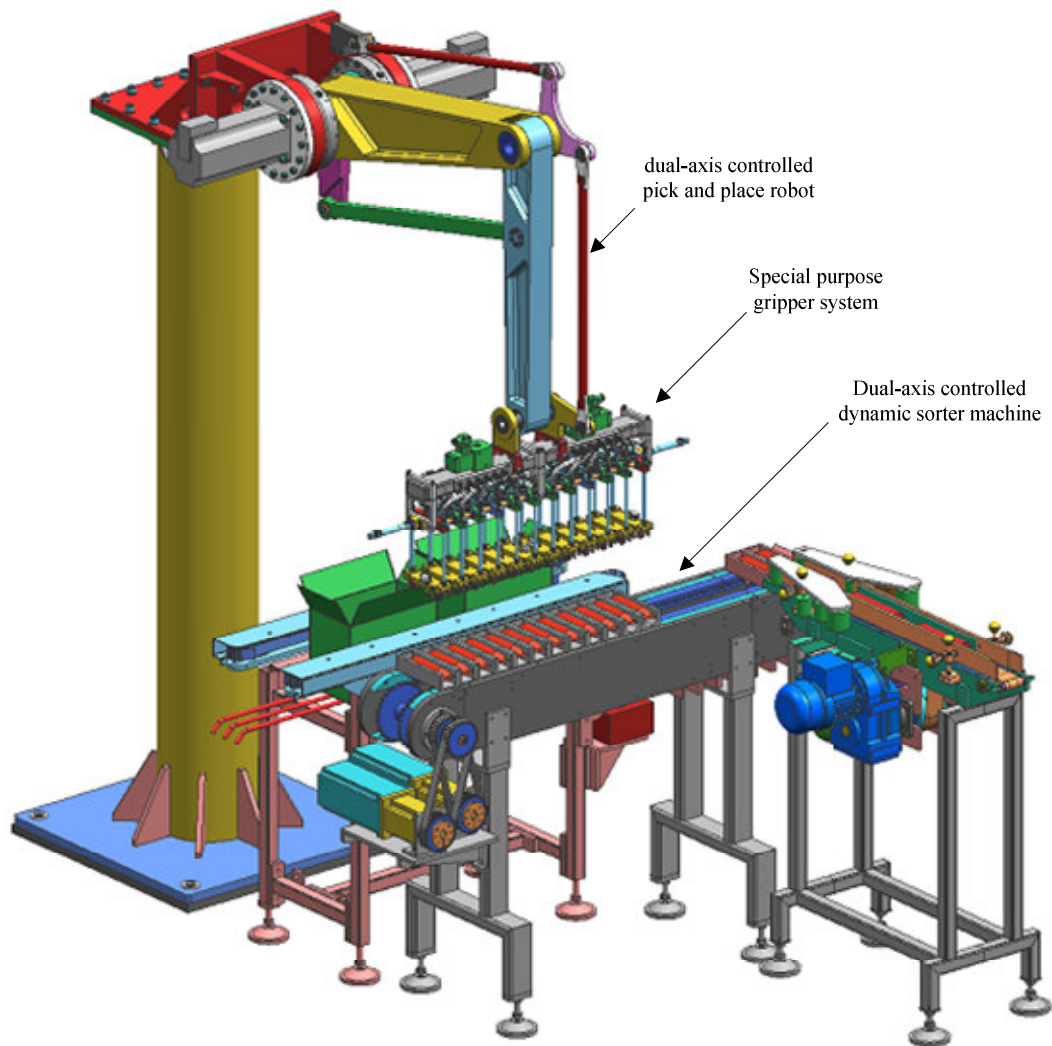
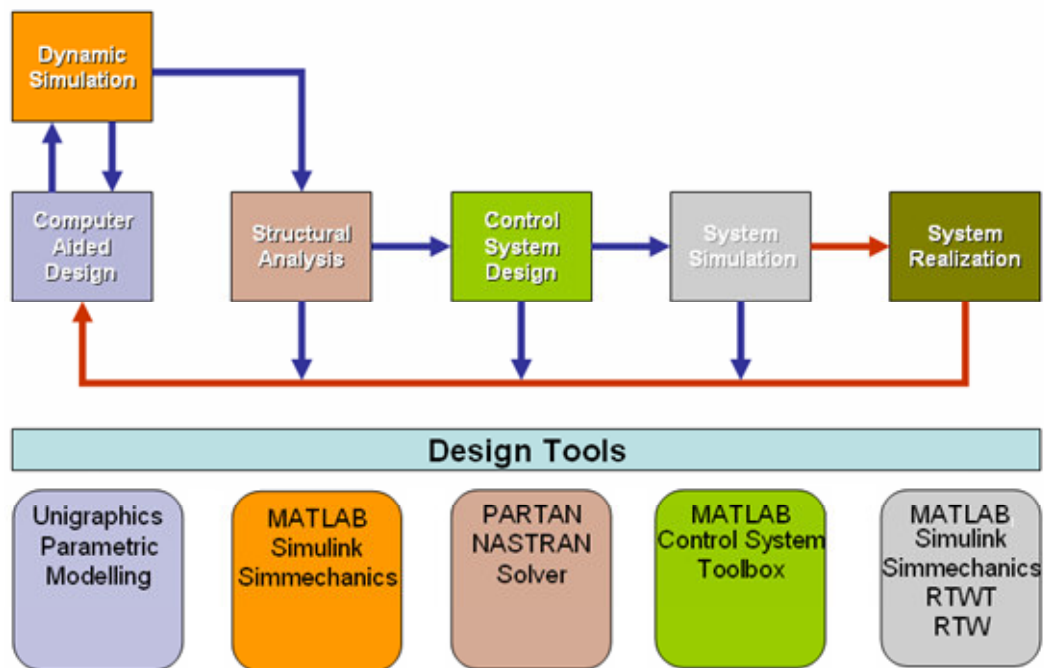


Figure 1.5 Secondary packaging robotic system

The design of robotic arms requires a systematic development and use of modern design tools. Starting from pure mechanical design, robotic arm design was performed in 5 distinct, but iterative, steps:

- Computer aided design stage. UNIGRAPHICS was used to construct the manipulator parametric 3-D solid models and their technical drawings.
- Dynamic simulation stage for obtaining dynamic parameters. MATLAB/Simulink and SimMechanics blockset was used to model the dynamics of the robotic arm.



### 1.6 Design procedure of robotic arm in SPRS

- Structural analysis stage for obtaining structural parameters. Msc. PATRAN together with Msc. NASTRAN solver was used for structural analysis.
- Control system design. MATLAB and Control Systems Toolbox was used to design the control system.
- System simulation stage for predicting the performance of overall system. MATLAB/Simulink, Real-time Windows Target, Real-time Workshop and a C compiler was used for the system simulation.

Robotic system development process is different from other development process in the sense that it spans over many closely coupled engineering domains. It is important to note that although a proper controller may enable building cheaper construction, a poorly designed mechanical system never be able to give a good performance by adding a sophisticated controller. Therefore, in structural development stage, special attention was paid to determine mechanical parameters that are directly relevant to performance of the robotic system.

### **1.5 Outline of the Thesis**

In this thesis, components of the developed secondary packaging robotic system are introduced and how they are constituted is described.

Chapter 2 describes the secondary packaging robotic system. The basic subsystems and overall system's control architecture are discussed.

Chapter 3 deals with the mechanical design of the robotic arm while chapter 4 discusses its control systems design.

Chapter 5 is devoted to system simulation techniques and application of these techniques to the developed robotic arm.

Chapter 6 describes the special purpose gripper unit.

### **1.6 Conclusion**

In this chapter fundamental processes in a generic food manufacturing line and the use of robotic systems in these processes have been discussed briefly. Technical and commercial difficulties blocking the use of robotic systems in food industry have been unveiled.

This thesis study has aimed the automation of secondary packaging process of the ETİ TUTKU production line. The reason behind selecting this line was unsystematic distribution of the labor force along the manufacturing line shown in figure 1.4. Therefore, the purpose of this thesis study was to design and implement a reliable and high performance secondary packaging robotic system for ETİ TUTKU manufacturing line.

In the design processes of secondary packaging robotic system, modern computer-aided design (CAD) and computer-aided engineering (CAE) tools were utilized. The importance of simultaneous development of hardware and software parts of a robotic system was emphasized by using these CAD/CAE tools.

## **CHAPTER 2**

### **INTRODUCTION TO SECONDARY PACKAGING ROBOTIC SYSTEM**

#### **2.1 Introduction**

In this chapter, the newly developed secondary packaging robotic system and its main components are introduced and how they are organized to perform intended task is described. The overall control architecture and operational state model of the system are also discussed.

Despite the recent advances in the application of robotics technology in food manufacturing, secondary packaging processes are generally performed by unskilled labors in food industry. Some of the technical and commercial reasons behind this fact are already discussed in chapter 1. In addition to mentioned hurdles, secondary packaging process presents additional challenges from the robotic handling point of view. Difficulties in matching human speed, dexterity, and flexibility, variable nature and number of products, high production volume rates, and lack of appropriate robot tools or end-effectors are still blocking the range of use of robotics in food production environments.

A closer look at secondary packaging process is essential to understand the working principal of secondary packaging robotic system. As stated in previous chapter, secondary packaging is the process of taking products coming from primary packaging process and placing them into cardboard boxes. The purpose of secondary packaging is not only to give an extra strength to products, but also to protect them

during transportation. Figure 2.1 depicts the input and output relations using block diagram representation.

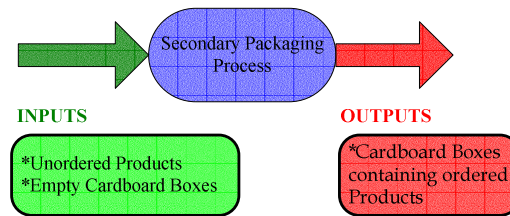


Figure 2.1 Inputs and outputs of secondary packaging

As seen in the figure, inputs of the secondary packaging process are unordered products coming from the primary packaging process and empty cardboard boxes. The output is cardboard boxes containing ordered products. The process can be further decomposed into three fundamental sub processes as shown in figure 2.2.

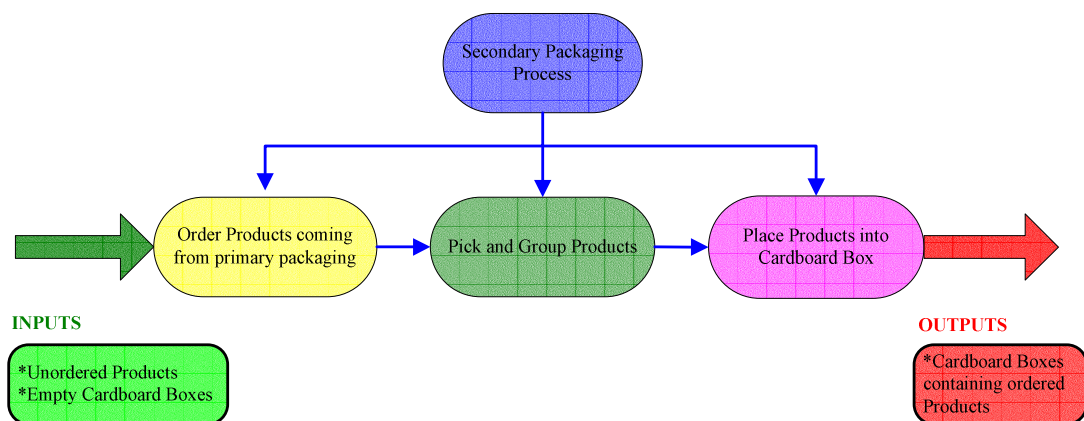


Figure 2.2 Sub processes of secondary packaging

## **2.2 Current State of the Art in Secondary Packaging Automation**

There are many companies offering secondary packaging automation solutions in the world market. OPM ([www.opm.it](http://www.opm.it)), Schubert ([www.gerhard-schubert.de](http://www.gerhard-schubert.de)), SIG ([www.sigdemaurex.com](http://www.sigdemaurex.com)), Delkor Systems ([www.delkorsystems.com](http://www.delkorsystems.com)), AMF Automation ([www.amfautomation.com](http://www.amfautomation.com)), The Blueprint Automation Group ([www.blueprintautomation.com](http://www.blueprintautomation.com)) are some examples. However, few of these automation solutions are mostly adopted by the food manufacturers. The main reasons behind this adoption are the flexibility, robustness and reliability of mentioned systems. Having a closer look at these companies' solutions will be useful to get general idea about the current state of the art in secondary packaging automation.

When different companies' secondary packaging automation systems are analyzed, it can be observed that a fully automated secondary packaging automation system consists of several distinct subsystems. While a special-purpose sorter machine prepares products coming from primary packaging process for robotic handling, a robot or robots equipped with special-purpose grippers and other peripheral devices, for instance vacuum system, take products and place them into the cardboard boxes. Primary and secondary packaging systems are often seamlessly integrated to form an automated packaging line.

### **2.2.1 OPM's Secondary Packaging Automation Solution**

OPM specializes in the robotic packaging of confectionary products, primarily assorted chocolates, biscuits and chocolate bars. As shown in figure 2.3, there are 5 modules in OPM's secondary packaging automation system;

- A product infeed system,
- A cardboard box infeed system,
- A dynamic sorter machine,

- A dual-axis controlled pick and place robot,
- A special-purpose end-effector.

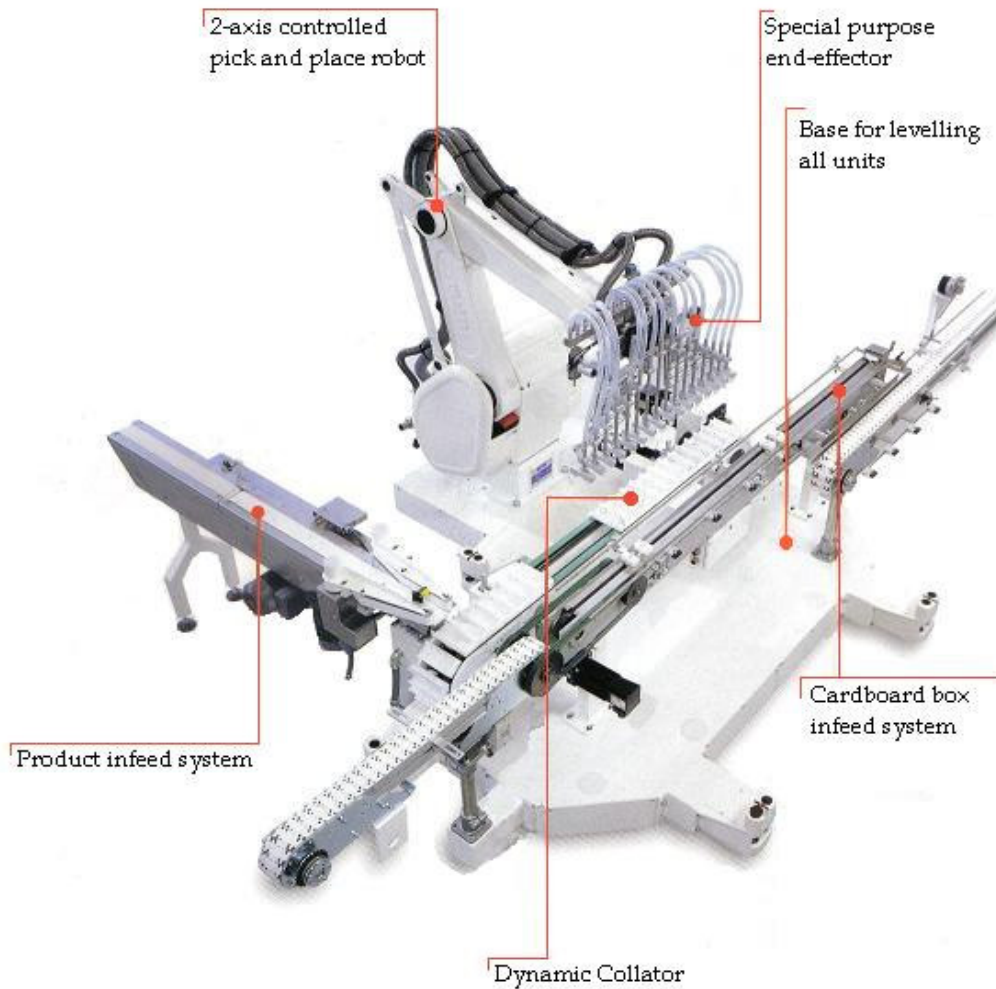


Figure 2.3 OPM's secondary packaging automation solution

### 2.2.2 Schubert's Secondary Packaging Automation Solution

Gerhard Schubert GmbH is one of the most mature and dedicated suppliers of robotic systems to the food industry. Schubert also specializes in the packaging of confectionary products, primarily assorted chocolates and biscuits like OPM. The

company's secondary packaging system, so called TLM packaging machines by the company, is a top loading system and ideal for packaging individual products. As seen in figure 2.4, the system composed of modules similar to that of OPM's system. The system erects a cardboard box from flat blanks, takes products from a dynamic sorting robot, which collects and orders products, and places them into cardboard box. The controls have been placed to the top of the system providing access to all moving parts. System can be reconfigured for different products.



Figure 2.4 Schubert's secondary packaging automation solution

### 2.2.3 SIG's Secondary Packaging Automation Solution

SIG, a major Swiss-owned food packaging company, realizes robotic solutions to meet secondary packaging requirements of the food manufactures. SIG's secondary packaging automation solution, shown in figure 2.5, differs from the other solutions. Delta robots are used for movements and dynamic collator system is eliminated by using a vision system. The Delta robot arrangement allows actuators to be located in fixed positions, greatly reducing the mass of the moving structure. 2 cycles per second can be achieved by these systems. However, speed of delta robot does not make significant influence in packaging capacity because of its low payload. Another major drawback of the system is its high cost compared to other solutions.

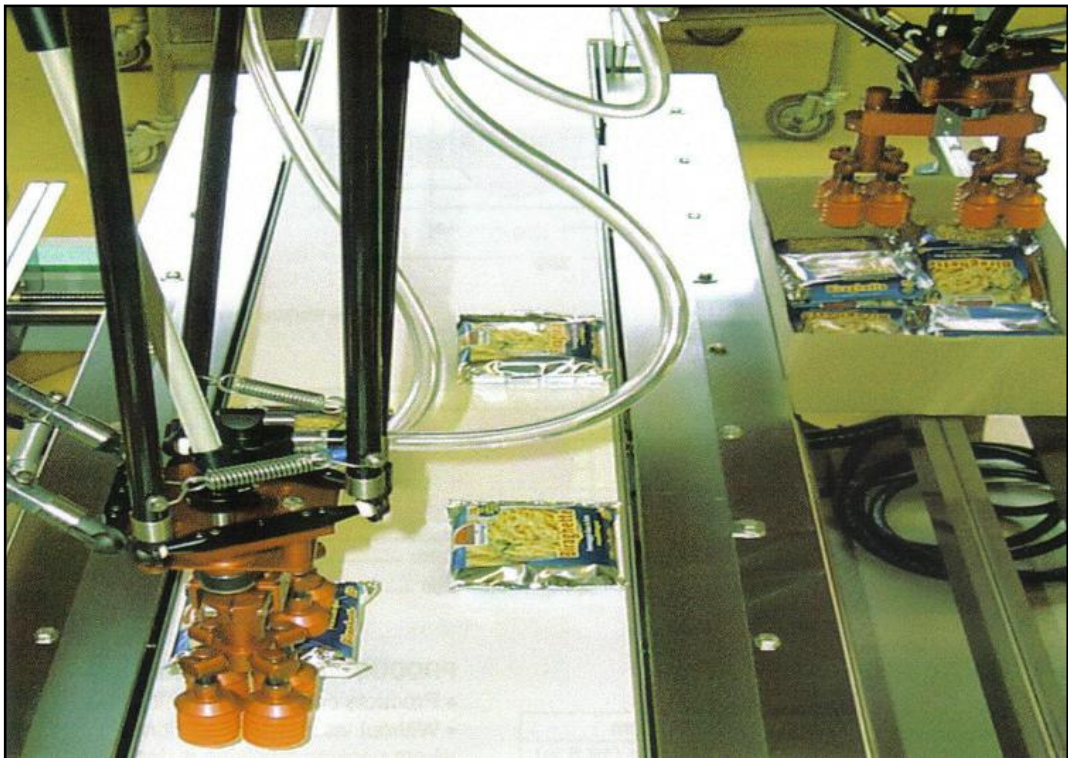


Figure 2.5 SIG's secondary packaging automation solution

### **2.3 Secondary Packaging Robotic System**

Newly developed secondary packaging robotic system, abbreviated as SPRS, for the purpose of secondary packaging automation of ETİ TUTKU manufacturing line is made up of several distinct subsystems to feed the products and cardboard boxes, to prepare products coming from the primary packaging process for robotic handling and to place them into the cardboard boxes. All of the components, except the actuators, pneumatic and control system hardware, were manufactured and assembled in the facilities of ETİ Machinery Industry and Trade Co. Inc. Figure 2.6 depicts the 3-D CAD view of SPRS.

Secondary packaging robotic system consists of the following components:

- A dynamic sorter machine, which is a dual-axis robot with the ability of sorting at a maximum rate of 240 products per minute.
- A dual-axis controlled pick and place robotic arm with the manipulation rate of 20 cycles per minute.
- A gripper unit with the ability of picking 12 workparts at one cycle and performing grouping action during the pick and place operation.
- Control systems hardware and a central motion control unit which executes control software and triggers software signals in order to accurately control the system.

Remembering the throughput of ETİ TUTKU production line, which is 200 products per minute at its maximum capacity, the system is able to respond to secondary packaging process with the capacity of 240 products per minute. It also has a 20 percent safety margin.

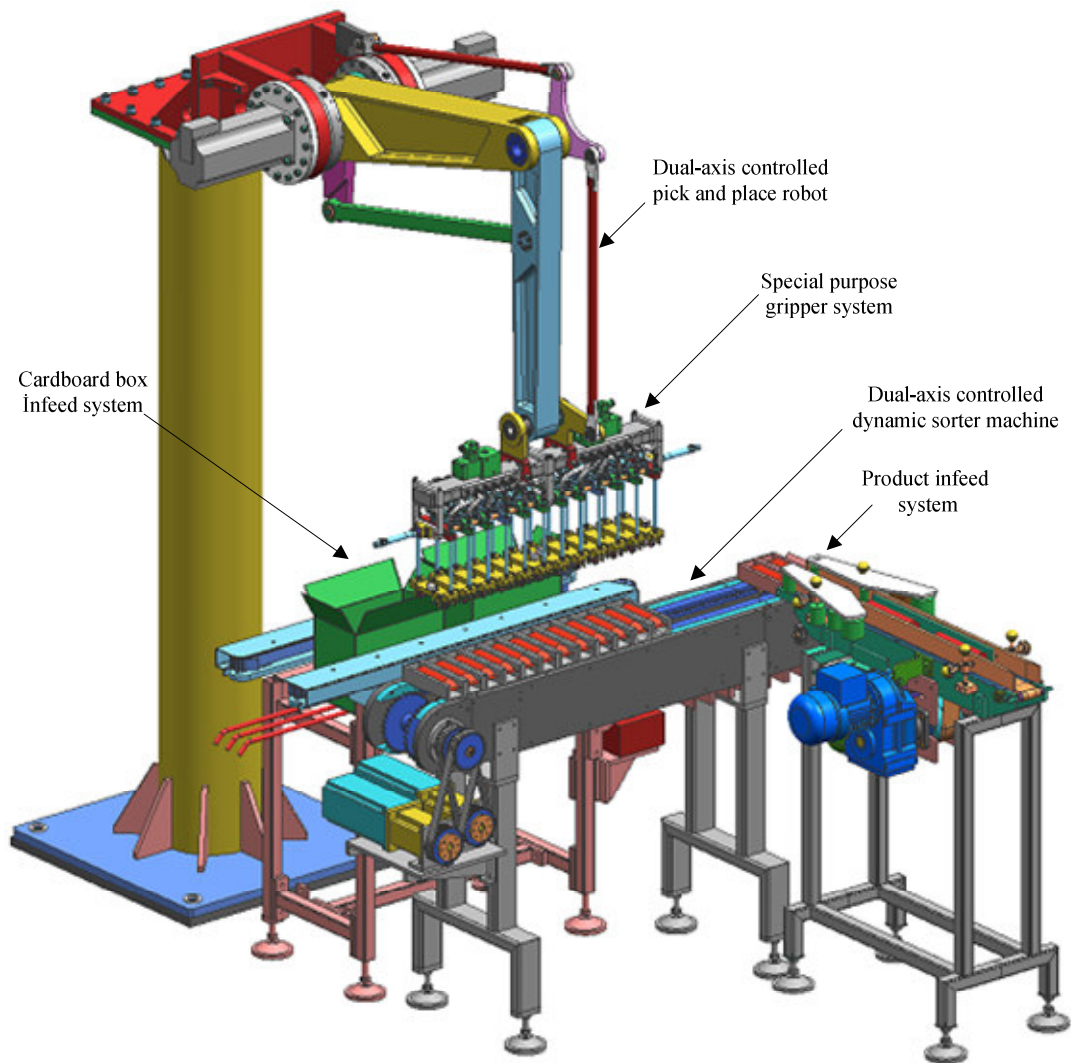


Figure 2.6 3-D CAD view of SPRS

In secondary packaging robotic system, pick and place operation is performed by a dual-axis controlled robotic arm equipped with a special purpose gripper system. The robotic arm is mounted to a cylindrical base in order to occupy less space in the factory floor as shown in figure 2.7.

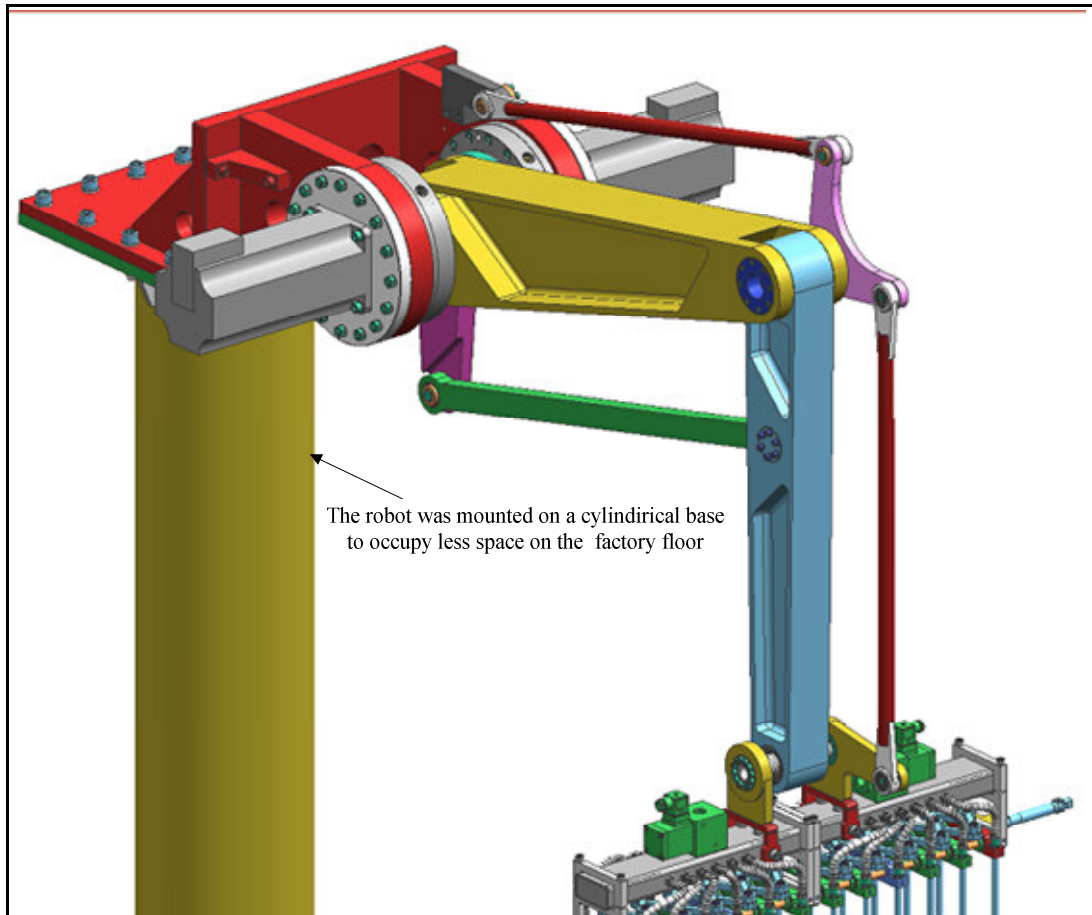


Figure 2.7 Dual-axis controlled pick and place robotic arm

Second basic component is the dynamic sorter machine. In order to sort products to a pattern that is suitable for robotic handling, a dynamic sorter machine, which is a dual axis robot, was utilized. Each individually driven axis of the robot carries a set of 12 specially designed pallets attached to chain. Figure 2.8 shows 3-D CAD view of the dynamic sorter machine. Safety guards of the power transmission system and guides are removed to show the details.

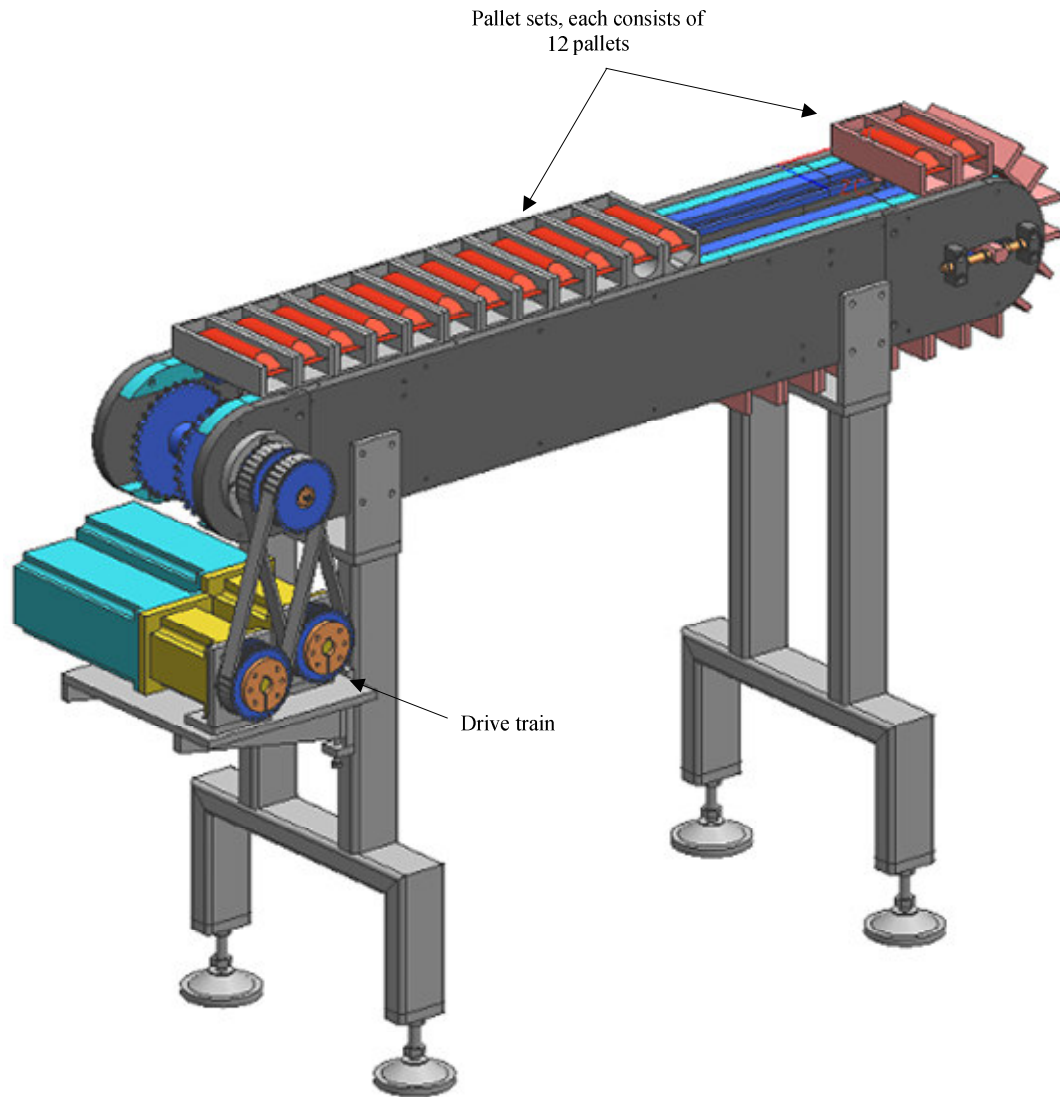
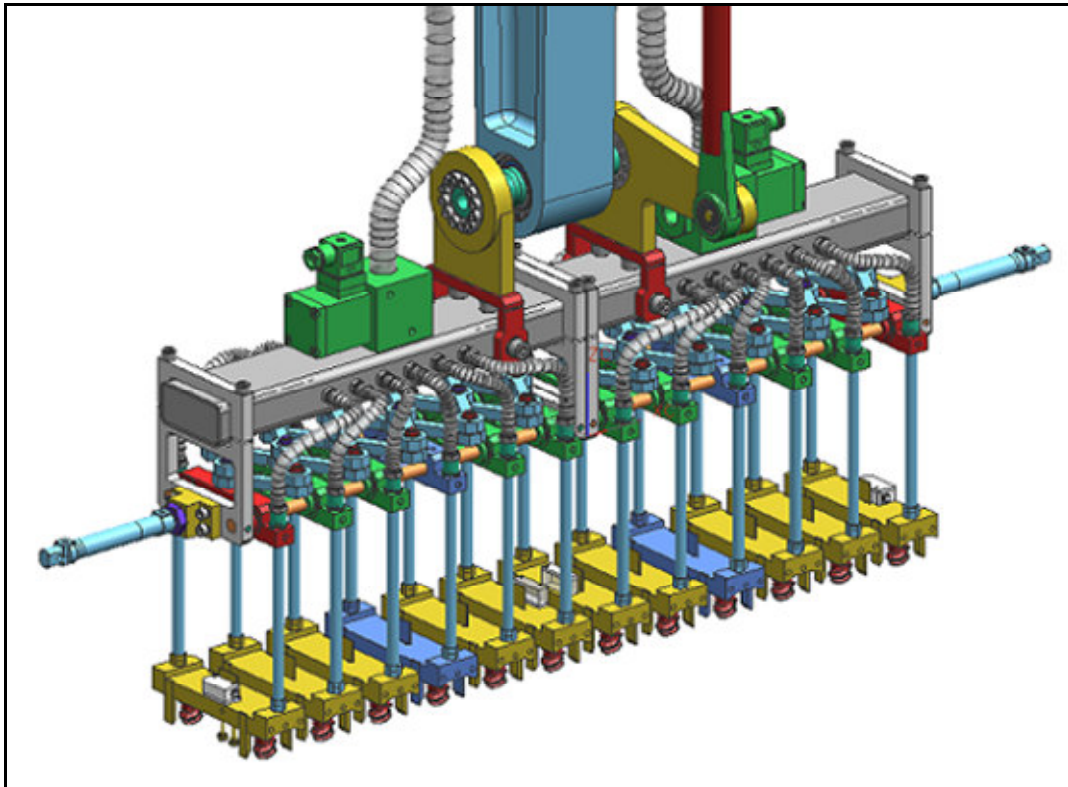


Figure 2.8 Isometric view of dynamic sorter machine

Another basic component of the system is the gripper. The robotic arm was equipped with a specially designed gripper to pick products from the dynamic sorter machine's pallets. Principle of pressure differential was used to create gripping force. The grasp geometry of the gripper was specially designed for the ETÍ TUTKU product. Figure 2.9 shows the isometric view of the gripper.



2.9 Isometric view of the gripper system

The working principle of SPRS is as follows. Randomly coming products from primary packaging process is fed to the dynamic sorter machine by product infeed system. Product feeding to dynamic sorter machine is one of the most critical processes because of the delicacy and fragility of the product. The dynamic forces created during the feeding process can easily damage to the product. Therefore, the feeding process was examined with great care. Figure 2.10 and 2.11 depict this process.

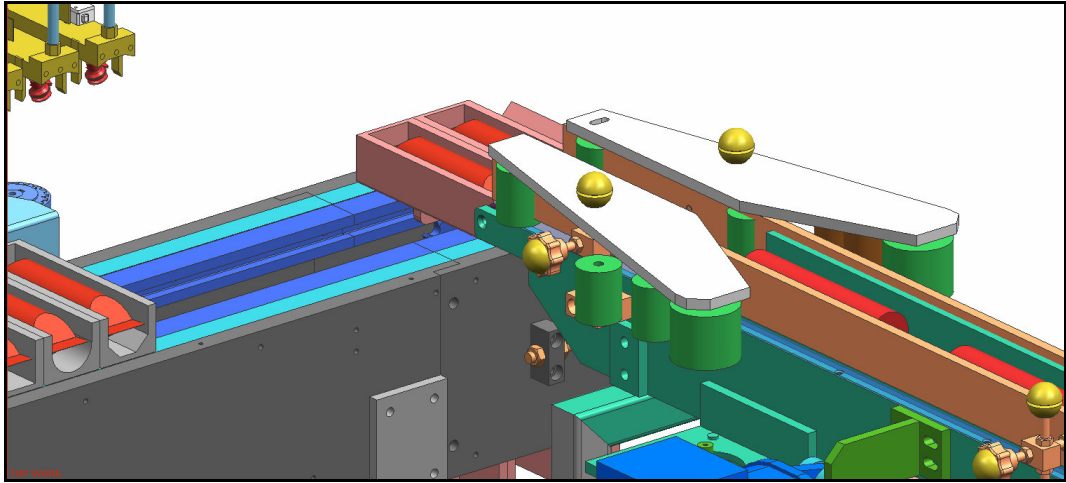


Figure 2.10 Isometric view of product infeed process

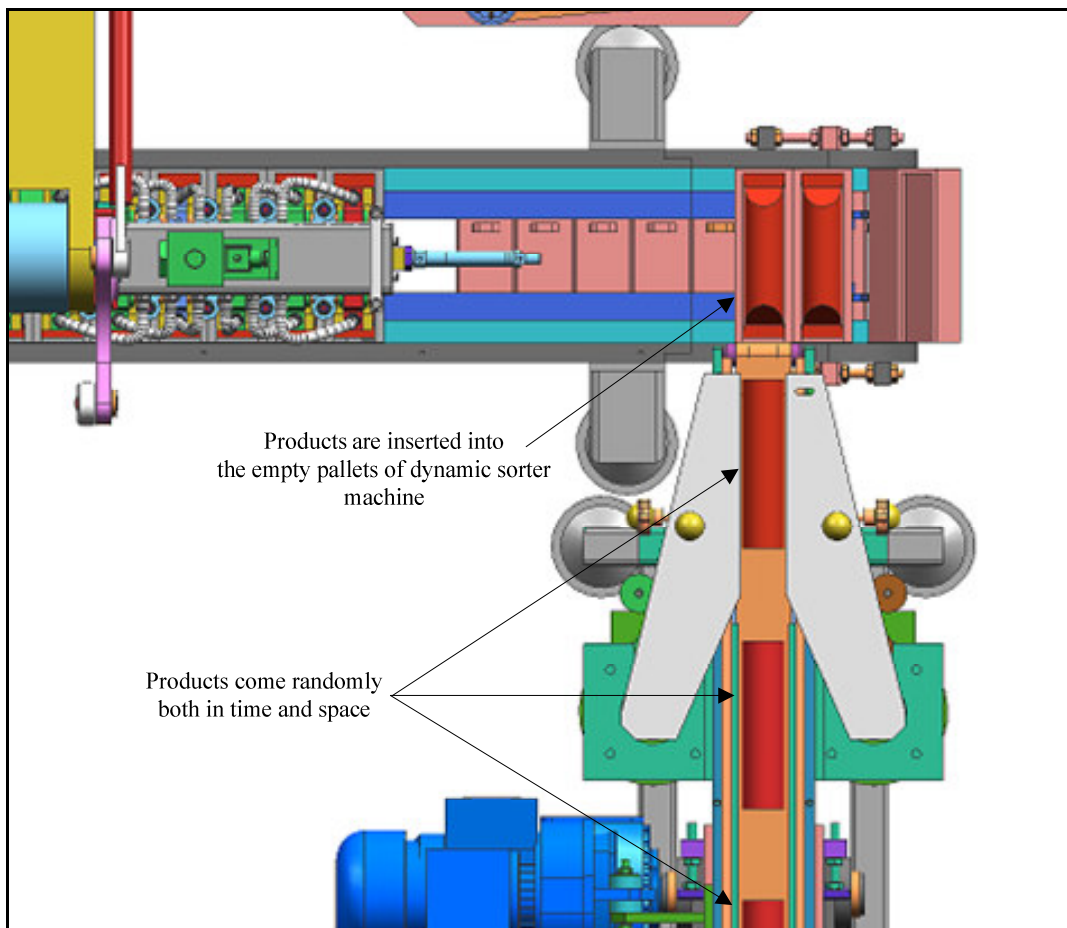


Figure 2.11 Top view of product infeed process

Once the product infeed process is completed; the loaded set is positioned to the unloading station. Products in unloading station are then picked and placed into the cardboard boxes by the robotic arm equipped with the special purpose gripper. Two cardboard boxes are filled simultaneously. While one set of pallets of the dynamic sorting robot are unloading, infeed process continues with the other set. After unloading, the axis carrying empty set of pallets synchronizes to the movement of the other axis, which is being loaded at that moment, until the infeed process is completed and the pallets are fully loaded. The operation cyclically continues while the dynamic sorter machine is in function. Figure 2.12 shows the dynamic sorting robot when one of its pallets are fully loaded and positioned to unloading station for pick and place operation.

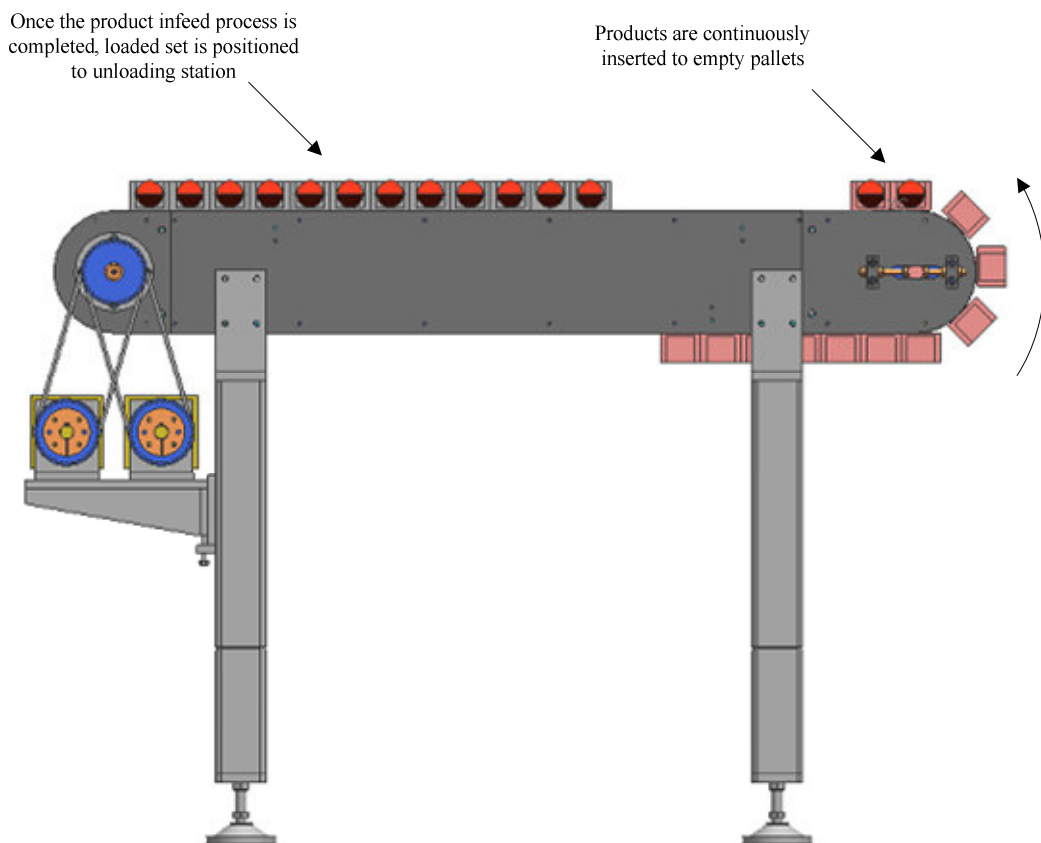


Figure 2.12 Front view of dynamic sorter machine

## 2.4 Control System Architecture

VisualMotion control system from Bosch-Rexroth Indramat was used in the SPRS control system. VisualMotion is a programmable multi-axis motion control system capable of controlling up to 32 digital intelligent motor drives. PC software used for motion control management is named as VisualMotion Toolkit (VMT). VisualMotion Toolkit (VMT) is software for motion control programming, parameterization, system diagnostics and motion control management. VMT also includes a DDE server which is a communication protocol between Microsoft Windows programs and motion control system. The hardware used with VisualMotion Toolkit is the PPC-R motion control card.

The SPRS control system consists of the following components:

- PPC-R motion control card
- RECO02 I/O modules
- VisualMotion Toolkit program
- ECODRIVE03-SGP01 motor drives
- Permanent magnet synchronous servomotors

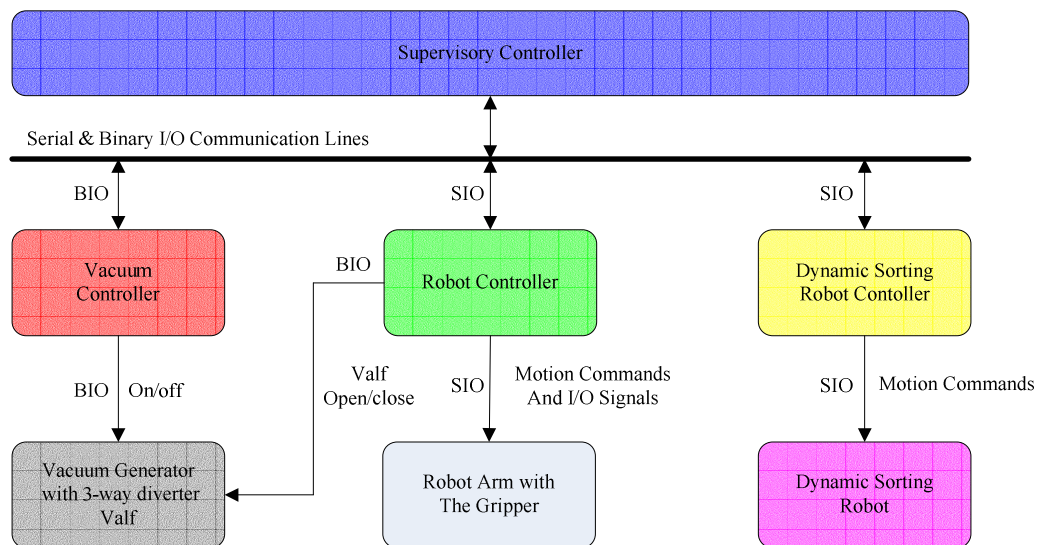


Figure 2.13 Block diagram representation of the SPRS

Figure 2.13 depicts the control architecture of the SPRS. As seen in the figure, there are one supervisory controller and three individual controllers in the system. The supervisory controller is used to trigger software signals that are relevant to the operation of overall system while individual controllers are used to control other basic subsystems. Communications between controllers are via the SERCOS fiber optic interface, which is an international standard for real-time communication.

## 2.5 SPRS Operational State Model

SPRS is designed as a finite state system, which is a popular mechanism for specifying what the system should be performing at a given time or circumstance. A state of SPRS completely defines the current condition of the system. Three state types are available:

- A final state represents a safe state, i.e. no moving parts.
- A transient state is one on which represents some processing activity. It implies a single or repeated execution of processing steps in a logical order, for a finite time or until a specific condition is reached. For example, packaging state is a transient state because it involves execution of number of processing steps in a logical order.
- A quiescent state is used to identify that a machine has achieved a defined set of conditions. In such a state the SPRS is holding or maintaining a status until transition to transient state.

Transitions between states occur:

- As a result of a command, or
- As a result of a status change. This is generated by change of state of one or a number of system conditions, either directly from I/O or completion of a logic routine. State model of the SPRS is depicted in Figure 2.14.

## 2.5.1 SPRS Operational State Descriptions

SPRS has 8 distinct states which fully describes the system conditions:

- **OFF:** All power to the system is switched off. There is no response from the system.
- **STOPPED:** The system is powered and stationary. All internal and external communications with the other systems are functioning.
- **STARTING:** This state allows the system to be prepared for running. It includes the activation of vacuum generator, initialization of the robotic arm, gripper and the dynamic sorting robot.

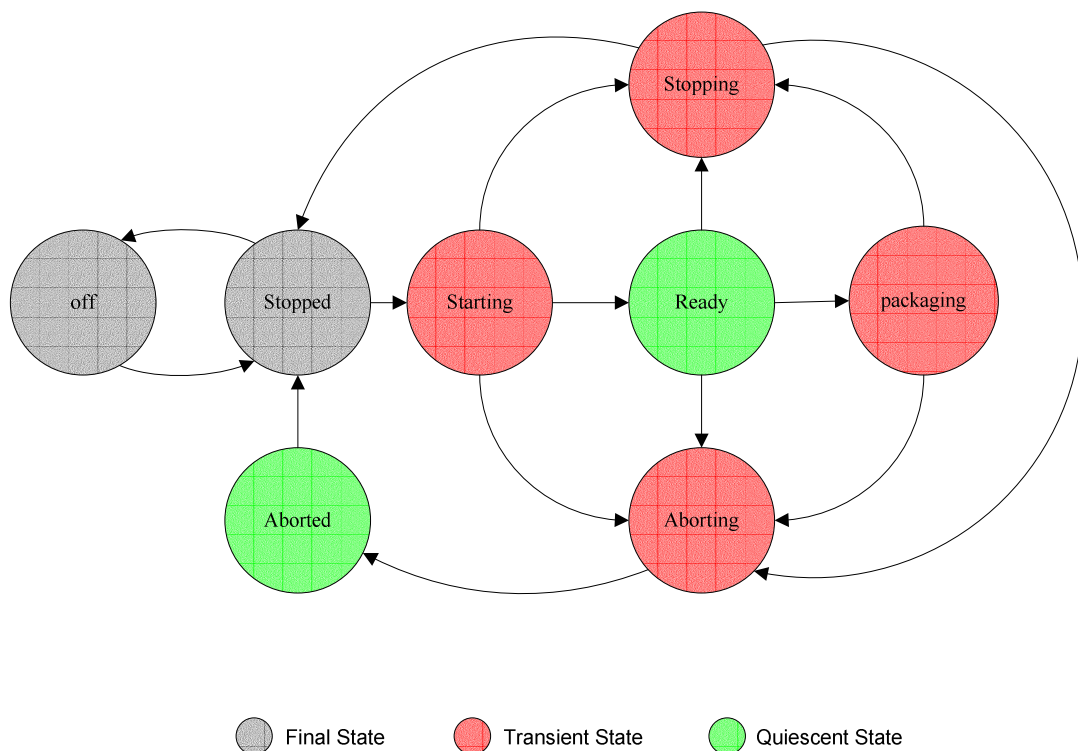


Figure 2.14 SPRS state model

- **READY:** This is a state that indicates that STARTING logic is completed. SPRS maintains its condition that is achieved during STARTING state.
- **PACKAGING:** In this state, SPRS performs packaging operation.
- **STOPPING:** This state executes the logic which brings the system to a controlled and safe stop.
- **ABORTING:** The system can enter to ABORTING state at any time in response to the ABORT command. The ABORTING logic brings the system to rapid, controlled safe stop. Operation of the emergency stop or “E-Stop” causes the system to enter ABORTING state.
- **ABORTED:** After the execution of ABORTING logic, SPRS enters to ABORTED state and maintains its status information relevant to the ABORT condition. The Stop command in this state forces transition to the STOPPED state. The ABORTED state is a quiescent state which indicates that the ABORTING logic has completed.

Table 2.1 Operational state transition matrix of SPRS

	Machine Status			Commands			
	Power on	Power off	State Completed	Prepare	Start	Stop	Abort
<b>Initial State</b>							
OFF	STOPPED						
STOPPED		OFF		STARTING			
STARTING			READY			STOPPING	ABORTING
READY					RUNNING	STOPPING	ABORTING
RUNNING			STOPPED			STOPPING	ABORTING
STOPPING							ABORTING
ABORTING			ABORTED				
ABORTED						STOPPED	

Table 2.1 shows the state transition matrix of the system. In order to perform packaging operation, SPRS should be in PACKAGING state. To bring the system to

this state, operator needs to switch on the power and issue the PREPARE command. Once the PREPARE command issued, SPRS enters to STARTING state and executes the starting logic. Supervisory controller sends the same signal to vacuum controller, robotic arm controller and dynamic sorting robot controller and waits for the relevant SYSTEM\_READY signals from individual controllers. Once the individual controllers issues this signal, each of them wait for the START command from the supervisory controller. When all components complete their corresponding starting logic, system automatically enters to READY state, which is a quiescent state. This state maintains the operating conditions of the system until the START command is issued and essentially represents that the STARTING state has been completed. Then, when the operator issues START command, supervisory controller sends same signal to each controller and system enters to packaging state. The ABORTING state can be entered in any time in response to the ABORT command of the operator. ABORTING causes the SPRS to a rapid controlled stop. The completion of the aborting logic results in the quiescent state ABORTED.

## **2.6 Conclusion**

In this chapter, current state of the art in secondary packaging automation has been briefly discussed and leading companies' secondary packaging automation solutions introduced. When different companies' secondary packaging automation systems are analyzed, it can be observed that a fully automated secondary packaging automation system consists of several distinct subsystems. While a special-purpose sorter machine prepares products coming from primary packaging process for robotic handling, a robot or robots equipped with special-purpose grippers and other peripheral devices, for instance vacuum system, take products and place them into the cardboard boxes.

Secondary packaging robotic system and its main components have also been introduced and how they are organized to perform intended task described. The

system is composed of three major components: a dynamic sorter machine, a two-axis controlled pick and place robotic arm and a special-purpose gripper system.

Overall control architecture and operational state model of the system have been briefly introduced. VisualMotion control system from Rexroth-Indramat was used in the SPRS control system. There are one supervisory controller and three individual controllers in the system. The supervisory controller is used to trigger software signals that are relevant to the operation of overall system while individual controllers are used to control other basic subsystems. Communications between controllers are via the SERCOS fiber optic interface, which is an international standard for real-time communication.

SPRS was designed as a finite state system, which is a popular mechanism for specifying what the system should be performing at a given time or circumstance. A state of SPRS completely defines the current condition of the system. Three state types are available: final state representing a safe state, a transient state representing some processing activity and quiescent state which is used to identify that a machine has achieved a defined set of conditions.

## CHAPTER 3

### MANIPULATOR MECHANICAL DESIGN

#### 3.1 Introduction

Manipulator is the main body of the robot. It is defined as [4] “a machine, the mechanism of which usually consists of a series of segments jointed or sliding relative to the one another, for the purpose of grasping and/or moving objects usually in several degrees of freedom”. Generally, an industrial manipulator is constructed of series of links, joints and other structural elements. It is characterized by an arm that ensures mobility, a wrist that provides dexterity, and an end-effector that performs the desired operation on the workpart.

Tasks that a robot can perform depend on the mechanical design of its manipulator. Although robots are perceived as universally programmable machines capable of wide variety of tasks, economical and practical constraints dictate basing the design of manipulators on task requirements. Therefore, there should be a harmony between the manipulator and the task to be executed. Taking into account this point, the mechanical design of the manipulator was performed based on the secondary packaging task requirements. All design decisions were based on the pick and place operation of products during secondary packaging. Several alternative configurations were considered in detail before one is chosen. Selection of the configuration was based on the sizing of the most important system components, evaluation of dynamic performance, mechanical simplicity, manufacturability and ease of control.

### 3.2 Manipulator Mechanical Design Procedure

The process of designing any mechanism can be divided into two fundamental phases as shown in the figure 3.1.

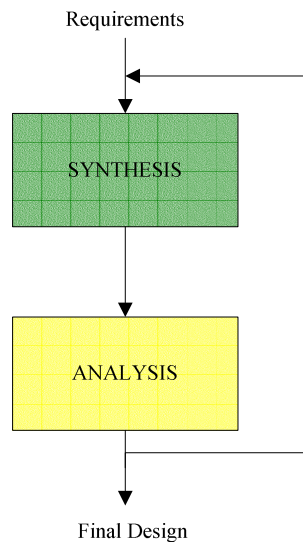


Figure 3.1 Main steps in the design of a mechanism

After a proper specification of the demands, the first step in the design cycle consists of the synthesis phase, in which the designer attempts to determine the type of mechanism and its dimensions, such that the requirements are met. In the analysis phase, the designer analyses the mechanism from both the dynamic and kinematic view points. Iteration continues until a satisfactory design is achieved. Mechanical design of a manipulator is similar to a mechanism design. However, it is difficult to design manipulators by the conventional methods of mechanism design because manipulators involve many parameters to be determined. Accordingly, following an efficient design procedure is the key point to achieve a suitable manipulator for intended tasks and saving manpower, time and cost.

Figure 3.2 shows the procedure adopted for the mechanical design of the manipulator in SPRS. According to the procedure, first step was the determination of design condition inputs which are prescribed by the objective task. Then, the manipulator mechanical design was performed in three distinct phases: fundamental mechanism design, drive system design, and detailed structural design. The fundamental mechanism design was based on kinematic requirements including work envelope, joint's maximum displacements, velocities and accelerations. A reference workpart trajectory is determined in this phase. In drive system design phase, motor allocations and the type of transmission mechanisms were determined based on rough evaluation of dynamics of the manipulator. Arm cross-sectional dimensions are calculated roughly, and motors, reduction units and machine elements were selected from catalog data. Modification of the arm cross-sectional dimensions and reselection of the machine elements based on precise evaluation of dynamics were performed in detailed structural design phase. Total weight, deflection of the manipulator under the effect of static and dynamic loading and natural frequency of mechanical structure were also evaluated.

### **3.3 Design Condition Inputs**

As stated in introductory chapter 1, the robotic arm in SPRS will perform pick and place operations on products. Therefore, all decisions about the mechanical design of the manipulator were based on pick and place task requirements. A reference trajectory, which is suitable for the packaging of products, was constructed for that purpose.

In addition to reference trajectory, there are 4 design condition inputs prescribed by the objective operation:

- maximum payload including the gripper system

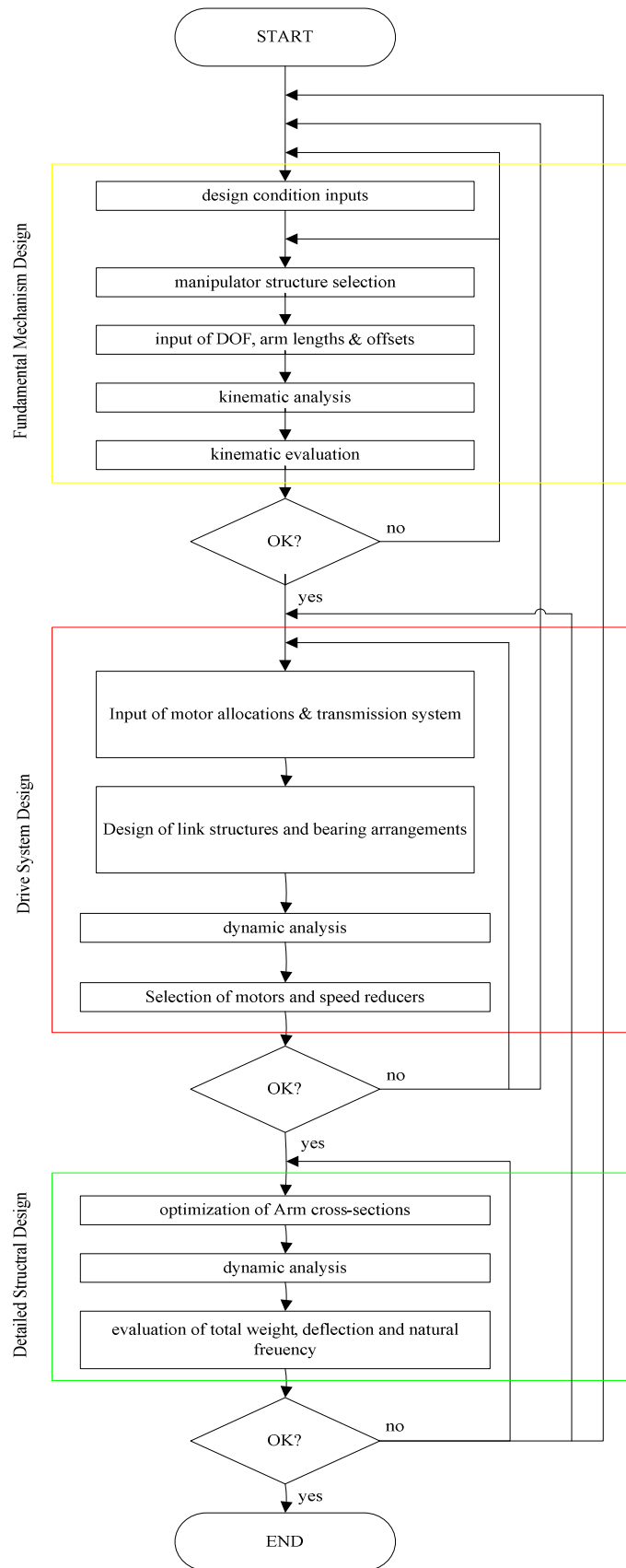


Figure 3.2 Mechanical design procedure of the manipulator

- allowable deflection at the tip point
- allowable natural frequency
- allowable product acceleration in x and y-direction

Design condition inputs are summarized in table 3.1.

Table 3.1 Design condition inputs

Description	Value	Units
Max. payload	20	kg
Max. deflection at the tip point	1	mm
Allowable min. natural frequency	40	Hz
Allowable product acceleration in		
horizontal direction	10	m/sec <sup>2</sup>
vertical direction	10	m/sec <sup>2</sup>

### 3.4 Fundamental Mechanism Design

Fundamental mechanism design was performed in three stages:

- Selection of manipulator structure
- Kinematic synthesis
- Kinematic analysis

First step in fundamental mechanical design phase was the construction of a reference trajectory for the intended pick and place operation. Taking into account the degrees of freedom of the manipulator in SPRS, a reference 2-D trajectory generator algorithm, presented in appendix A, was developed. Main consideration in trajectory generation was the smoothness of the motion since rough, jerky motions tend to increase wear on the mechanism and cause vibrations by exciting resonances of the mechanical structure. Linear interpolation method was used in reference

trajectory generation. However, in order to remove discontinuities, parabolic blend regions were added at the path points. During the blend portion of the trajectory, constant acceleration equal to the allowable product acceleration is used to change velocity smoothly. Figure 3.3 depicts the constructed reference trajectory of products in Cartesian space while figure 3.4 and 3.5 shows the position, velocity and acceleration profiles of products in x (horizontal) and y (vertical) directions.

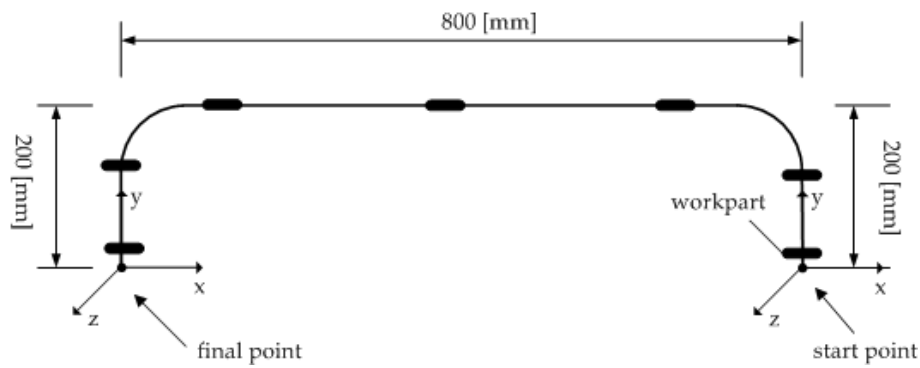


Figure 3.3 Reference trajectory of products in Cartesian space

### 3.4.1 Selection of Manipulator Structure

Particular structure of the manipulator strongly influences the kinematic and dynamic characteristics of the robot. Selection of the configuration was based on the sizing of the most important system components, evaluation of dynamic performance, mechanical simplicity, manufacturability and ease of control.

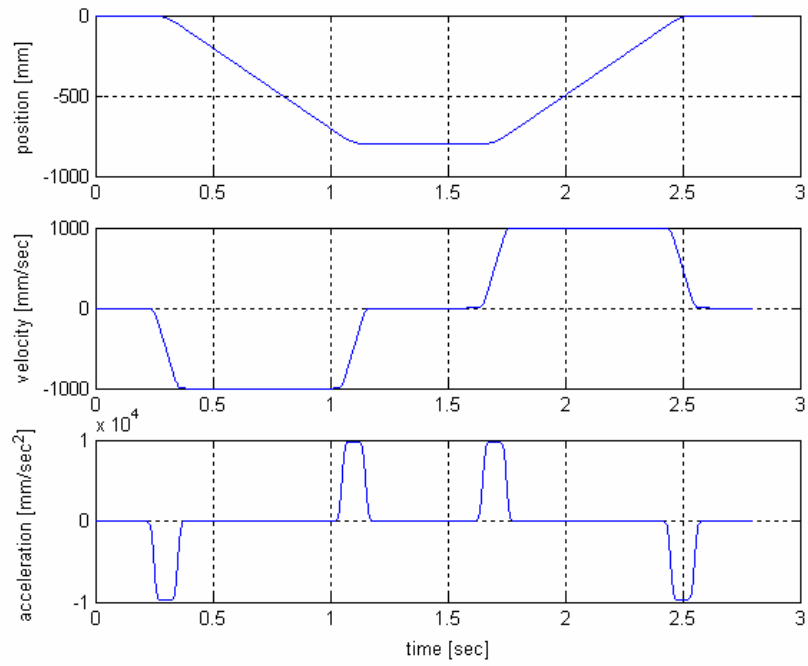


Figure 3.4 Trajectory of products in horizontal direction

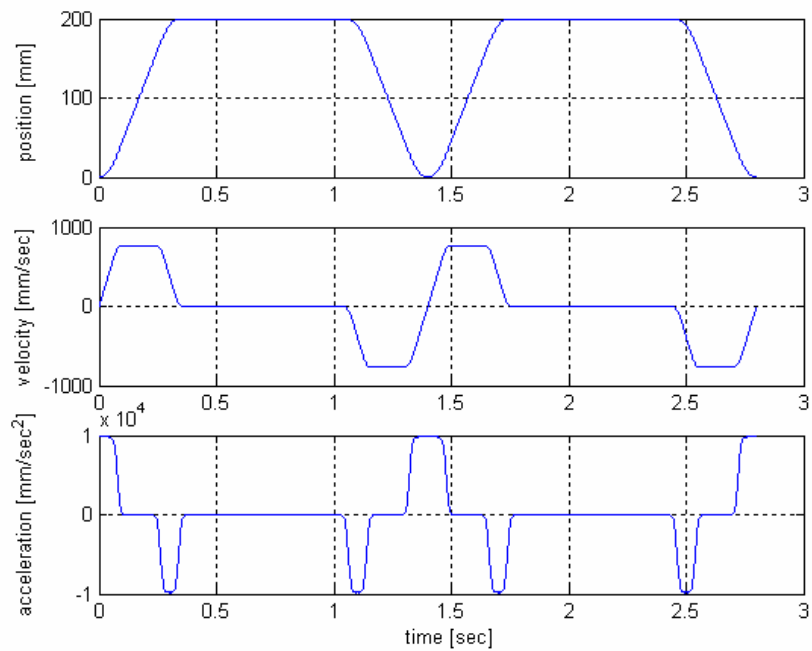


Figure 3.5 Trajectory of products in vertical direction

Most industrial manipulators designed so that the first 3 joints position the wrist point and the last 2 or 3 joints, having axes intersecting at the wrist point, orient the end-effector. Manipulators having this design can be divided into two structures; a positioning structure and an orientation structure. Since the orientation structures are out of scope of the current study, only positioning structures are investigated.

Although positioning structure of manipulators varies widely in configuration, there are mainly 5 categories; Cartesian, cylindrical, spherical, SCARA, and articulated arm manipulators. There are advantages and disadvantages for each category in precision, rigidity, speed, workspace, and ease of control.

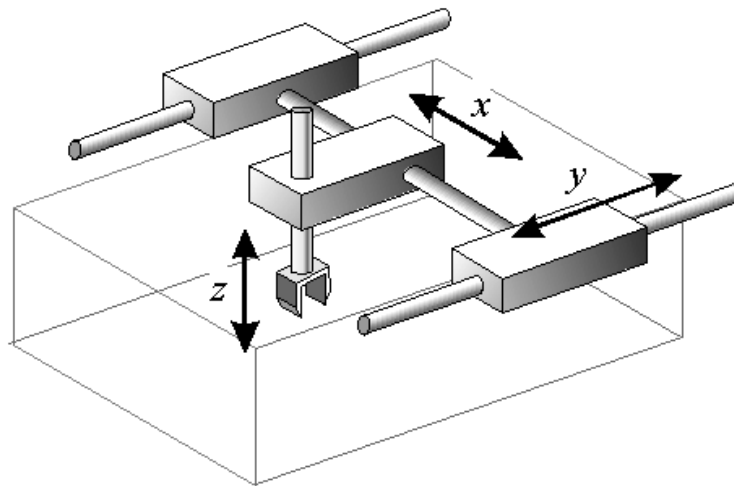


Figure 3.6 Kinematic structure of a Cartesian manipulator

Cartesian manipulators have the simplest kinematic configuration. The Cartesian geometry is composed of three prismatic, mutually orthogonal joints, as shown in the figure 3.6. Because of the orthogonality of joint axes, the inverse kinematic solution is trivial and does not produce any kinematic singularities in the workspace. Each

degree of freedom corresponds to that of the Cartesian space. Cartesian manipulators have the simplest transform and control solutions. Their prismatic orthogonal axes make it easy and quick to compute desired positions of the links for any gripper position. Because, their motion axes do not dynamically couple, their control equations are also simplified. They are also easy to control. Mechanical structure of this kinematic configuration provides very good stiffness.

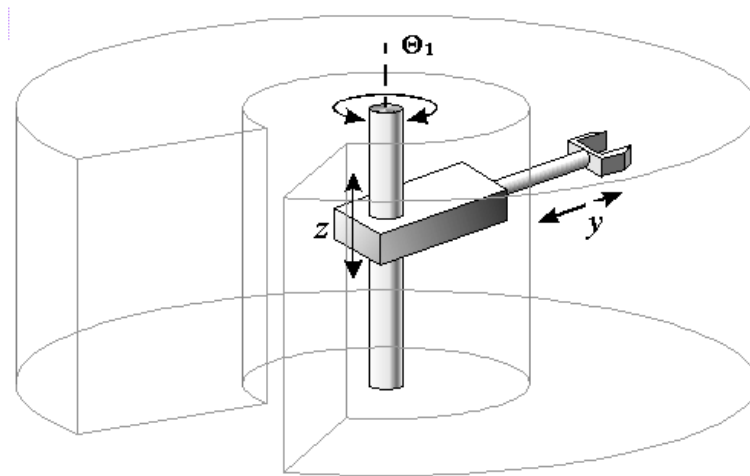


Figure 3.7 Kinematic structure of a cylindrical manipulator

Figure 3.7 shows the kinematic structure of cylindrical coordinate manipulators. They are constructed of a prismatic joint for translating the arm vertically, a revolute joint with a vertical axis and another prismatic joint orthogonal to the revolute joint axis. Cylindrical coordinate robots are best suited when the task to be executed or machines to be loaded/unloaded are located radially from the robot and no obstacles are present. Thanks to their unique kinematic configuration, cylindrical coordinate robots have good mechanical stiffness. Therefore they are mainly employed for carrying objects in gross dimensions.

A spherical manipulator differs from the cylindrical one in that the second prismatic joint is replaced with a revolute joint. The kinematic structure is shown in figure 3.8. Each degree of freedom corresponds to that of the task if the task is described in spherical coordinates. Mechanical stiffness is lower and mechanical construction is more complex compared to the previous kinematic configurations. Positioning accuracy is not uniform in the workspace and decreases as the radial stroke increases. The workspace is a portion of hollow sphere. Manipulators in this configuration are generally actuated by electrical actuators.

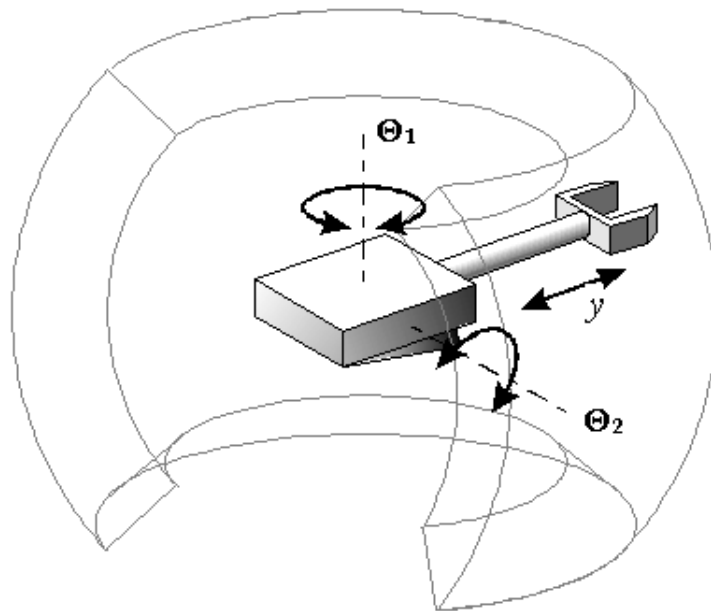


Figure 3.8 Kinematic structure of a spherical manipulator

The SCARA configuration, shown in figure 3.9, has two parallel revolute joints allowing it to move and orient in a plane and a prismatic joint moving the end-effector in vertical direction. The acronym SCARA stands for Selective Compliance Assembly Robot Arm.

The chief advantage of SCARA configuration is that the first two joints do not have to support the weight of the manipulator or payload. Thanks to its unique structure, actuators can be placed in base. This allows using very large actuators, so the robot can move very fast. The SCARA robots are generally employed in planar tasks.

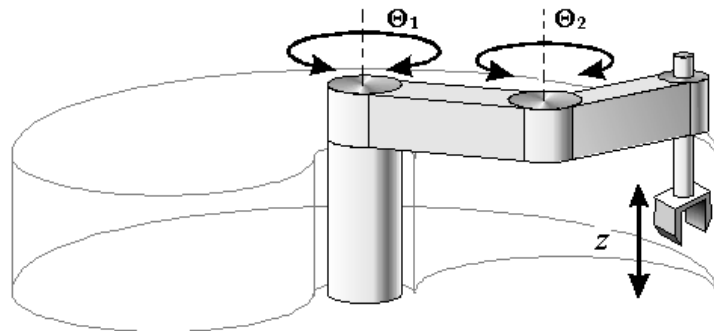


Figure 3.9 Kinematic structure of a SCARA manipulator

An articulated manipulator resembles human arm. Manipulators in this configuration consist of two shoulder joints and an elbow joint. While the first joint axis rotates about the vertical axis, the second joint elevates out of the horizontal plane. Third joint, whose axis is usually parallel to second joint, positions the wrist point of the manipulator. Axes are also called as pitch, yaw and roll. Figure 3.10 shows the kinematic structure.

Articulated manipulators generate large volume of workspace relative to their size. Positioning accuracies are low due to the cumulative effects of errors in each of the joints. Payload capacities are also limited. The main advantage of articulated manipulators is that they provide least intrusion of the manipulator into the workspace. In addition, less material is needed to build an articulated manipulator compared to other kinematic configurations, making them cheaper and economically justifiable. They are widely used in many industries for diverse purposes.

In this study, Cartesian and articulated manipulators were considered because of their suitability for intended pick and place operation. As a comparison, simple kinematic configuration, decoupled joint motions, high mechanical stiffness, and high positional accuracy are clear advantages of Cartesian manipulators. However, they are bulky structures, which is unsuitable for flow-line manufacturing systems like ETİ TUTKU manufacturing line. On the other hand, articulated manipulators generate larger volume of workspace than Cartesian manipulators relative to their size. In addition, less material is required to build an articulated manipulator than to build a Cartesian manipulator of similar workspace volume. This makes the articulated manipulator cheaper and economically justifiable. Relatively low positional accuracy due to the cumulative effects of errors in each of the joints and low payload are clear disadvantages of this type.

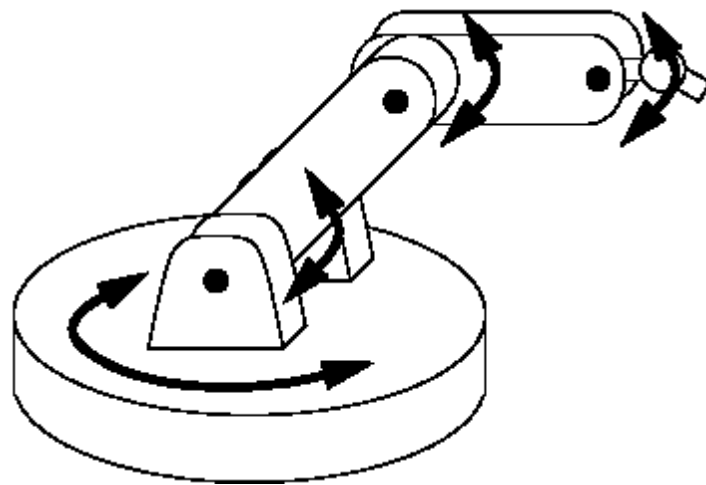


Figure 3.10 Kinematic structure of an articulated manipulator

Based on the above discussion and regarding the geometry of reference trajectory, articulated kinematic configuration seems most suitable for the project. Therefore, articulated manipulator configuration with two revolute joints, shown in figure 3.11,

was chosen. It was decided to mount the manipulator to a base structure which is perpendicular to the ground in order to save space on the factory floor. Link structures and joints are represented by lines and black dots respectively; while base structure is represented by a ground symbol in the figure.

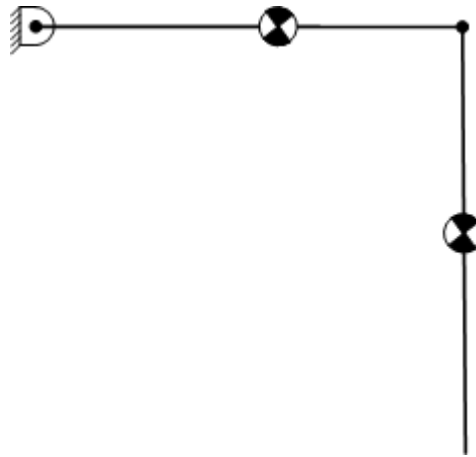


Figure 3.11 Selected kinematic configuration of the manipulator

### 3.4.2 Kinematic Synthesis

Actually, intended pick and place operation in a 2-D plane requires three degrees of freedom, two of which are for positioning and another one for orientation. However, a careful analysis of reference trajectory in figure 3.3 reveals that the orientation of the workpart does not change with respect to a non-moving frame such as a frame attached to ground. It means it remains its orientation during motion. However, selected kinematic configuration with 2 degrees of freedom is deficient for the intended task. So the kinematic configuration is modified by adding several light parallel links to keep the workpart orientation constant during the pick and place operation. Modified kinematic structure is shown in figure 3.12.

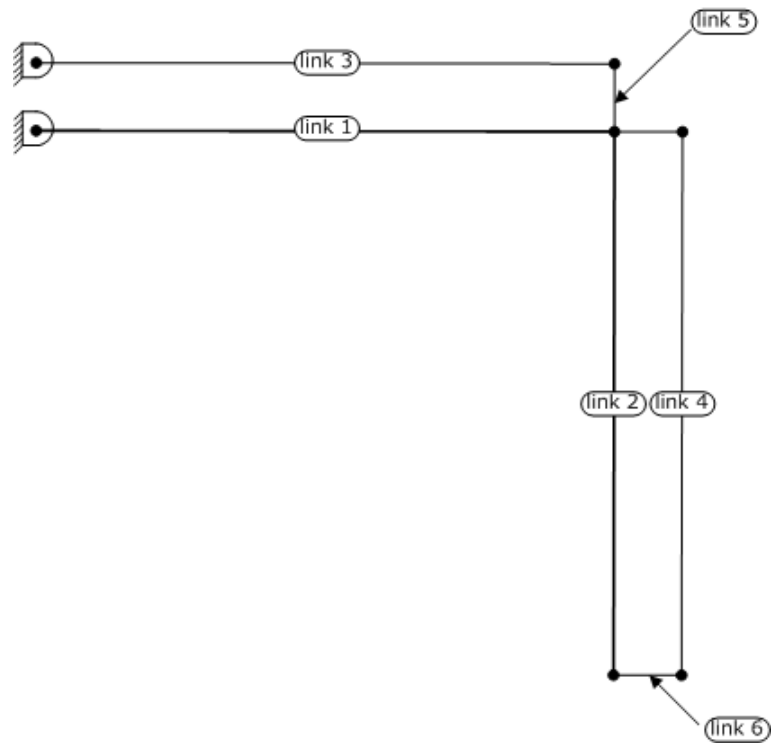


Figure 3.12 Modified manipulator kinematic structure

Following the determination of manipulator's kinematic configuration, arm lengths were determined based on required workspace for reference trajectory. They are shown in table 3.2. Dimensions of the single ternary link, link 7, is shown in figure 3.13.

Table 3.2 Arm lengths

Link numbers	Length [mm]
1	875
2	800
3	875
4	800
6	160

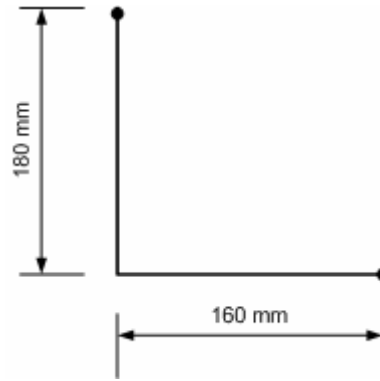


Figure 3.13 Dimensions of link 7

### 3.4.3 Kinematic Analysis

Kinematic analysis consists of four distinct analyses: forward kinematics, inverse kinematics, workspace analysis, and velocity/acceleration analysis. Forward kinematics computes the tip point position of the robot based on known joint angle set, while inverse kinematics is used to compute joint angles based on a given tip point position. Kinematics is usually performed at the position, velocity, and acceleration level. One way of computing the forward position solution is to formulate homogenous transformation matrices for each joint of a robot. These matrices can then be multiplied to get a description of the position and orientation of tip point of the manipulator. The homogenous transformation matrices for each joint can be formulated using the Denavit-Hartenberg (DH) parameters. More detailed descriptions can be found in standard books on robotics [4], [5], [6], [7], [8], [9], [10].

#### 3.4.3.1 Forward Kinematics Analysis

Forward kinematics analysis of the manipulator was performed in order to find the mapping between the joint displacements and the tip point position with respect to

base frame. Kinematic parameters were determined according to Denavit-Hartenberg convention and shown in figure 3.14.  $\theta$  and  $\alpha$  represents joint and actuator displacements respectively. The light parallel links was not shown in the figure for the sake of simplicity.

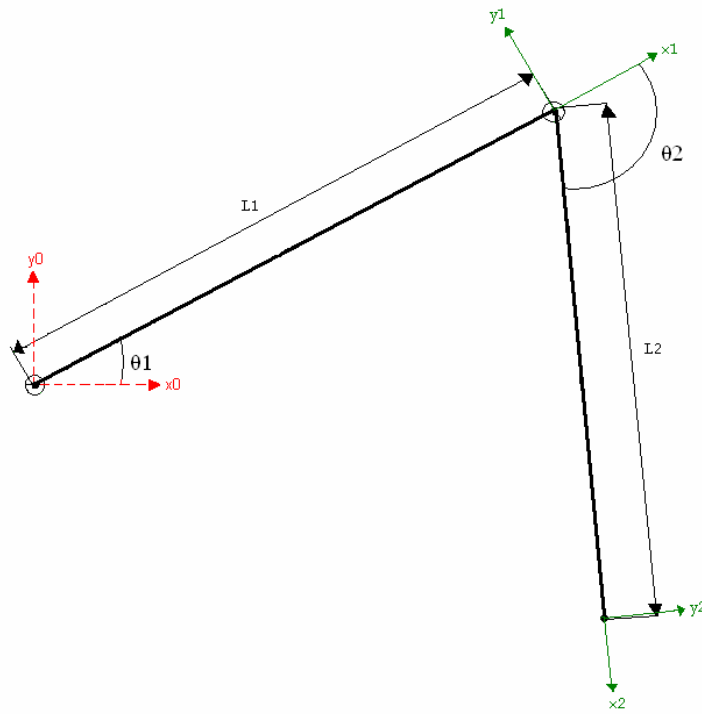


Figure 3.14 Kinematic parameters of the manipulator

Simplicity of the kinematic configuration allows writing the forward position of the tip point with respect to base frame directly as shown below.

$$\begin{bmatrix} P_x \\ P_y \end{bmatrix} = \begin{bmatrix} L_1 \cos(\theta_1) + L_2 \cos(\theta_1 + \theta_2) \\ L_1 \sin(\theta_1) + L_2 \sin(\theta_1 + \theta_2) \end{bmatrix}$$

where  $P_x$  and  $P_y$  denote the tip point position in x and y-direction.

### 3.4.3.2 Inverse Kinematics Analysis

While forward kinematics establishes the functional relationship between the joint space and Cartesian space, inverse kinematics concerns the determination of the joint variables corresponding to given tip point position. In reality, inverse kinematics equations are more important since the robot controller will calculate the joint values using these equations and move the robot to commanded position and orientation. Although there are numerous methods in the literature to find the inverse kinematics equations of a manipulator, relative simplicity of forward kinematics equations allowed inverting the equations by using standard algebraic methods. Inverse kinematic equations were found to be:

$$\begin{bmatrix} \theta_1 \\ \theta_2 \end{bmatrix} = \begin{bmatrix} \frac{\cos^{-1}(P_x^2 + P_y^2 - L_1^2 - L_2^2)}{2L_1L_2} \\ a \tan 2(P_y(L_1 + L_2 \cos \theta_2) - P_x L_2 \sin \theta_2), P_x(L_1 + L_2 \cos \theta_2) + P_y L_2 \sin \theta_2 \end{bmatrix}.$$

### 3.4.3.3 Workspace Analysis

The workspace, also sometimes called as work volume or work envelope, represents a portion of the space that the manipulator can access. The workspace of the manipulator was calculated based on the link lengths and joint limits. Calculation of the workspace was performed under the following joint motion limits:

$$\begin{aligned} -20^\circ &\leq \theta_1 \leq 30^\circ \\ -135^\circ &\leq \theta_2 \leq -45^\circ. \end{aligned}$$

### 3.4.3.4 Velocity and Acceleration Analysis

The Jacobian is a representation of the geometry of the elements of a mechanism in time. It allows the conversion of differential motions or velocities of individual joints

to differential motions or velocities of points of interest. It also relates the individual joint motion to overall mechanism motion. Manipulator Jacobian reveals the relationship between the joints velocities and accelerations and the tip point Cartesian velocities and accelerations as follows:

$$\begin{bmatrix} V_x \\ V_y \end{bmatrix} = \begin{bmatrix} Robot \\ Jacobian \end{bmatrix} \begin{bmatrix} \dot{\theta}_1 \\ \dot{\theta}_2 \end{bmatrix} \quad or \quad \bar{V}_p = \tilde{J} \bar{V}_\theta$$

where  $\bar{V}_p$  is the vector of Cartesian velocities, and  $\bar{V}_\theta$  is a vector of joint rates of the manipulator. In this study, manipulator's Jacobian was calculated by taking the derivatives of each forward kinematic equation with respect to all variables. The result is as follows:

$$J = \begin{bmatrix} \frac{\partial f_1}{\partial \theta_1} & \frac{\partial f_1}{\partial \theta_2} \\ \frac{\partial f_2}{\partial \theta_1} & \frac{\partial f_2}{\partial \theta_2} \end{bmatrix} \Rightarrow \begin{bmatrix} -L_1 \sin \theta_1 - L_2 \sin(\theta_1 + \theta_2) & -L_2 \sin(\theta_1 + \theta_2) \\ L_1 \cos \theta_1 + L_2 \cos(\theta_1 + \theta_2) & L_2 \cos(\theta_1 + \theta_2) \end{bmatrix} \begin{bmatrix} \dot{\theta}_1 \\ \dot{\theta}_2 \end{bmatrix}$$

where  $f_1$  and  $f_2$  denote forward kinematic equations. Velocity and acceleration of each joint for a given Cartesian trajectory were calculated by using following relations:

$$V_\theta = \tilde{J}^{-1} \bar{V}_p$$

$$\dot{V}_\theta = \dot{\tilde{J}}^{-1} \bar{V}_p + \tilde{J}^{-1} \dot{\bar{V}}_p.$$

### 3.4.4 Kinematics Evaluation

The workspace analysis demonstrated that the manipulator is capable of generating sufficient workspace volume with the determined arm lengths for the reference trajectory. Figure 3.15 shows the resulting workspace.

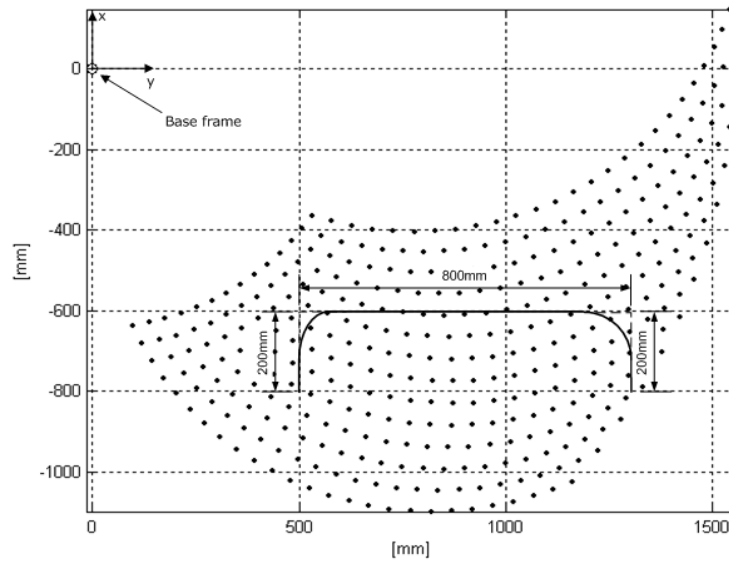


Figure 3.15 Manipulator workspace

The position, velocity and acceleration profiles of each joint for the reference trajectory were calculated based on manipulator Jacobian. Results are shown in figure 3.16 and 3.17. The analysis demonstrated that the joint 1 and 2 have the maximum angular velocity of 90 [deg/sec] and 50 [deg/sec] respectively. Maximum acceleration of joint 1 is 650 [deg/sec<sup>2</sup>] while that of joint 2 is 1100 [deg/sec<sup>2</sup>].

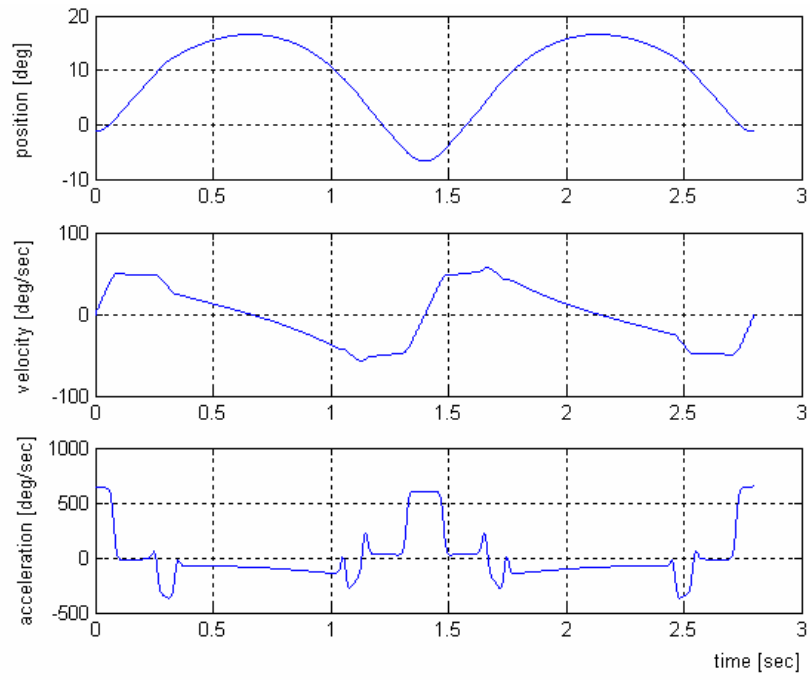


Figure 3.16 Position, velocity and acceleration profile of joint 1

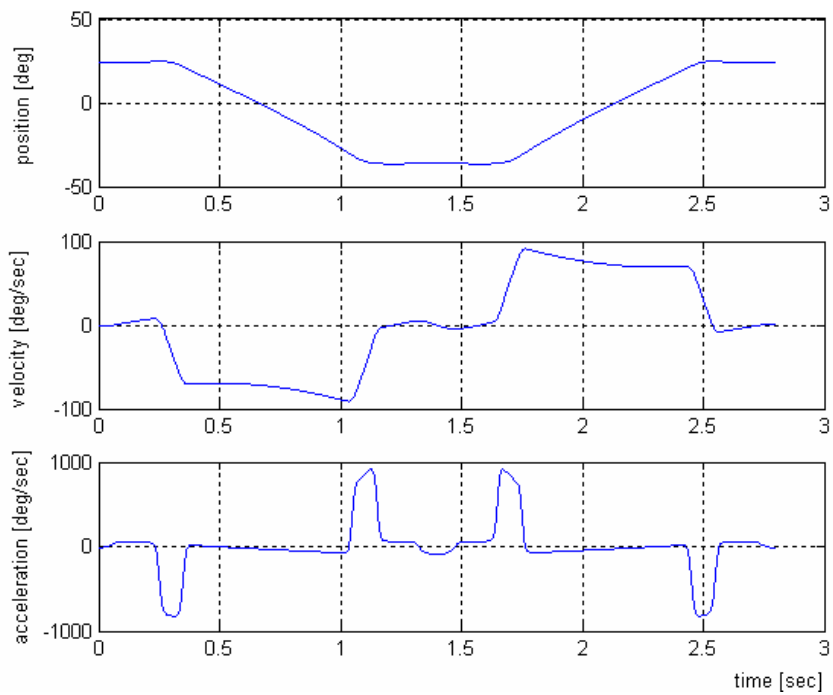


Figure 3.17 Position, velocity and acceleration profile of joint 2

### **3.5 Drive System Design**

Drive system design consists of determining the following design parameters:

- Motor allocations,
- Types of transmission system,
- Motors selection,
- Reduction units and their reduction ratio,
- Structural design of links and bearing arrangements.

In the first stage of the drive system design, following the determination of motor allocations and types of transmission systems, links' cross-sectional dimensions are calculated roughly. Then the motors and reduction units were selected from their catalogs temporarily, based on rough dynamic analysis. Finally the link structures are modified regarding the actuation system and bearing arrangements are determined.

#### **3.5.1 Motor Allocations and Transmission Systems**

Actuators of articulated manipulators with open-chain kinematic configuration are generally located at the corresponding joints and they exert torque between adjacent links. However, placing actuators on the base creates arm having better static and dynamic characteristics by reducing the total mass and inertia of the moving parts. On the other hand, this concept introduces the need for transmission mechanisms which connects actuators with the corresponding joints.

There are mainly three different articulated manipulators in terms of transmission systems, as shown in figure 3.18.

While joint manipulator is an open-linkage arm, parallelogram and Gopalswamy's manipulators are typically closed-linkage arms, which are becoming more and more often used because of their static and dynamic advantages over open-linkage arms. Closed-linkage configurations allow placing actuators on the base by adding extra links to transmit motion. The overall reduction in the total mass and inertia that can be achieved with these manipulators makes them very suitable specifically for tasks demanding high velocities and accelerations. On the other hand, more complicated design and higher manufacturing costs are clear disadvantages.

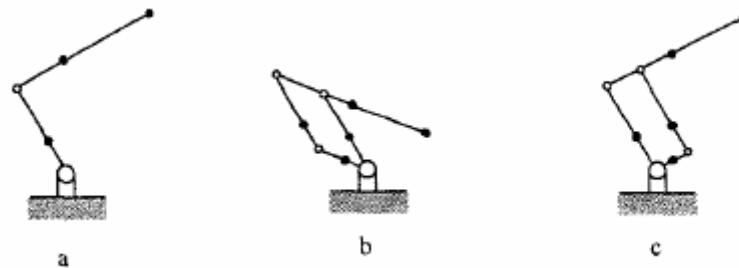


Figure 3.18 a) Joint manipulator b) Parallelogram manipulator c) Gopalswamy's manipulator

In addition to better static and dynamic performance, no Coriolis terms appear in the dynamic equations of parallelogram and Gopalswamy's manipulators. Absence of Coriolis terms improves further the dynamic behavior of the manipulator. For open-linkage manipulators all non-linear terms, i.e. Coriolis and centripetal forces, is present in the required actuator torque. The situation will be explained in greater detail in the mechanical modeling section of the following chapter.

For the current study, Gopalswamy's manipulator shown in figure 3.18c was chosen because it was found more suitable for the task. Gopalswamy's manipulator differs from classical parallelogram manipulator in a way that it allows counterbalancing the

gravity terms by using torsional springs [11]. Therefore, smaller actuators can be used. However, this situation was not handled for the current study and reserved for future studies. In addition, building a Gopalswamy's manipulator requires less material than building a parallelogram manipulator. This reduces the overall weight and operational cost of the robot.

Figure 3.19 shows the kinematic parameters of manipulator according to the Denavit-Hartenberg convention. In the figure,  $\alpha_i$  denotes i-th actuator position. Parallel links keeping the orientation of the products constant during the pick and place operation were not shown in the figure for the sake of simplicity.

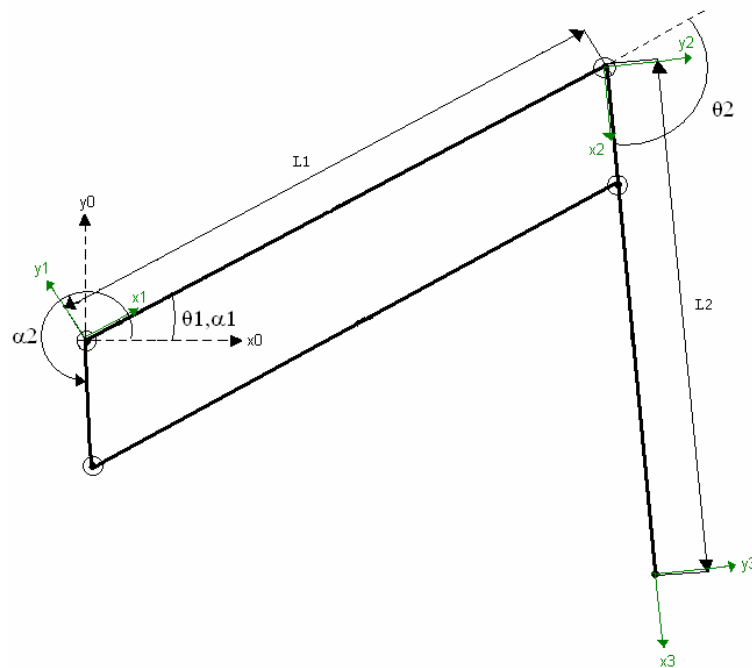


Figure 3.19 Kinematic parameters of the manipulator

Figure 3.20 depicts the manipulator final kinematic configuration and modified link numbers. According to final kinematic configuration, actuator 1 directly coupled to

link 1 while motion of the actuator 2 is transmitted to link 2 by means of transmission links, link 3 and 4. Table 3.3 lists final link lengths.

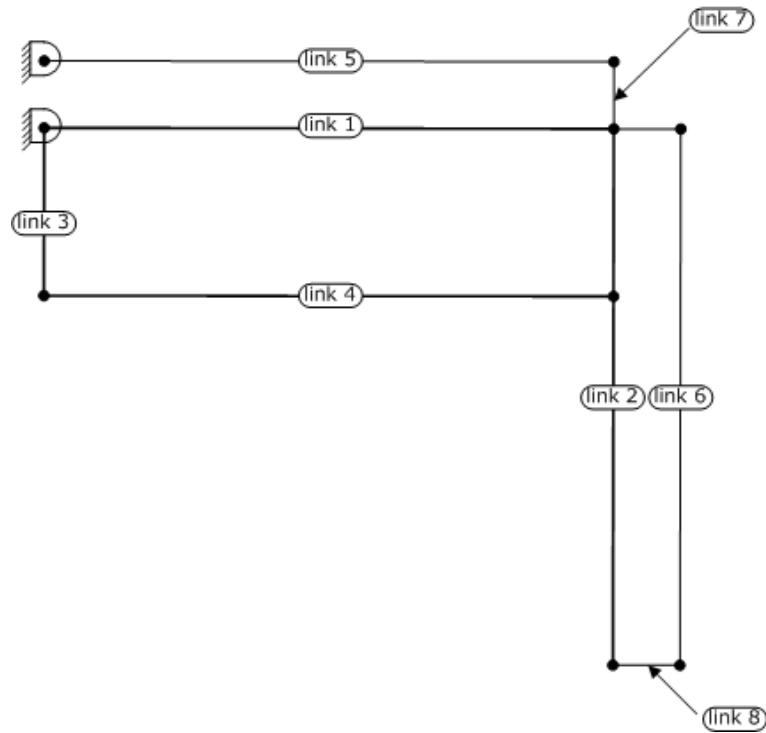


Figure 3.20 Final kinematic configuration of the manipulator

An adverse effect of placing actuators remotely from corresponding driven joints is that a motion coupling problem arises. It means that the torque applied by an actuator is not necessarily applied to one joint but affects several joints. Similarly, displacement of one actuator causes a displacement in more than one joint axis. Thus, it is necessary to study the effects of motion coupling. Simple trigonometry was used to find the relation between the displacements of joints and actuators as follows:

$$\theta_1 = \alpha_1$$

$$\theta_2 = \alpha_1 - \alpha_2.$$

In matrix form,

$$\begin{bmatrix} \theta_1 \\ \theta_2 \end{bmatrix} = \begin{bmatrix} 1 & 0 \\ 1 & -1 \end{bmatrix} \begin{bmatrix} \alpha_1 \\ \alpha_2 \end{bmatrix}.$$

Table 3.3 Final link lengths

Link numbers	Length [mm]
1	875
2	800
3	270
4	875
5	875
6	800
8	160

### 3.5.2 Design of Link Structures

After the determination of kinematic configuration, placement of actuators, and selection of proper transmission systems, structural design of links were performed based on strength and deflection requirements. Two common types of structures for manipulators are monocoque or shell structures and beam structures. Although the monocoque structures have lower weight or higher strength-to-weight ratios, they are more expensive and generally more difficult to manufacture. Cast, extruded, or machined hollow beam based structures are more cost effective although they are not

structurally efficient as pure monocoque structures. Taking into account of these points and available manufacturing facilities of ETİ Machinery Industry, main links of the manipulator was designed as I-beam structures.



Figure 3.21 Actual manipulator

Method of assembly was another important consideration in manufacturing. Distinct mechanical components were assembled by using bolted joints. Although bolted assembly is straightforward, inexpensive and easily maintained, there are associated problems including creep and hysteresis at the bolted connections and dimension changes resulting from assembly and disassembly. Therefore, number of bolted connections was tried to minimize to avoid these adverse effects.

Structural design of the manipulator was performed by utilizing computer aided design technologies. Utilization of computer aided design technology reduced the mechanical design period and increased the design quality of the manipulator. UNIGRAPHICS was used in the 3D modeling process. Figure 3.21 and 3.22 show actual view and 3D CAD model of the manipulator.

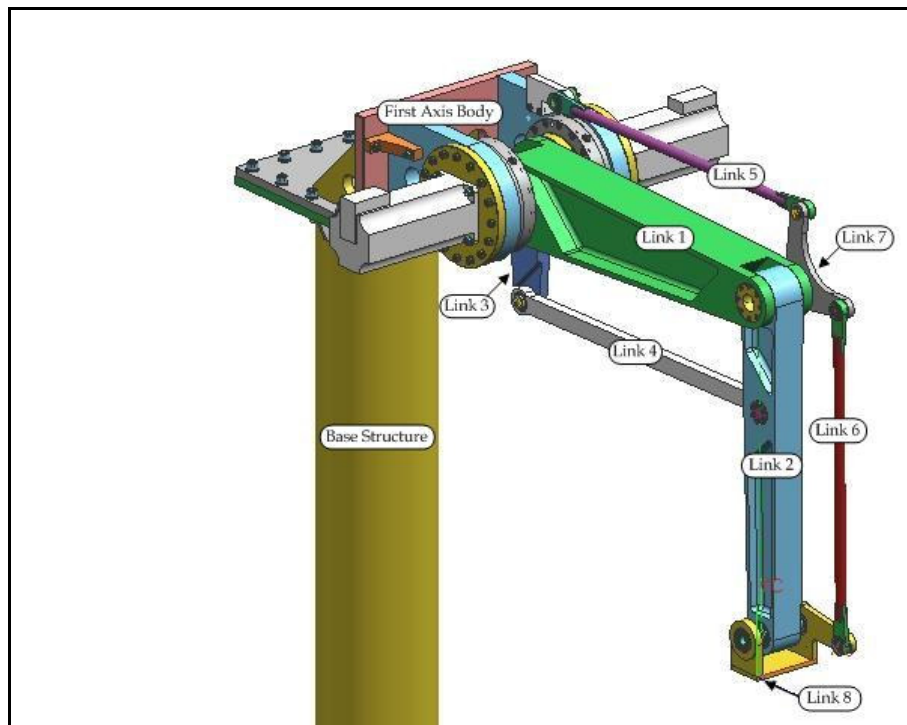


Figure 3.22 3D CAD model of the manipulator

The manipulator was anchored to ground by a base structure shown in figure 3.23. In order to obtain a stable operation, base structure should have enough strength to resist shaking forces and moments created by the manipulator during operation. In addition, the material of the base structure should have adequate level of damping capacity to eliminate mechanical vibrations. Regarding these requirements, the main body of the base structure was designed as a hollow cylinder made up of steel and having large wall thickness. Two flanges were welded to the top and bottom surface of the cylinder. The manipulator mounted on the upper flange and the base structure was rigidly attached to the ground by the lower flange using steel rods. Ribs were

utilized to increase the strength of the welded joints. Openings were added to the main body and the upper flange to pass the electrical and mechanical harness.

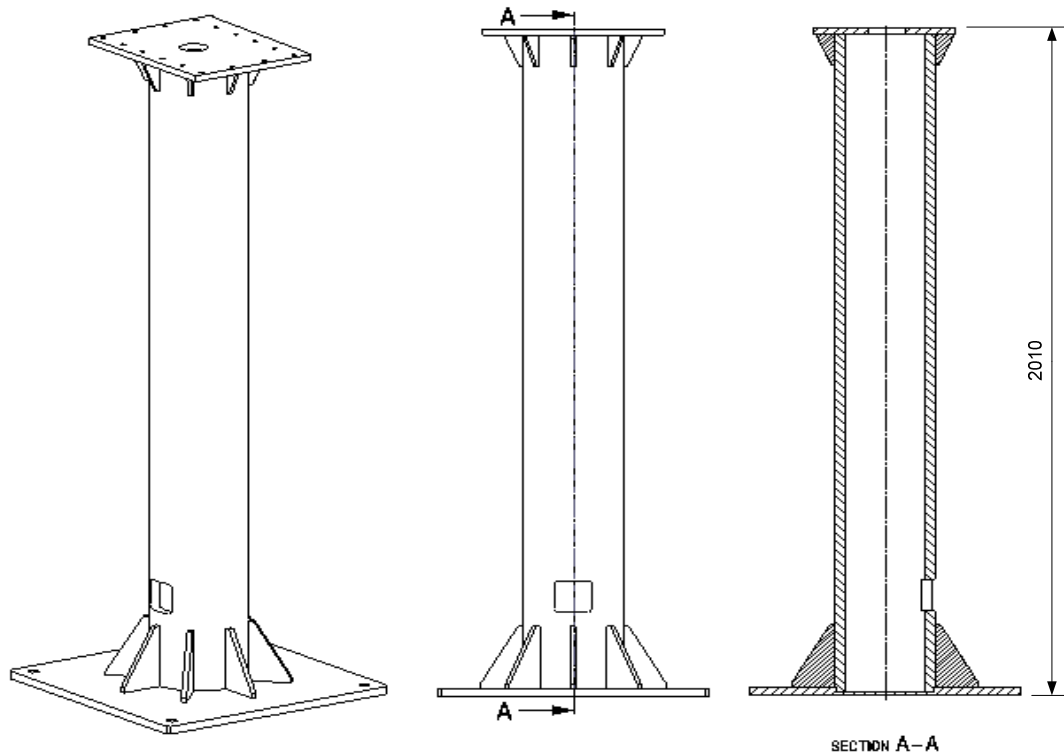


Figure 3.23 Base Structure

Drawing of the first joint body is shown in figure 3.24. First axis body houses both of motors, speed reducers and the first link. Considering the difficulties in the manufacturing and assembly process, it was designed in three distinct parts, one center part and two side panels. All parts are made up of steel. Actuators were mounted on the side panels. Each part was separately dimensioned regarding the required geometric tolerances between mating components. Side panels were mounted to the center part by using bolts. One fixing pin per each panel was used to compensate angular misalignments arising from the difference between the bolt and

hole diameters. Perpendicularity of side panels to center part was ensured by mounting precisely machined parts between them.

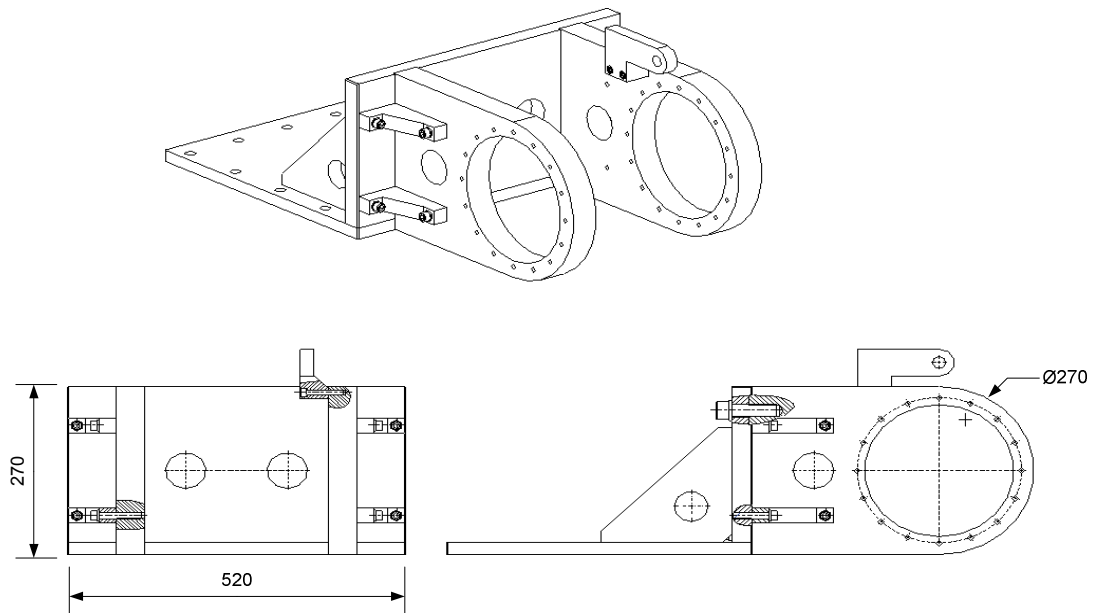


Figure 3.24 First axis body structure

Figure 3.25 shows the drawing of the first link. As stated previously, considering the loading condition and ease of manufacturing, link 1 was designed as an I-beam. It is made up of aluminum like other links to keep the weight of the moving parts minimum. Also, in order to decrease the weight further, gross dimensions were configured so the link becomes smaller at the end closer to the payload. Protrusions were created at both ends of the link. Protrusions at the lower side were used to mount the link on the first joint. They were designed in such a way that the first axis shaft and the bearing that supports the structure can be assembled easily. Actuator 1 is directly coupled to link 1 by using bolts. Bolt holes can be seen on the left lower protrusion.

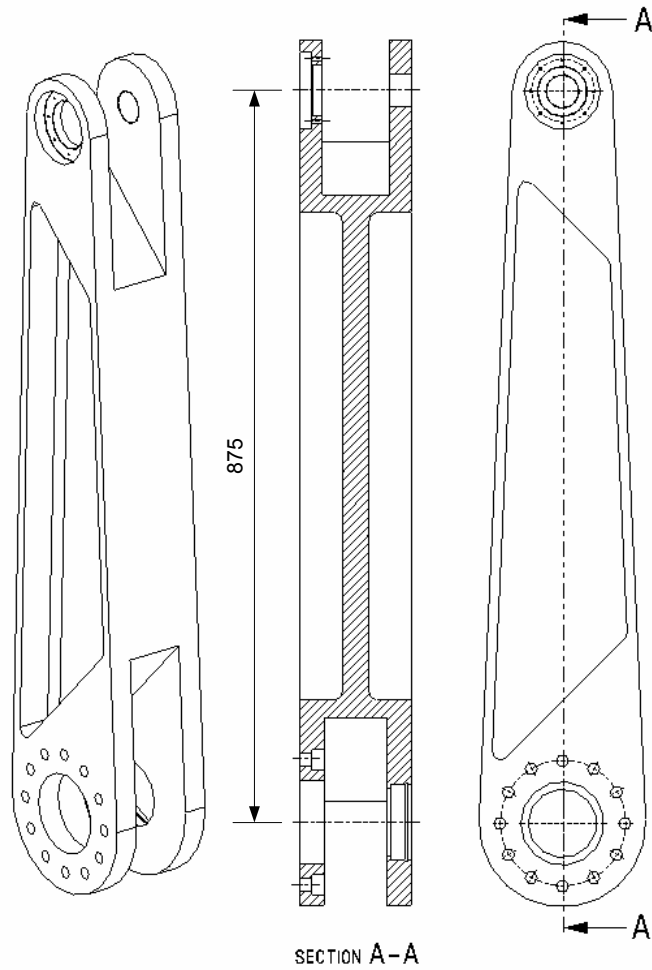


Figure 3.25 Link 1

Link 2 was also designed as a tapered beam like link 1. It was mounted to link 1 using the upper protrusions. Material was removed from the middle section in order to create necessary space for the joint between link 2 and link 4. As explained in previous sections, motion of the second actuator was transmitted to link 2 by using transmission links 3 and 4. Figure 3.26 shows the drawing of link 2.

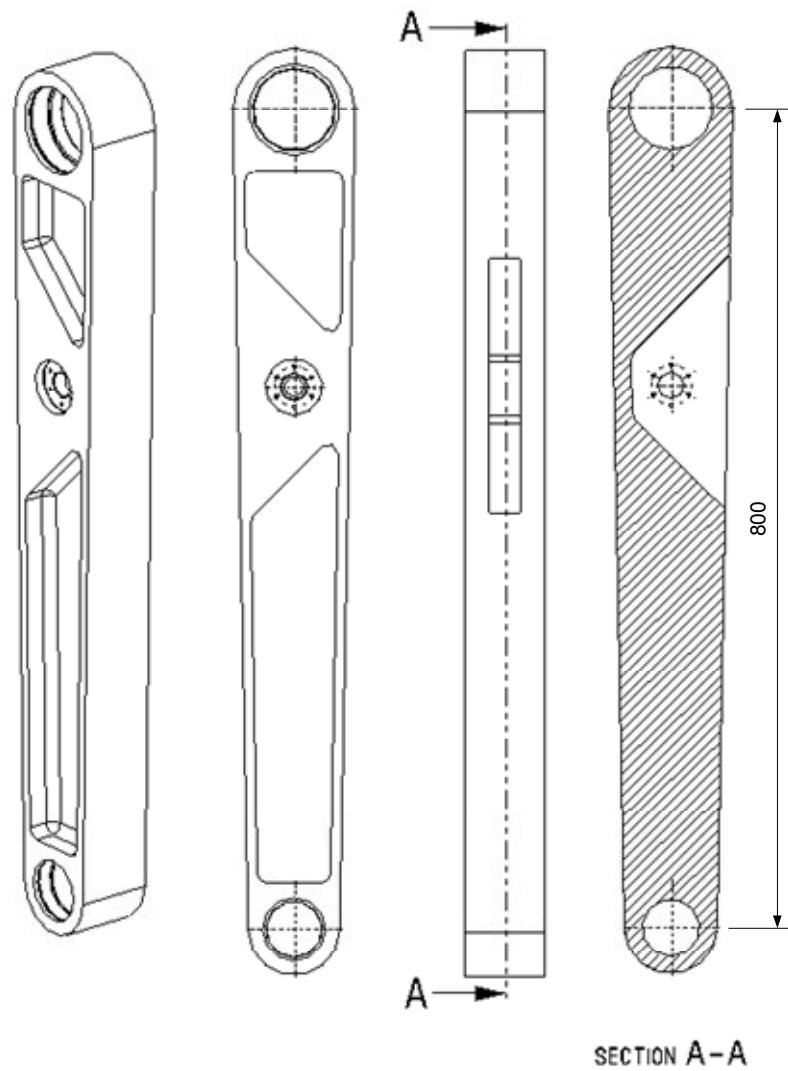


Figure 3.26 Link 2 structure

Link 3 is shown in figure 3.27. Material was removed from the lower part in order to prevent interference between the link 3 and 4. Link 3 is directly coupled to second actuator. It is connected to second actuator's shaft by using locking assembly. The concept will be further explained in the following sections about bearing arrangements.

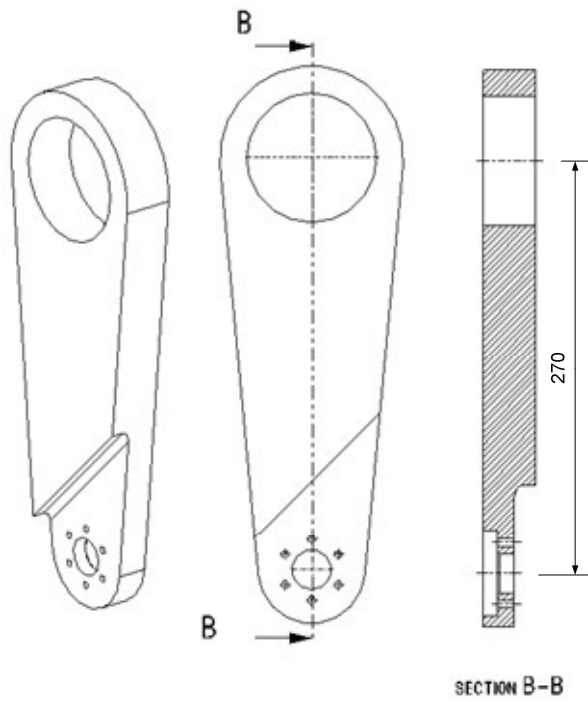


Figure 3.27 Link 3 structure

Link 4 is shown in figure 3.28. It is a binary link like link 3 and mounted between link 2 and link 3. Link 4 transmits the motion of link 3 to link 2.

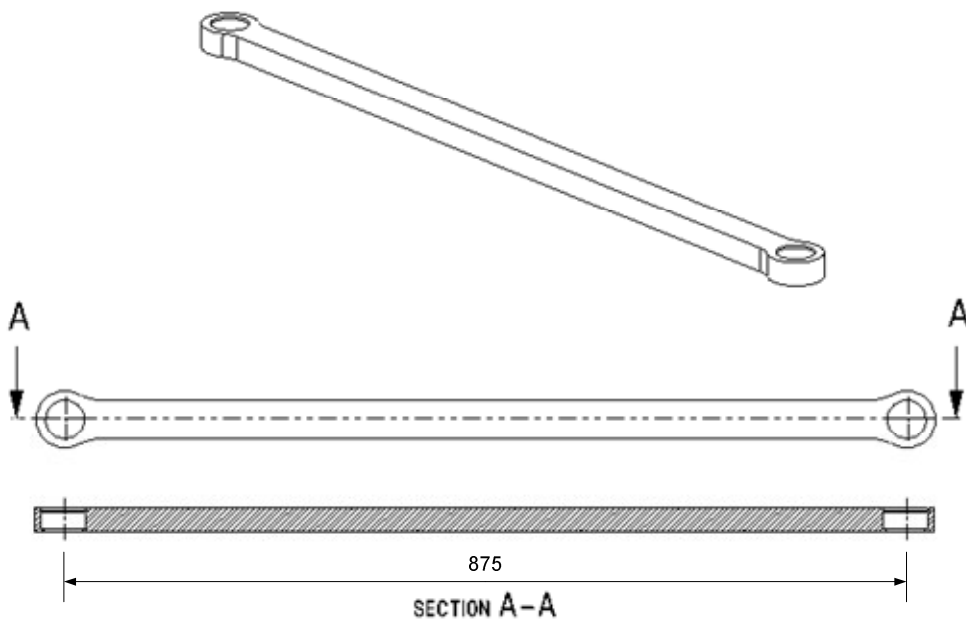


Figure 3.28 Link 4

Orientation of the workpart was ensured by links 5 and 6. Since only the reaction forces are acting on the links, they were designed as light structures. Hollow steel rods were used as the main body and two steel parts welded to the both ends in order to create place for bearings. Link 5 and 6 differ from each other only in dimension.

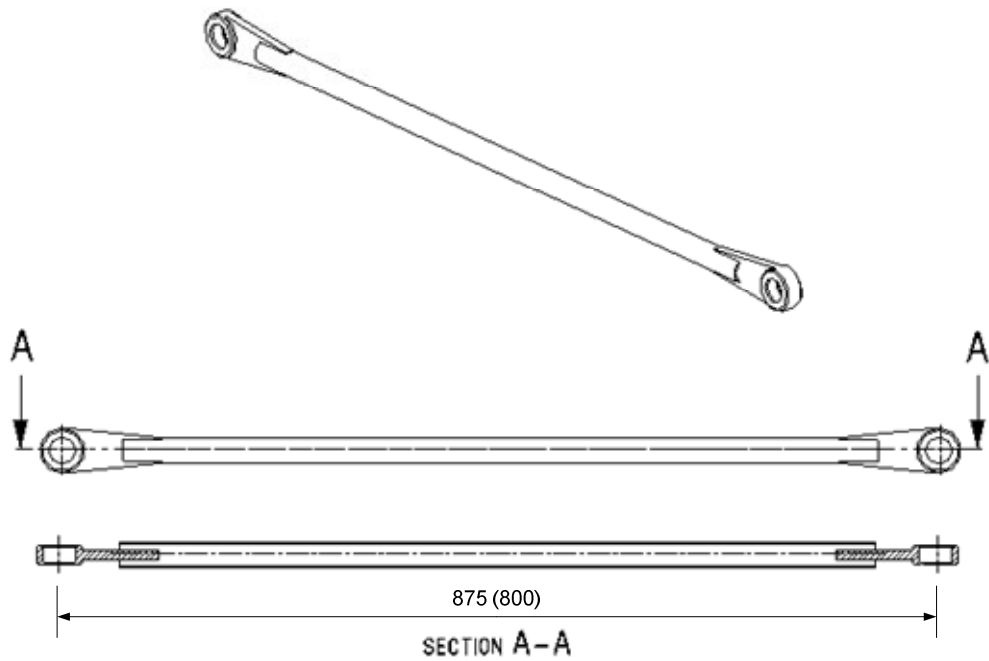


Figure 3.29 Links 5 and 6

Link 7 was designed as a ternary link to make mechanical connection between links 5 and 6. It is made up of aluminum. Figure 3.30 shows the drawing of link 7.

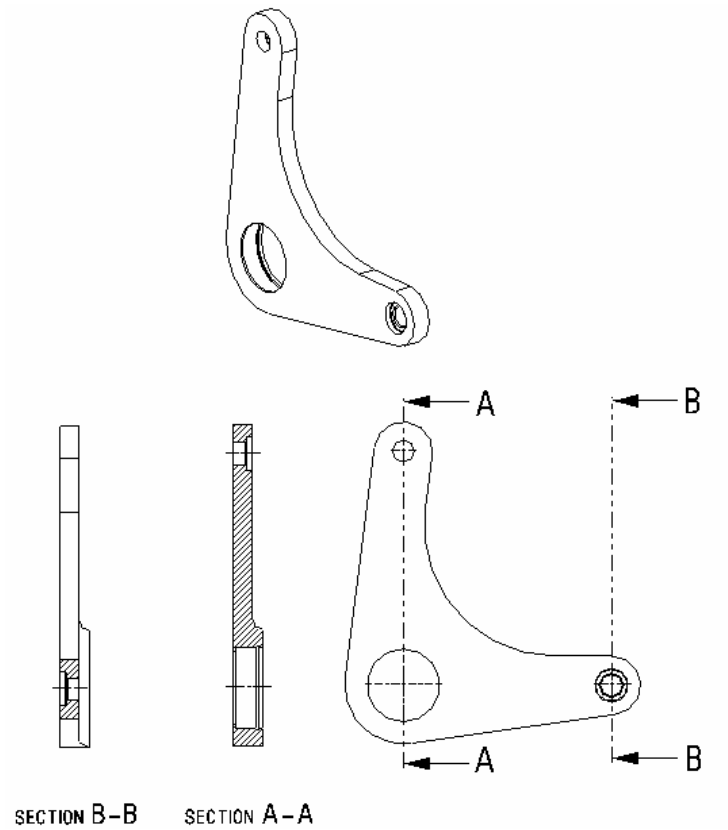


Figure 3.30 Link 7

Figure 3.31 shows the drawing of last link, link 8. It is a part of orientation links. Link 8 was mounted on the shaft that changes the orientation of the gripper system. Orientation of the gripper system is kept constant by constraining the motion of this shaft by links 5, 6, 7, and 8.

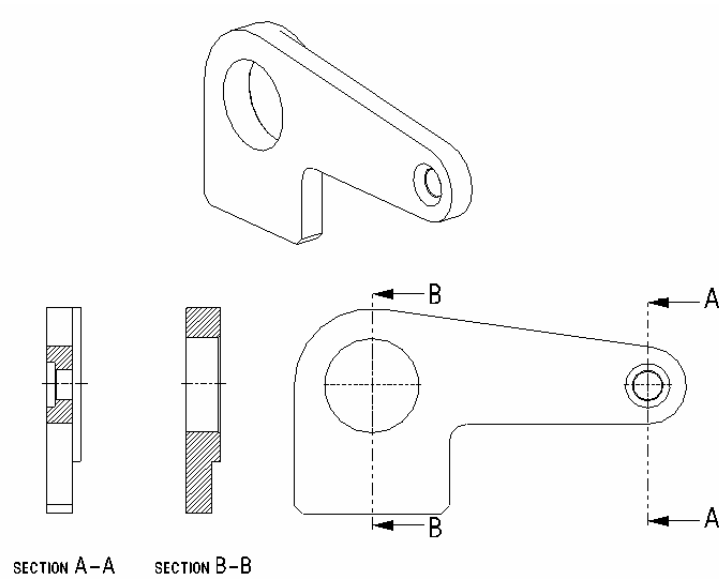


Figure 3.31 Link 8 structure

### 3.5.3 Materials Selection

Materials selection was based on the strength, weight, vibration characteristics, ease of manufacturing, and availability. In order to obtain a stable operation, structures near the base were selected such that they can create enough counter-balance for the moment loads that will be transmitted from the first axis body to the base structure.

For the linkages of the manipulator, the most important consideration was the weight, since they create additional load on the actuators. In addition, heavier structures end up with a reduced payload capacity. Taking into account these points, aluminum (Al 7075) was used for linkages. Depending on the strength and heat treatment requirements, different types of steel were used for other flanges, parts, shafts, retainers etc.

### **3.5.4 Bearings and Bearing Arrangements**

Control system of an industrial robot has very strong effect on the characteristics of its motion. However, no matter how good the control system is, required characteristics of motion can not be obtained if the manipulator does not have adequate precision. Precision in the design and manufacturing processes of the manipulator is needed in order to achieve high degree of control on the motion of the robot. Since the bearings and bearing arrangements play crucial role on the precision and characteristics of the robot, it is necessary to pay particular attention to bearings and bearing arrangements. There are several factors that should be taken into account when making selection of the bearings:

- Rigidity
- Torque
- Dimensions
- Precision

Rigidity is a measure of the bearing displacement under the influence of fluctuations in bearing load. For an industrial manipulator, fluctuations in bearing load may be caused by the weight of things being carried or changes in the posture of the manipulator.

The absolute value of the torque acting on the bearing is an important consideration. However, minimum variation is also desired because the alterations in torque make the control of the manipulator difficult. Regarding the dimensions of bearings, lightness and smallness are desirable features particularly when the bearings are used in moving parts.

Precision is also an important point in achieving high degree of control and positioning accuracy. Bearing housings was machined with extreme care because it is difficult, sometimes impossible, to obtain required level of precision by using purely housed bearings. Other aspects such as bearing life, tolerances on the shaft

and housing dimensions, the materials of the bearings, the structure of fittings, methods of lubrication, assembly and dismantling were also considered in bearing selection.

Environmental conditions affect the lubrication life considerably. Since the bearing performance and durability are strongly affected by lubricant properties, it is necessary to take these conditions into account.

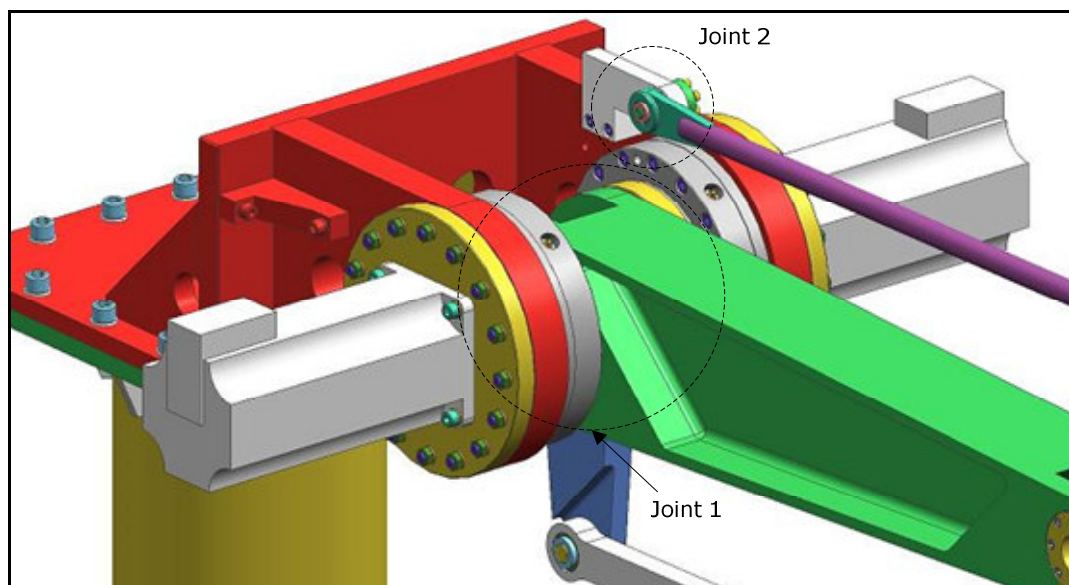


Figure 3.32 Joint 1, and 2

Taking into account the points mentioned above, using large and heavy bearings in moving parts of the manipulator was avoided because it increases the weight and inertia of the overall system and adversely affects the speed and positioning precision of the pick and place robotic arm. Selection of bearings type was performed based on size and type of the load acting on particular bearing. Bearing dimensions were selected according to required dimensions and space permitted. Environmental

conditions were also investigated since bearings used in special environments require special consideration with regard to materials, heat treatment, surface treatment, etc. It was also concluded that the environment in which the manipulator will function does not require special consideration. Cost and availability of the bearing were also thought in bearing selection.

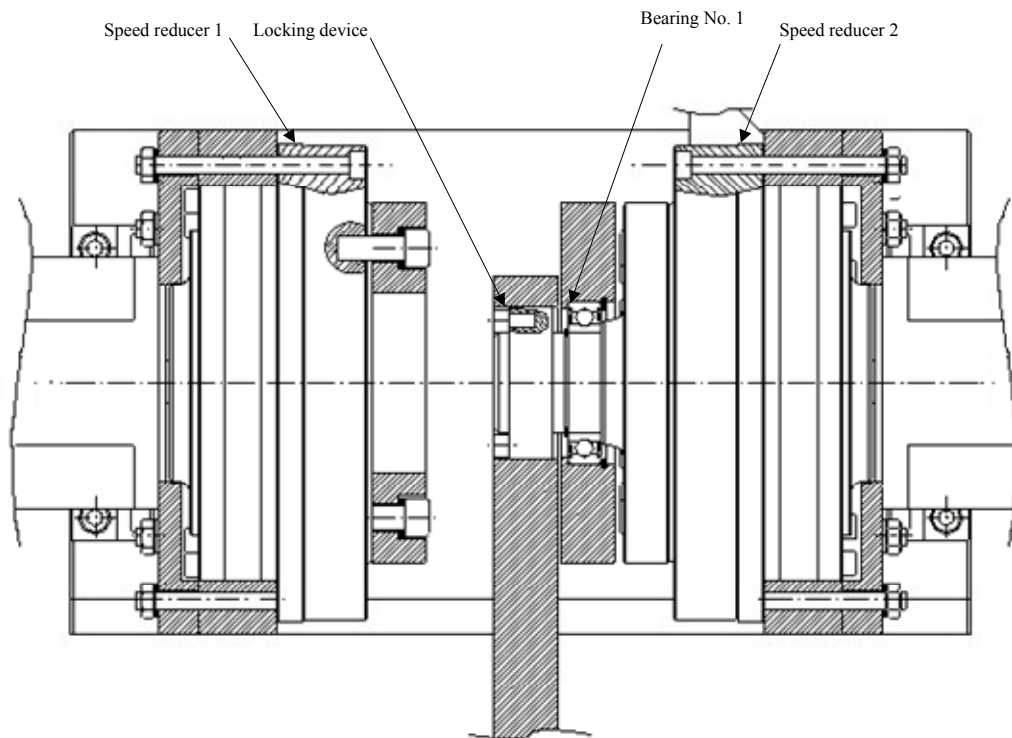


Figure 3.33 Joint 1 bearing arrangement

Joint 1 and 2 and corresponding bearing arrangements are shown in figure 3.32, 3.33 and 3.34. Joint 1 has particularly important bearing arrangement because it integrates the power train and link 1. Integration of the structure with power train hardware poses a strong design challenge. Positioning of bearings for transmission elements was extremely important since the deformation in the joint at the bearing housings could adversely affect precision by allowing backlash and free play.

As shown in the figure 3.33, link 1 was connected to speed reducer 1 by bolts. In order to transmit power link 1 securely, high strength steel bolts were used in the connection. Link 1 was also seated to the shaft driving link 3 to distribute the static and dynamic forces to both of the first joint body side panels. Taking loading conditions into consideration, single row deep groove ball bearing with contact seals on both sides was used in the joint. In addition to loading condition, this type of bearing was preferred because of its simplicity in design, and robustness in operation.

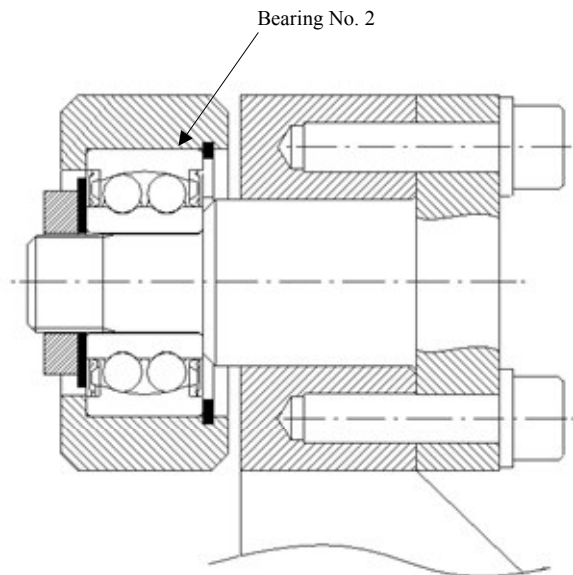


Figure 3.34 Joint 2 bearing arrangement

Locking device was used to transmit power to the link 3. Locking devices employs steel rings with opposing mating tapers held together with a series of fasteners. Initially there was a small clearance between the inside diameter of the locking device and the shaft as well as the hub bore. This clearance facilitated the assembly and positioning of the hub. After the hub was positioned on the shaft, the fasteners

were tightened by a torque wrench to a specified torque in a specific sequence. As the bolts were tightened, they pulled the opposing tapered rings together, generating a radial movement of the inner ring toward the shaft and simultaneous outward movement of the outer ring toward the hub. Once the initial clearance was eliminated, further tightening of the bolts resulted in a high pressure against the shaft and the hub. This pressure combined with friction allowed for the transmission of power from shaft to link 3.

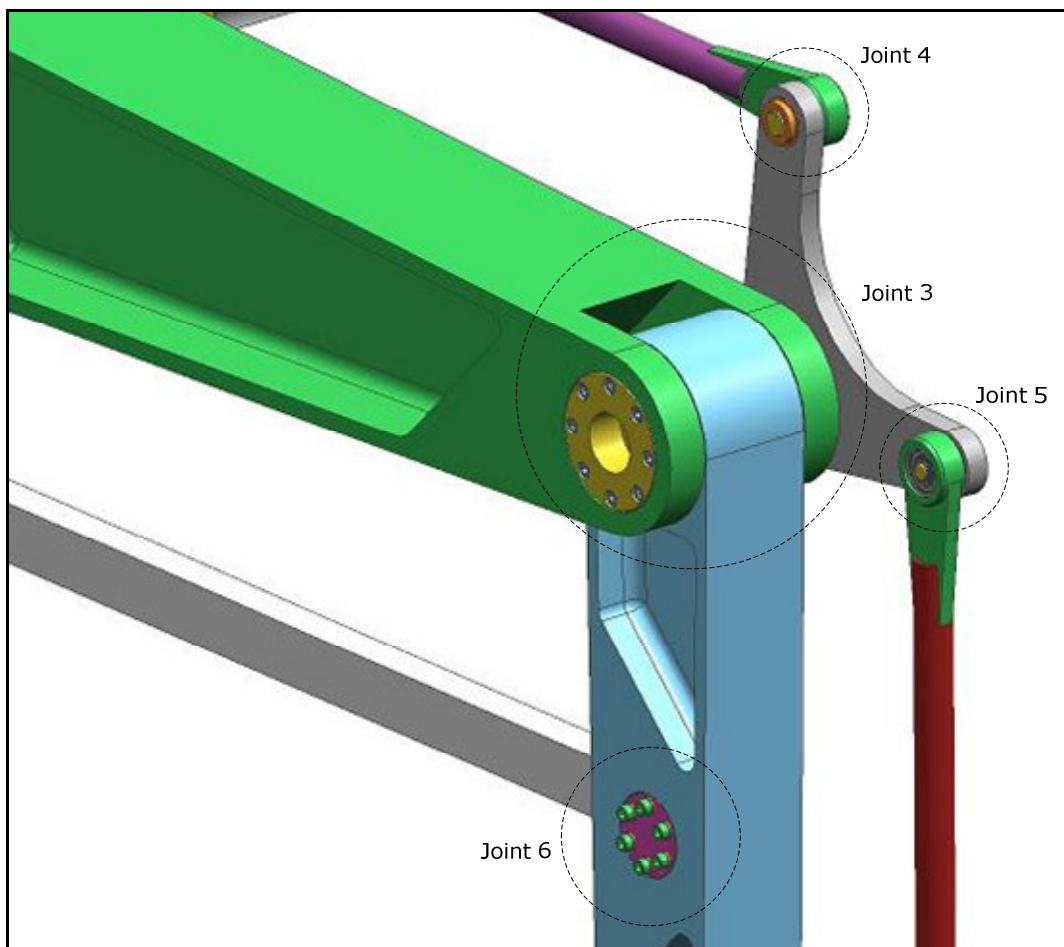


Figure 3.35 Joint 3, 4, 5, and 6

In joint 2, self-aligning ball bearing was used to compensate the angular misalignments caused by the manufacturing process of link 5. Self-aligning ball

bearings have two rows of balls and a common sphered raceway in the outer ring. The bearing is consequently self-aligning and insensitive two angular misalignments of the shaft relative to the housing.

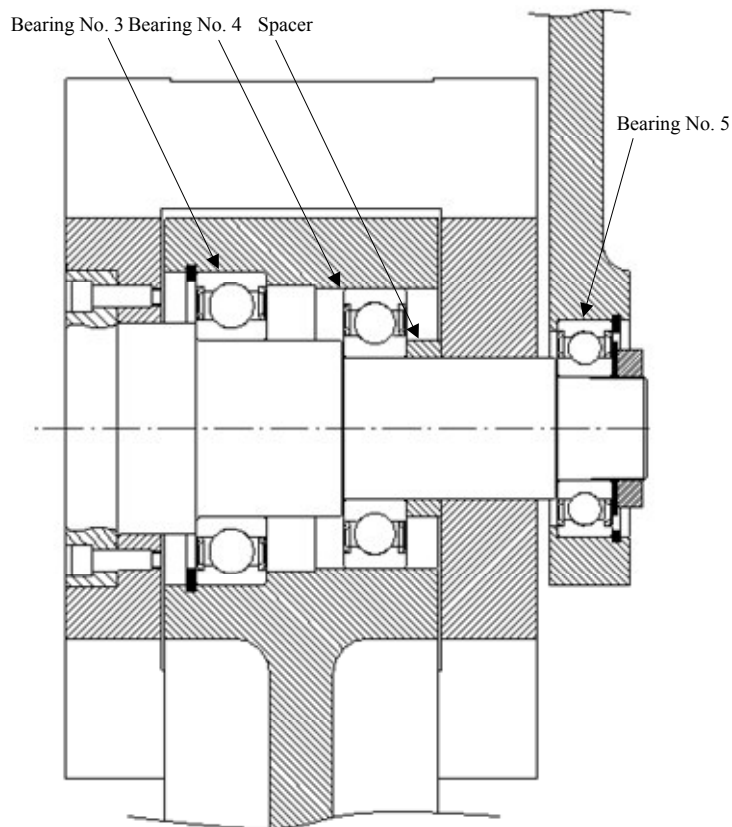


Figure 3.36 Joint 3 bearing arrangement

Location of the bearing was fixed with a locknut threaded at the end of the shaft. The internal tab on the lockwasher engaged the groove in the shaft, and one of the external tabs was bent into the groove on the nut after it was seated to keep the nut from backing off.

Joint 3,4,5,6 and corresponding bearing arrangements are depicted in figure 3.35, 3.36, 3.37, 3.38, 3.39, respectively. Shaft made up of steel was rigidly mounted to link 1 by bolts and Link 2, and 7 were mounted on this shaft, as shown in figure 3.35. Single row deep groove ball bearings were mounted on the shaft in order to provide rotational degrees of freedom between links. Axial movement of link 2 and 4 along the shaft axes was prevented by locating spacers on the shaft against the bearings. Locknut and lockwasher was used to fix the location of link 7.

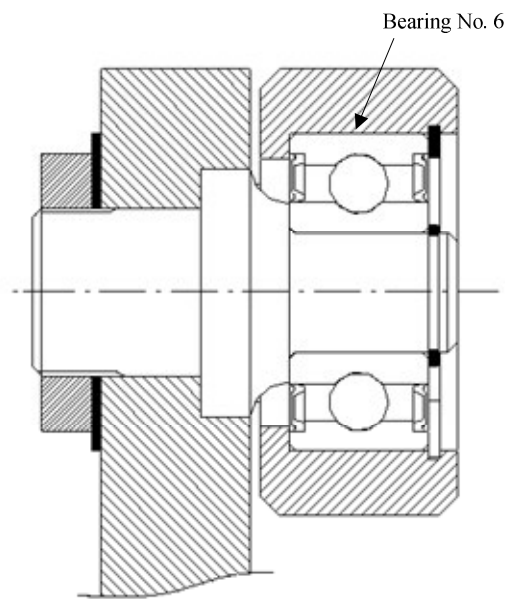


Figure 3.37 Joint 4 bearing arrangement

One practical consideration in the matter of axial location of ball bearings mounted on link 2 was that these machine elements should not have been overconstrained. Under certain conditions of differential thermal expansion or because of the manufacturing errors, bearings would be forced together so tightly causing dangerous axial stresses. This situation was prevented by locating only one bearing positively on the shaft and permitting the outer race of the other bearing to float slightly in the axial direction.

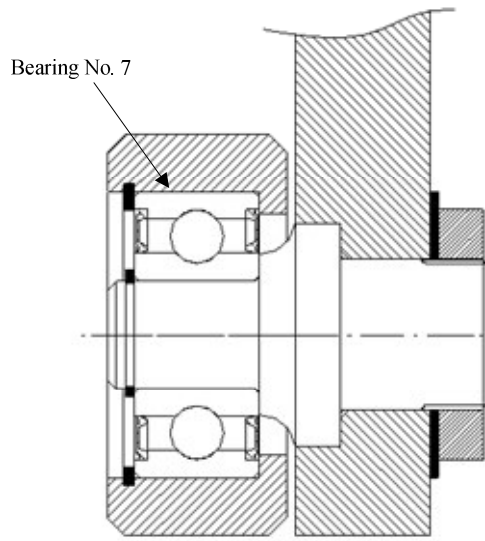


Figure 3.38 Joint 5 bearing arrangement

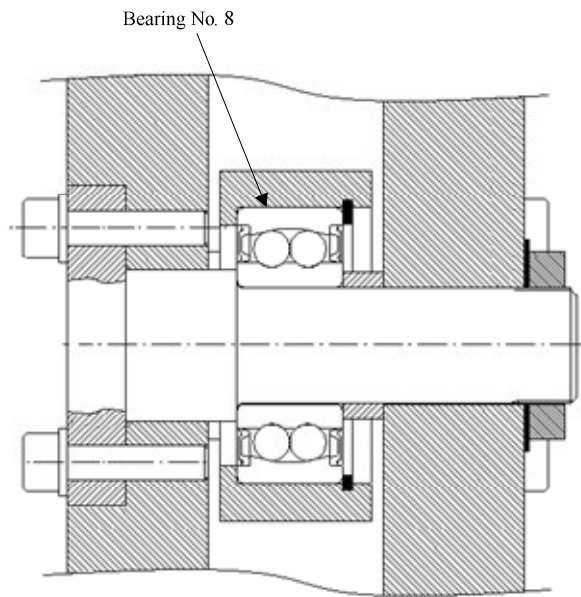


Figure 3.39 Joint 6 bearing arrangement

Figure 3.40 and 3.41 shows joint 7 and its bearing arrangements, respectively. In joint 7, location of the bearing was fixed with a locknut threaded at the end of the shaft like in joint 2.

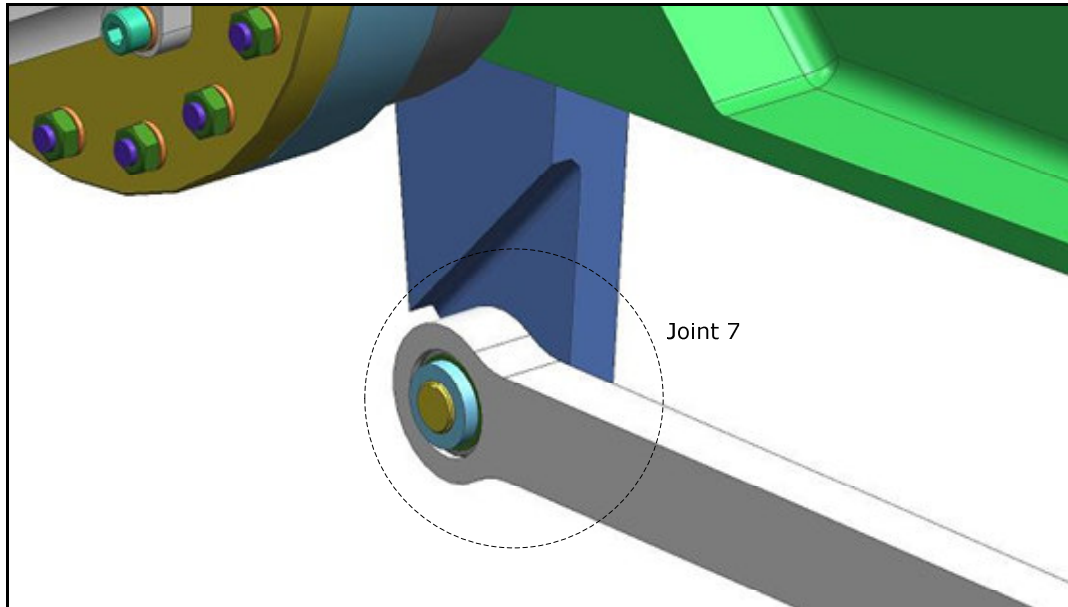


Figure 3.40 Joint 7

Figure 3.42, 3.43, and 3.44 shows joint 8, 9 and corresponding bearing arrangements. In joint 8, locking device was used to transmit the motion of the shaft to link 8. Similar to joint 3, bearings were not overconstraint by locating only one bearing positively on the shaft and permitting the outer race of the other bearing to float slightly in the axial direction.

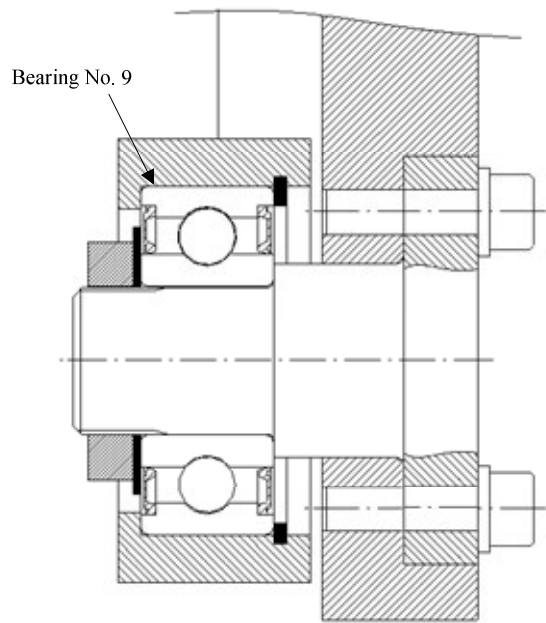


Figure 3.41 Joint 7 bearing arrangement

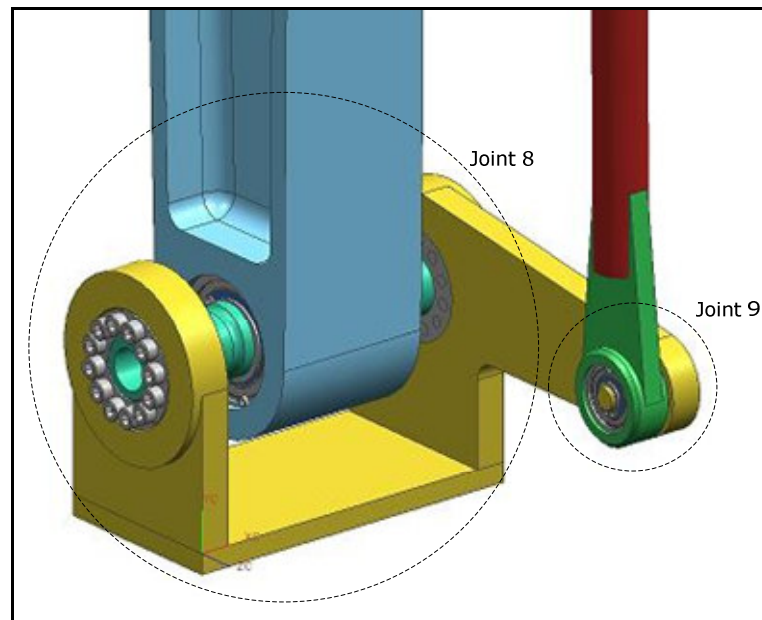


Figure 3.41 Joint 8, and 9

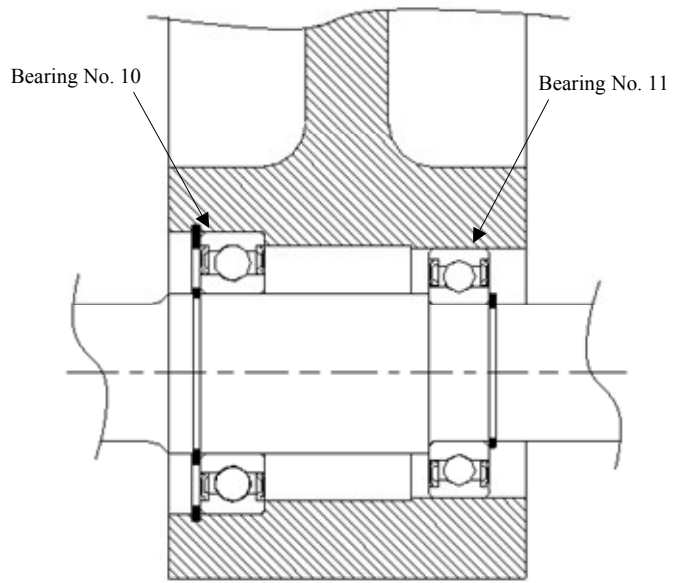


Figure 3.44 Joint 8 bearing arrangement

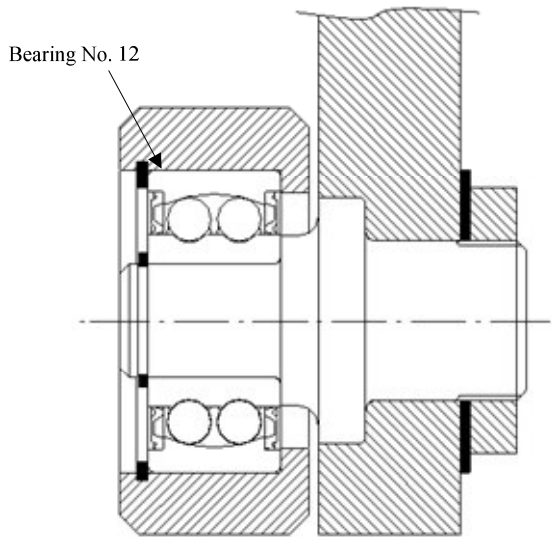


Figure 3.45 Joint 9 bearing arrangement

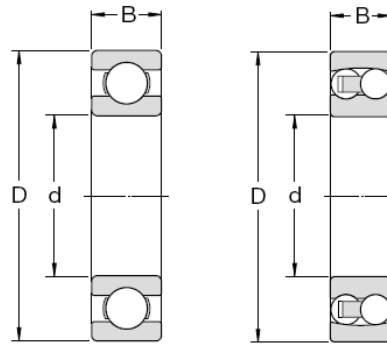


Figure 3.46 Cross-sectional views of ball bearings

Table 3.4 Bearings specifications

Bearing number	Principal Dimensions			Basic load ratings		Mass	Bearing Designation
	d	D	B	Dynamic, C	Static, C <sub>0</sub>		
	mm			kN		kg	-
1	55	90	18	29.60	21.20	0.39	6011
2 (S.A.)	12	32	14	8.52	1.90	0.05	2201
3	50	90	20	37.10	23.20	0.46	6210
4	40	80	18	35.80	20.80	0.34	6208
5	30	62	16	20.30	11.20	0.20	6206
6	12	32	10	7.28	3.10	0.06	6201
7	12	32	10	7.28	3.10	0.06	6201
8 (S.A.)	20	47	18	16.80	4.15	0.14	2204
9	20	47	14	13.50	6.55	0.11	6204
10	35	62	14	16.80	10.10	0.16	6007
11	30	55	13	13.80	8.30	0.12	6006
12(S.A.)	12	32	14	8.52	1.9	0.05	2201

Both deep groove ball bearings and self-aligning ball bearings were selected from SKF bearing catalogue. Figure 3.46 depicts cross-sectional views of the bearings while table 3.4 includes basic dimensions and technical specifications of the bearings used in the manipulator.

### 3.5.5 Dynamic Analysis

The aim of kinematic synthesis was to determine the kinematic configuration that allows following the desired position, velocity and acceleration profiles, without regarding the forces and torques causing motion. However, Mechanical design of the manipulator has to be performed by taking the static and dynamic loading conditions into account. Actuators and speed reducers should be selected in such a way that they can deliver required power to the system. Therefore, it is important to predict and understand the dynamic behavior of the system.

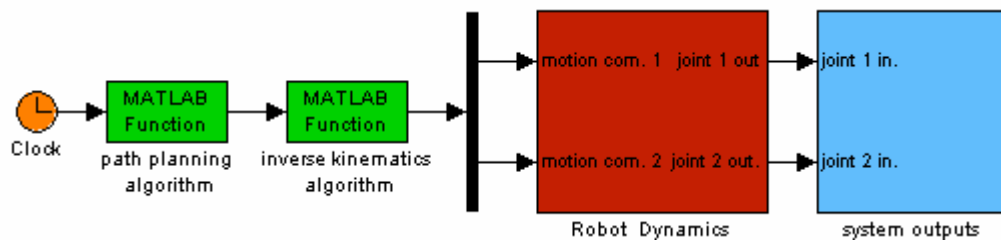


Figure 3.47 Dynamic analysis block diagram

Figure 3.47 shows the block diagram of dynamic simulation. In this block diagram, path planning algorithm, presented in appendix A, accepts the time signal and generates the reference trajectory in Cartesian space. The reference trajectory and corresponding kinematic attributes are shown in figure 3.3, 3.4, and 3.5. Then, the inverse kinematic algorithm accepts the reference trajectory in Cartesian space and converts it to joint space of the manipulator. Finally, the equations governing the

motion of the mechanical system are solved in robot dynamics block and the outputs are written to system outputs.

Dynamics of the manipulator was modeled by using MATLAB/Simulink together with SimMechanics blockset. SimMechanics is a blockset that extends the capabilities of MATLAB/Simulink with tools for modeling and simulating mechanical systems. SimMechanics is a set of block libraries and special simulation features for use in the Simulink environment. Mechanical systems consisting of any number of rigid bodies, connected by joints representing translational or rotational degrees of freedom can be modeled by the blocks in these libraries. Figure 3.49 shows the resulting physical model of the manipulator by using SimMechanics blockset.

There were three main steps in building the dynamic model of the manipulator:

- Inertial parameters, degrees of freedom, and constraints, along with coordinate systems attached to bodies to measure desired kinematic or dynamic parameters were specified.
- Actuators and sensors were placed in order to actuate the driven joints and record the resulting motion.
- Dynamic simulation was performed by calling the Simulink Runge-Kutta differential equation solver.

Linkages were specified by their masses and inertia tensors using “body” block in “Bodies” library of SimMechanics, shown in figure 3.48. Actuating and sensing are performed by specifying local coordinate frames on the mechanical bodies.

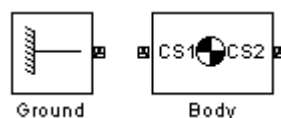


Figure 3.48 SimMechanics “Bodies” library

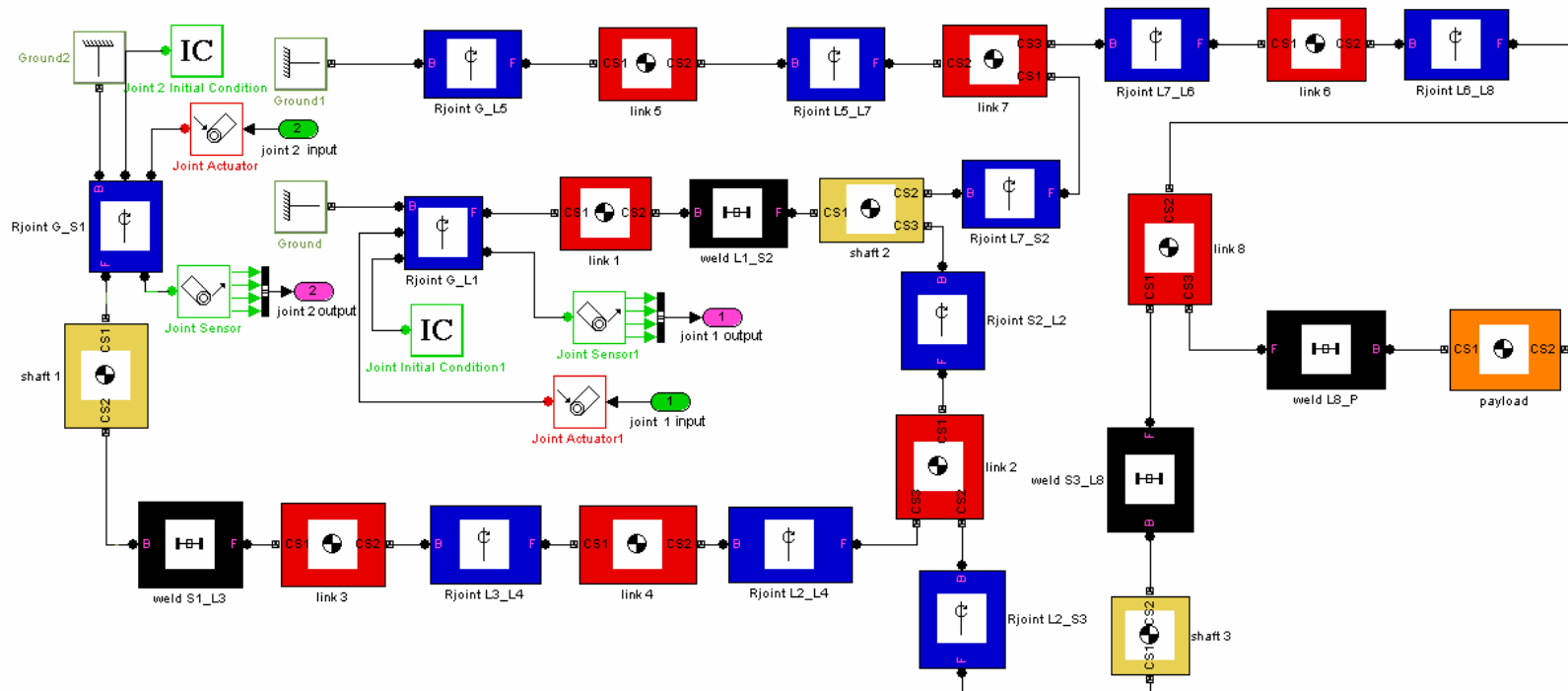


Figure 3.49 Physical modeling of the manipulator using SimMechanics

Blocks in “Joints” library, shown in figure 3.50, were used to make connections between bodies. Joints represent the possible motions of linkages of the manipulator relative to each another.

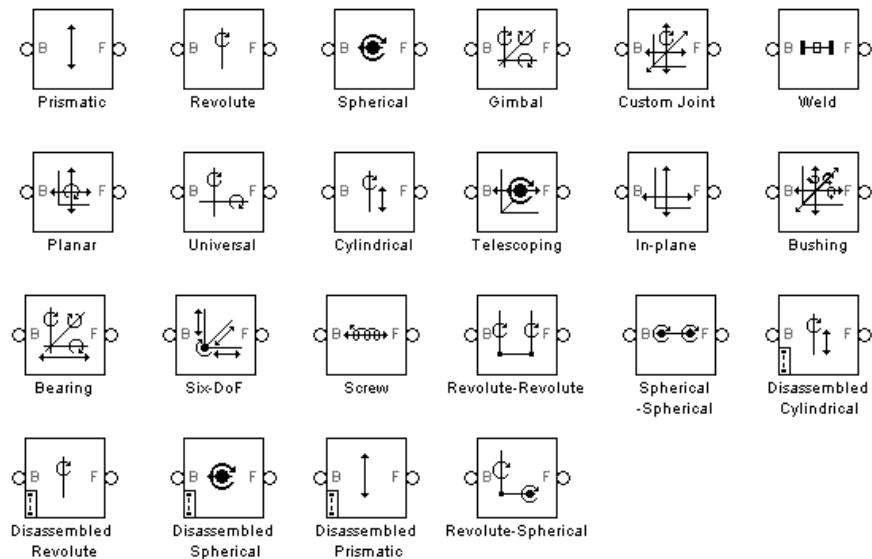


Figure 3.50 SimMechanics “Joints” library

In order to interface non-SimMechanics Simulink blocks in other subsystems of system simulation and SimMechanics blocks “Sensors & Actuators” library, shown in figure 3.51, were used.

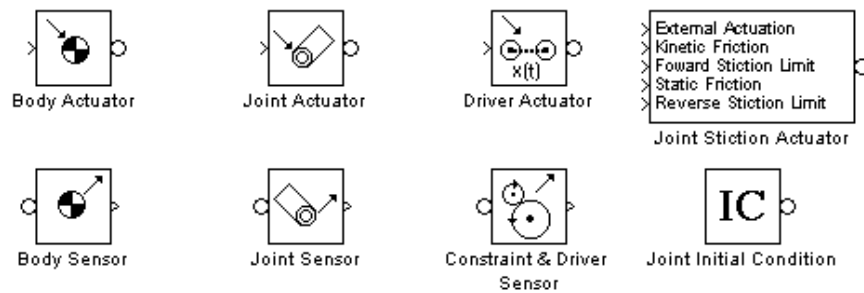


Figure 3.51 SimMechanics “Sensors & Actuators” library

Torque and speed requirements for the reference trajectory, which are two critical parameters in the selection of actuators and speed reducers, are shown in Figure 3.52 through 3.55.

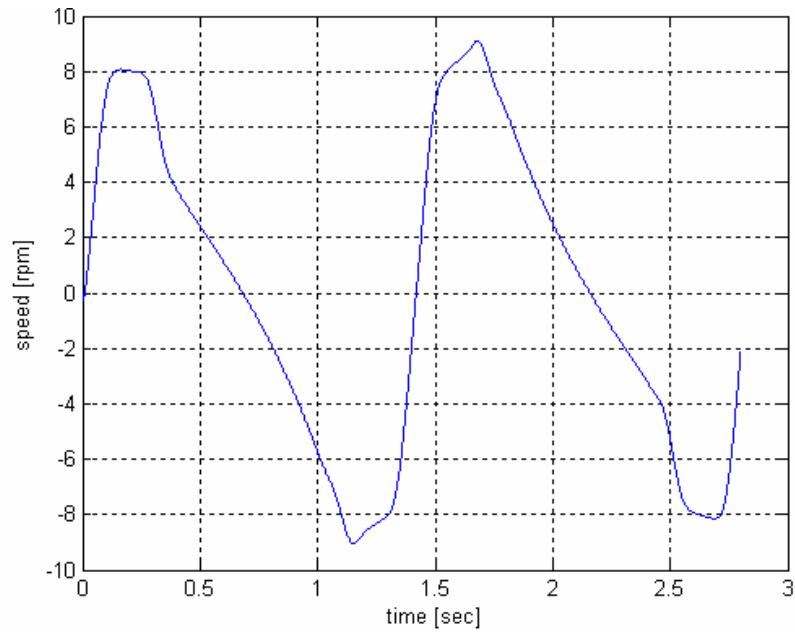


Figure 3.52 Joint 1 speed

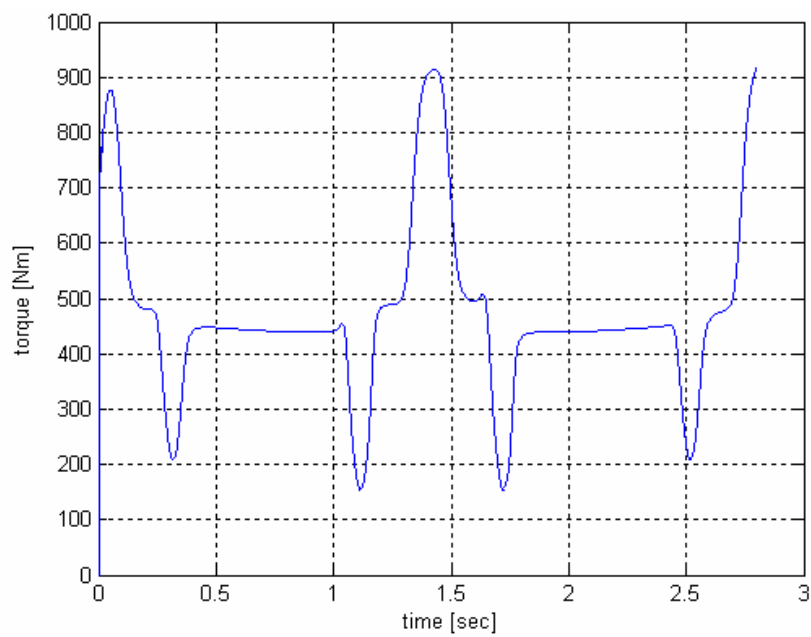


Figure 3.53 Joint 1 torque

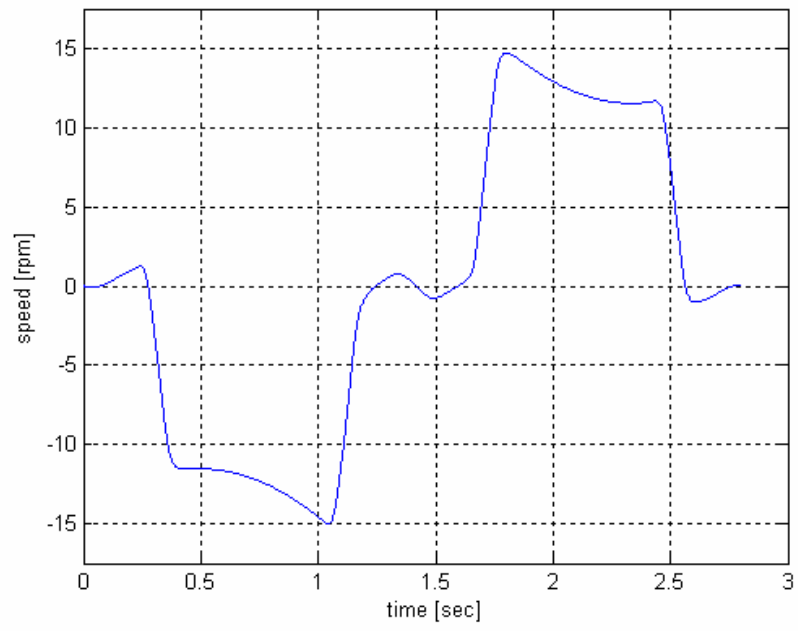


Figure 3.54 Joint 2 speed

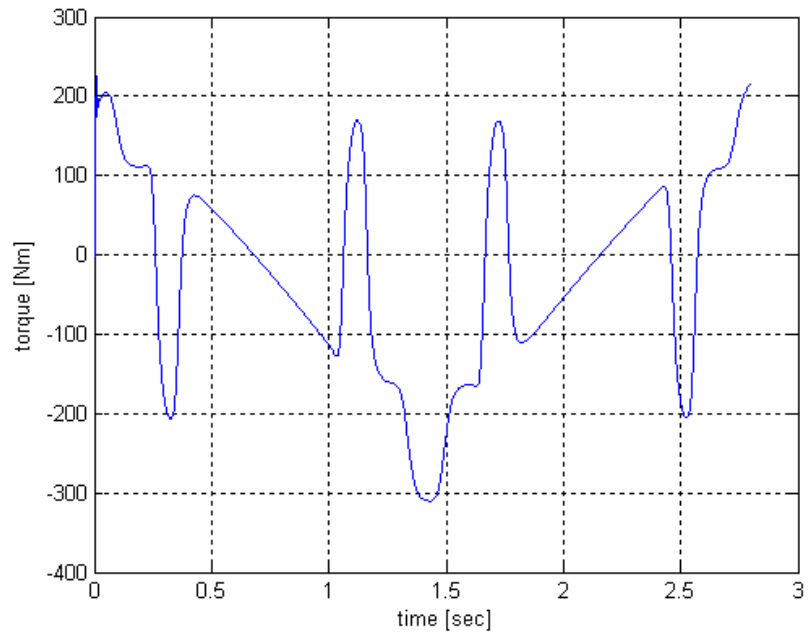


Figure 3.55 Joint 2 torque

### 3.5.6 Selection of Motors and Speed Reducers

Industrial manipulators were usually driven by permanent magnet DC servomotors in the past. Mechanical commutator and brushes of DC servomotor impose limitations on the motor performance. They can also cause maintenance problems. Alternatively, by eliminating DC servomotor's mechanical commutator and armature winding on the rotor, maintenance-free motors were realized. In a brushless servomotor, mechanical commutator is replaced by an electronic one. This design certainly results in lower rotor inertias, higher rotor speeds, higher motor supply voltages and potential for high reliability compared to DC servomotors. Because of superior features of brushless servomotors over DC motors, three-phase brushless permanent magnet synchronous servomotors manufactured by Bosch-Rexroth Indramat were used in the manipulator.



Figure 3.56 A three-phase synchronous servomotor

A brushless servomotor system consists of a stator with winding, a permanent magnet rotor, a rotor position sensor and a solid state switching assembly. Figure

3.56 and 3.57 shows the cross-sectional and actual view of the mentioned servomotors.

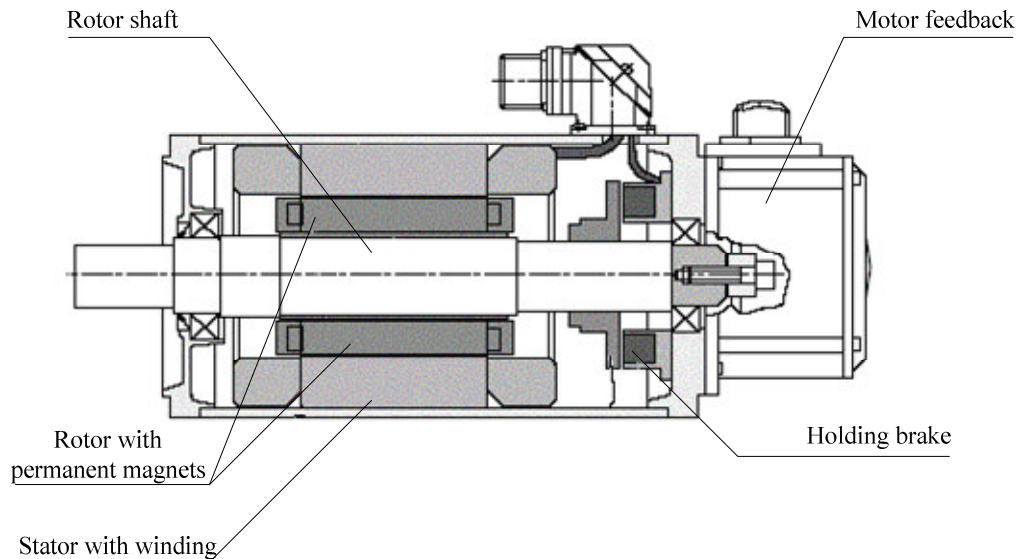


Figure 3.57 Cross-sectional view of a three-phase synchronous servomotor

In present design, Cyclo speed reducers produced by SUMITOMO Drive Technologies were used. There are essentially four major components in the CYCLO reducer:

- High speed shaft with an eccentric bearing
- Cycloid discs
- Ring gear housing with pins and rollers
- Slow speed shaft with pins and rollers

As the eccentric part rotates, it rolls one or more cycloid discs around the internal circumference of the ring gear housing. The resulting action is similar to that of a disc rolling around the inside of a ring. As the cycloid discs travel in a clockwise path around the ring gear, the discs themselves turn in a counter-clockwise direction

around their own axes. The teeth of the cycloid engage successively with the pins of the fixed ring gear, thus producing a reverse rotation at reduced speed. The reduction ratio is determined by the number of cycloid teeth on the cycloid disc. There is at least one ring gear housing which results in the reduction ratio being numerically equal to the number of teeth on the cycloid disc. Therefore, for each complete revolution of the high speed shaft, cycloid discs move in the opposite direction by one tooth.

Figure 3.58 shows actual view of a Cyclo speed reducer while figure 3.59 depicts the main components.



Figure 3.58 A Cyclo speed reducer

In this study, motors and speed reducers were selected for optimum power transmission. Fundamentally, power transmission is optimized in a mechanical system if the load inertia matches the motor inertia. That is, for a specific motor, if load inertia reflected to the motor shaft can be made to match the motor inertia,

disregarding added inertia and efficiency of the speed reducer, power transfer will be optimized and the maximum acceleration of the load will result.

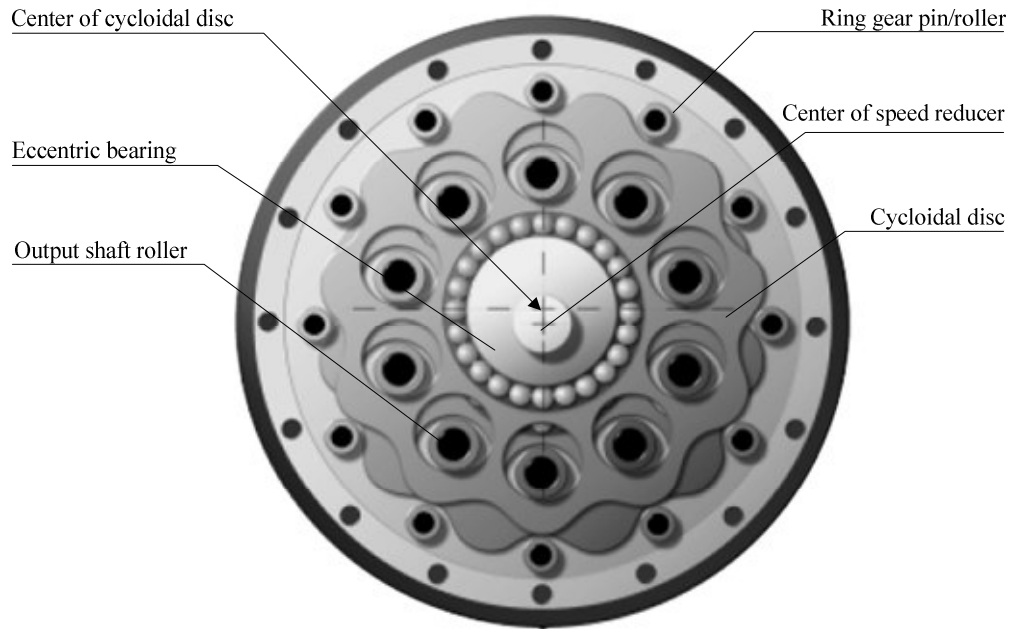


Figure 3.59 Main components of a Cyclo speed reducer

Ignoring the speed reducer efficiency and friction and considering the inertia of the speed reducer as a part of the load inertia, the total torque on the motor can be found as:

$$\tau_m = \left[ J_m + \frac{J_L}{N^2} \right] \ddot{\theta}_m \quad (3.1)$$

where  $\tau_m, J_m, \ddot{\theta}_m$  are motor torque, inertia, and angular acceleration, and  $J_L, N$  are load inertia and reduction ratio of the speed reducer. Angular acceleration of the motor can be represented in terms of that of the load as follows:

$$\ddot{\theta}_m = N \ddot{\theta}_L. \quad (3.2)$$

Combining and rearranging the eq. (1) and (2) yields:

$$\ddot{\theta}_L = \frac{\tau_m N}{J_m N^2 + J_L}. \quad (3.3)$$

In order to find the value of the reduction ratio,  $N$ , that maximize the angular acceleration of the load for a given motor torque, derivative of  $\ddot{\theta}_L$  with respect to  $N$  are taken. The result is as follows:

$$\frac{\partial \ddot{\theta}_L}{\partial N} = \frac{(J_m N^2 + J_L)\tau_m - \tau_m N(2J_m N)}{(J_m N^2 + J_L)^2}. \quad (3.4)$$

Rearranging yields:

$$\frac{\partial \ddot{\theta}_L}{\partial N} = \frac{\tau_m (J_L - J_m N^2)}{(J_m N^2 + J_L)^2}. \quad (3.5)$$

setting the derivative equal to zero finds the gear ratio that gives the maximum load acceleration:

$$\frac{\tau_m (J_L - J_m N^2)}{(J_m N^2 + J_L)^2} = 0 \Rightarrow J_L - J_m N^2. \quad (3.6)$$

Rearranging results in:

$$N = \sqrt{\frac{J_L}{J_m}}. \quad (3.7)$$

This result basically states that for a given motor of a known torque capability, maximum power transfer can be achieved with matched inertias. However, this may or may not be practically implemented with gearing between motor and load. Gearing inertia, efficiency of the speed reducer, mechanical limits and cost are points that can prevent to realize an optimum power transmission.

Following section presents the mechanical modeling of the manipulator. Such an analysis is necessary to calculate the inertia,  $J_L$  acting on motors.

### 3.5.6.1 Mechanical Modeling

Dynamic equations of motion for a manipulator relate joint torques or forces to positions, velocities, and accelerations in terms of the specific kinematic and inertial parameters of the mechanical system. There are mainly two procedures for generating the dynamic equations of motion. These are the Lagrange-Euler (L-E) and the Newton-Euler (N-E) method. In spite of the fact that two methods are “equivalent” to each other in the sense that they describe the dynamic behavior of the same manipulator, L-E method are generally used in the derivations because of its relative simplicity [12].

The equations of motion of the manipulator are [11]:

$$\begin{aligned}\tau_1 &= J_{11}\ddot{\theta}_1 + J_{21}\ddot{\theta}_2 + (\partial J_{12} / \partial \theta_2)\dot{\theta}_2^2 + G_1 \\ \tau_2 &= J_{21}\ddot{\theta}_1 + J_{22}\ddot{\theta}_2 + (\partial J_{21} / \partial \theta_1)\dot{\theta}_1^2 + G_2\end{aligned}\tag{3.8}$$

, where

$$G_1 = (m_1 l_{c1} + m_4 l_{c4} + m_2 l_1 + m_p l_1) g \cos(\theta_1)$$

$$G_1 = (m_3 l_{c3} + m_4 l_3 + m_2 (l_3 + l_{c4}) + m_p l_2) g \cos(\theta_2)$$

$$J_{11} = m_1 l_{c1}^2 + m_4 l_{c4}^2 + m_2 l_1^2 + m_p l_1^2 + (I_{zz})_1 + (I_{zz})_4$$

$$J_{12} = J_{21} = (m_4 l_{c4} l_3 + m_2 l_1 (l_3 + l_{c2}) + m_p l_1 l_2) \cos(\theta_1 - \theta_2)$$

$$J_{22} = m_3 l_{c3}^2 + m_4 l_3^2 + m_2 (l_3 + l_{c2})^2 + m_p l_2^2 + (I_{zz})_3 + (I_{zz})_2$$

All symbols in eq. (8) are shown in figure 3.60.

To simplify the equations of motion, it can be rewritten as a single matrix equation in the following form:

$$\bar{\tau} = \bar{J} \ddot{\theta} + \bar{C}(\theta, \dot{\theta}) + \bar{G}(\theta) \quad (3.9)$$

where

$$\bar{J} = \begin{bmatrix} J_{11} & J_{12} \\ J_{21} & J_{22} \end{bmatrix}, \quad \bar{G}(\theta) = \begin{bmatrix} G_1 \\ G_2 \end{bmatrix}, \quad \text{and} \quad \bar{C}(\theta, \dot{\theta}) = \begin{bmatrix} (\partial J_{12} / \partial \theta_2) \dot{\theta}_2^2 \\ (\partial J_{21} / \partial \theta_1) \dot{\theta}_1^2 \end{bmatrix}. \quad (3.10)$$

In the above matrix equation (9), while the first term in the right hand side represent effective and coupling inertia acting on joints, following two terms represent torques induced by centripetal and gravity forces.

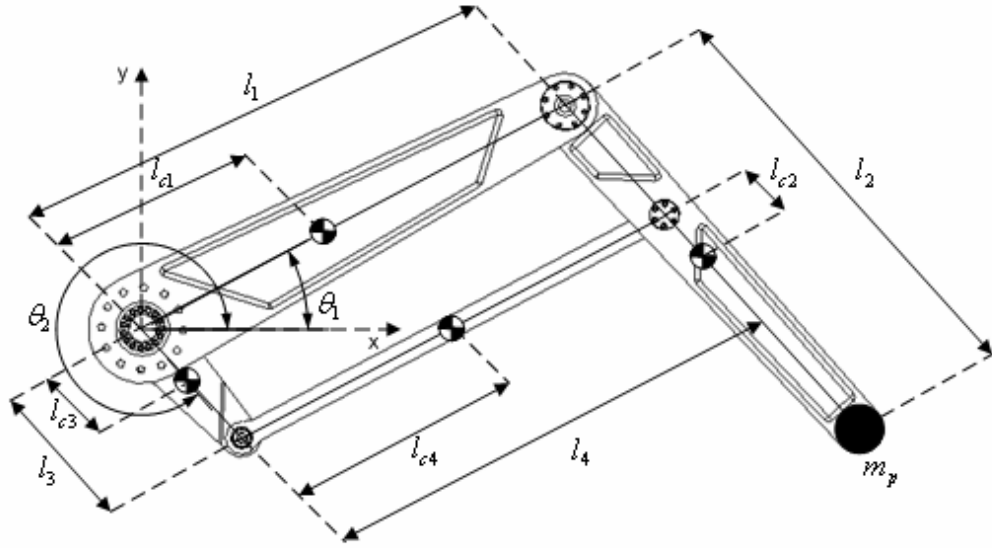


Figure 3.60 Kinematic parameters of the manipulator

It is clear from eq. (8) that the coupling inertias depend on the posture of the manipulator. In fact, it is well known fact that the anthropomorphic manipulators are inertia-varying machines. However, motors and speed reducers were selected for optimum power transfer by assuming load inertia that is the average of the maximum and minimum inertias acting on the motor during operation. Average inertias were calculated as 52.06 and 21.7 [kg m<sup>2</sup>] for the first and second joints, respectively. In calculations, bearings and shafts were also considered as point masses attached to corresponding linkages. The numerical values were calculated by using UNIGRAPHICS software packages and presented bellow.

$$\begin{aligned}
 m_1 &= 24.2 \text{ [kg]} & m_2 &= 11.75 \text{ [kg]} & m_3 &= 3.08 \text{ [kg]} & m_4 &= 2.77 \text{ [kg]} \\
 l_1 &= 0.875 \text{ [m]} & l_2 &= 0.800 \text{ [m]} & l_3 &= 0.270 \text{ [m]} & l_4 &= 0.875 \text{ [m]} \\
 l_{c1} &= 0.350 \text{ [m]} & l_{c2} &= 0.080 \text{ [m]} & l_{c3} &= 0.085 \text{ [m]} & l_{c4} &= 0.437 \text{ [m]} \\
 (I_{zz})_1 &= 2.14 \text{ [kg m}^2\text{]} & (I_{zz})_2 &= 0.87 \text{ [kg m}^2\text{]} & (I_{zz})_3 &= 0.027 \text{ [kg m}^2\text{]} & (I_{zz})_4 &= 0.21 \text{ [kg m}^2\text{]}
 \end{aligned}$$

, and  $m_p = 20[kg]$ .

Resulting load to motor inertia ratios are presented in table 3.5 shown below.

Table 3.5 load to motor inertia ratios

Joints	Motor inertia $J_m$	Load inertia $(J_L + J_{sr})$	Reduction ratio	Inertia ratio
	$kg\ m^2$	$kg\ m^2$	-	-
1 <sup>st</sup> joint	0.0043	69.04	119	1.13
2 <sup>nd</sup> joint	0.0043	31.20	89	0.91

As stated previously, optimum power transmission could not be achieved because of practical reasons. However, Load to motor inertia ratios was tried to keep around unity in order to improve the performance. Technical specifications of selected servo motors are presented in table 3.6. As seen in the table, identical servo motors (designated as MKD090 by Bosch-Rexroth Indramat) were used for both driven joints.

Table 3.6 Technical specifications of selected servo motors

	Power	Rated torque	Peak Torque	Rated Speed	Rotor inertia
	$kW$	$Nm$	$Nm$	$rpm$	$kg\ m^2$
1 <sup>st</sup> motor	2.8	7.2	43.5	3000	0.0043
2 <sup>nd</sup> motor	2.8	7.2	43.5	3000	0.0043

Technical specifications of selected Cyclo speed reducers manufactured by SUMITOMO Drive Technologies are presented in table 3.7.

Table 3.7 Technical specifications of selected speed reducers

	Designation	Reduction	Rated torque	Input speed	inertia
	-	<i>Nm</i>	<i>Nm</i>	<i>rpm</i>	<i>kg m<sup>2</sup></i>
1 <sup>st</sup> S. reducer	F1C-A45-119	1/119	1830	3150	0.0012
2 <sup>nd</sup> S. reducer	F1C-A45-89	1/89	1830	3150	0.0012

After selecting servo motors and speed reducers, torque-speed relations of servo-motors for the reference trajectory generated in fundamental design process were analyzed. Results were also compared to other available servo motors manufactured by Bosch-Rexroth Indramat. Figure 3.61 through 3.66 show these relations for motor 1 and motor 2. Technical specifications of servo motors are presented in table 3.8.

Table 3.8 Technical specifications of servo motors

Designation	Power	Rated torque	Peak Torque	Rated Speed	Rotor inertia
	<i>kW</i>	<i>Nm</i>	<i>Nm</i>	<i>rpm</i>	<i>kg m<sup>2</sup></i>
MKD041	0.32	0.82	11.3	3000	0.00017
MKD071	1.6	5.2	32	2500	0.00087
MKD090	2.8	7.2	43.5	3000	0.0043
MKD112	3.2	10.1	54	2500	0.0110

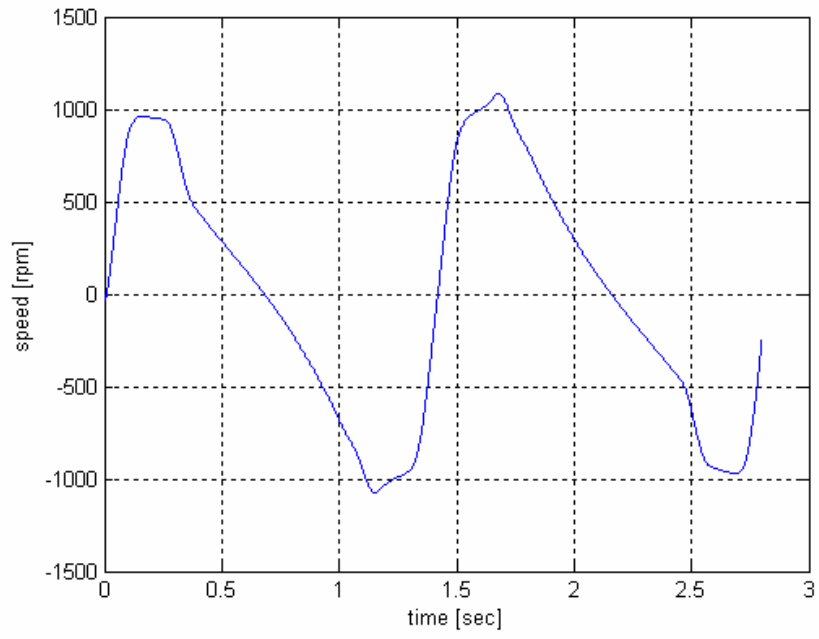


Figure 3.61 Motor 1 speed

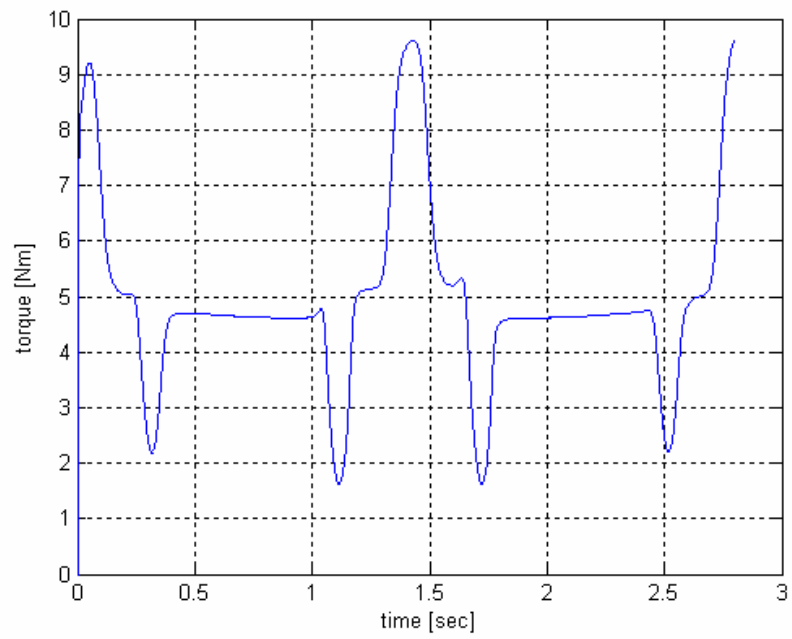


Figure 3.62 Motor 1 torque

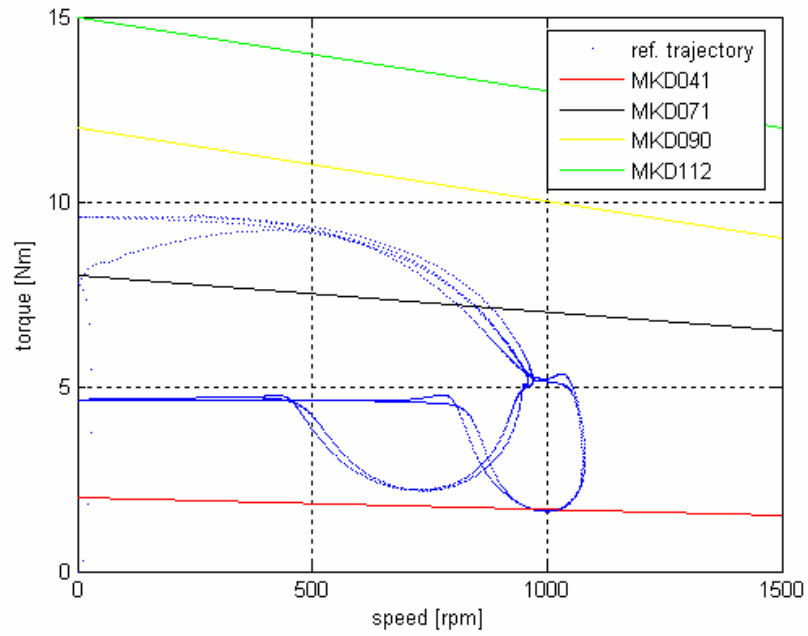


Figure 3.63 Torque-speed curve of motor 1 for reference trajectory

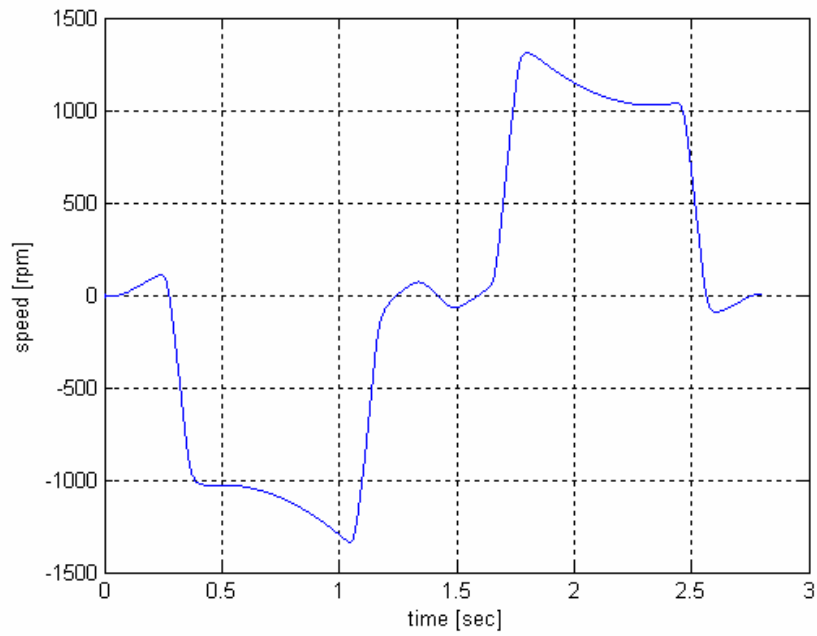


Figure 3.64 Motor 2 speed

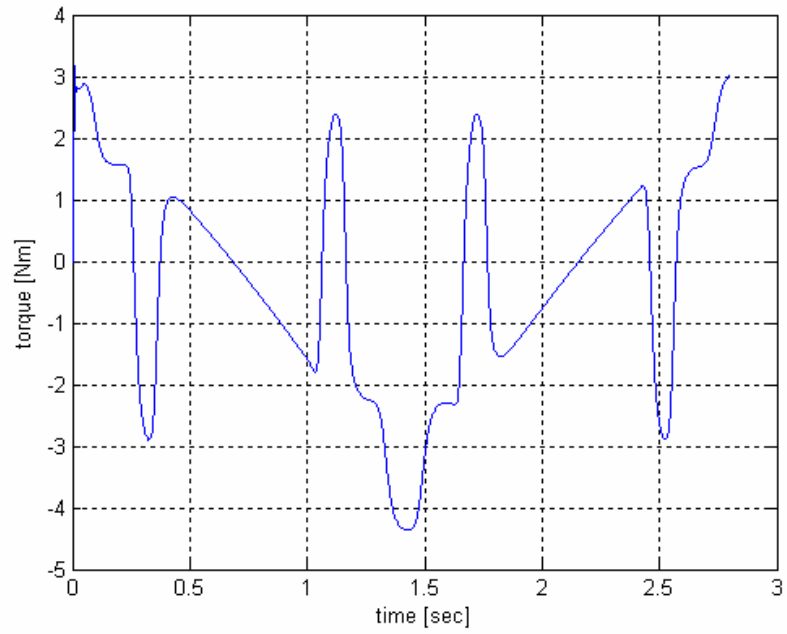


Figure 3.65 Motor 2 torque

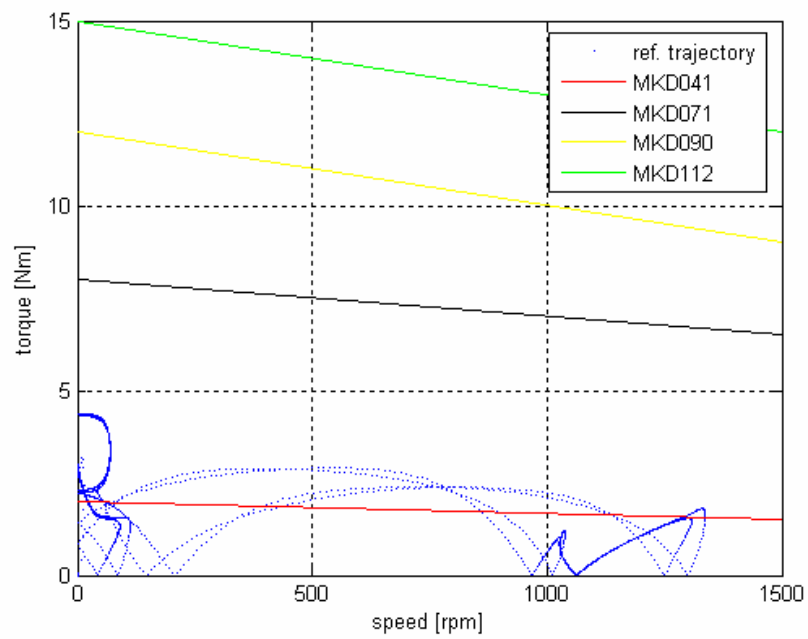


Figure 3.66 Torque-speed curves of motor 2 for reference trajectory

### **3.6 Detailed Structural Design**

After the drive system design of the manipulator was completed, detailed structural design was performed. In this design phase, modification of the arm cross-sectional dimensions was performed. Stress, deflection, and natural frequency analysis of the manipulator mechanical structure were performed by using various computer aided engineering package software as discussed in the following sections.

#### **3.6.1 Stress and Deflection Analysis**

It is obvious that the manipulator should not fail during its expected service life due to the forces and torques acting on the mechanical system. This means that stress and deflection levels must be kept within acceptable limits for the material chosen and the environmental conditions encountered. Therefore, it is necessary to investigate the stresses and deflections occurring on the mechanical structure under the effect of static and dynamic loading conditions.

Stress and deflection analysis of the structural components was performed by using finite elements method. Because of the geometric complexity of the manipulator structure, finite element analysis was performed using software MSC. PATRAN together with the MSC. NASTRAN solver. Based on the geometry of the link structures as presented in section 3.5.2, design of link structures, finite element analysis was performed for the worst case condition in the reference trajectory. At the worst case condition, it was assumed that the payload of the manipulator and acceleration at the tip point are at their corresponding maximum values given in the design condition inputs in table 3.1. When the results were examined, it was concluded that the stress values calculated for the link structures are below the limits that may lead to failure on the structures. Figure 3.67 shows the stress analysis results. As seen in the figure, maximum stress was found to be 9.78 [MPa] in link 1, which is much lower than the yield strength of the material of the link 1 structure.

In order to determine the tip deflection at the tip point, posture of the manipulator is very important. At the different configurations of the manipulator depending on the different combinations of velocity and acceleration values and the superposition of deflections from the base structure to the tip point, the accuracy varies in the workspace. For this reason, deflection analysis was performed for the worst case condition as in the stress analysis and the maximum deflection at the tip point was found to be 0.058 [mm]. Remembering the design condition input of the maximum deflection at the tip point, which is 1 [mm], it was concluded that the deflection of the manipulator at the worst case condition fulfills the design condition input.

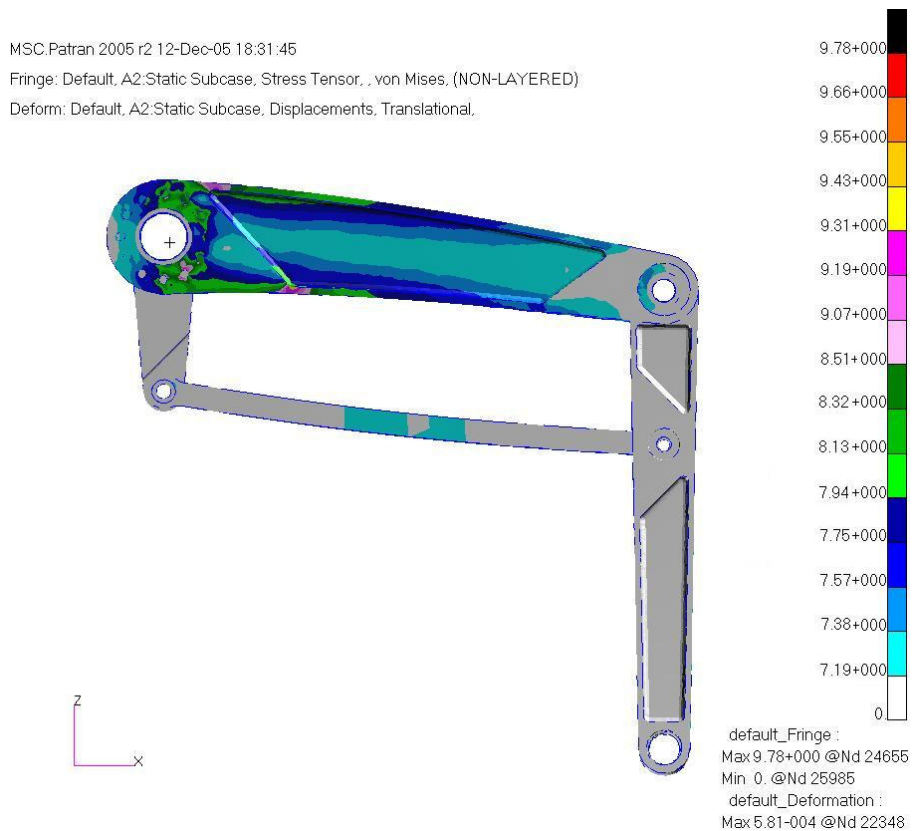


Figure 3.67 Stress and deflection analysis of the manipulator

### **3.6.2 Natural Frequency Analysis**

All manipulator structures have some resonant frequencies that are high and far enough the servo drive bandwidth so that they can be ignored. However, there can be a predominant resonant frequency that could possibly cause a stability problem of the overall system. Therefore, resonant frequencies of a manipulator should be evaluated. In this thesis study, resonant frequencies of the manipulator structure were found by using MSC. ADAMS package software. Lowest resonant frequency was found to be 42 [Hz], which is higher than the design condition input value of minimum 40 [Hz]. Animations showing resonant frequencies can be found in accompanying CD-ROM.

## CHAPTER 4

### CONTROL SYSTEM DESIGN

#### 4.1 Introduction

In this chapter, control system design of the robotic arm is described. The control system of the manipulator was designed based on linear control techniques. Actually, the use of linear control techniques are only valid if the dynamics of the system to be controlled can be mathematically modeled by linear differential equations. For the case of manipulator control, linear control techniques must be comprehended as approximate methods since the dynamics of the manipulator is more properly represented by non-linear differential equations as shown in eq. (3.8). However, utilization of speed reducers with high reduction ratios in the transmission systems suppressed the effects of non-linear terms in the equations governing the manipulator motion and the use of linear techniques in control system design was justified, as shown in the following sections.

Mechanical modeling of the manipulator was presented in chapter 3. In this chapter, both mechanical and electro-mechanical modeling of the transmission system were presented and then tuning of the control system parameters was described.

#### 4.2 Modeling of the Transmission System

As stated in the mechanical design of the manipulator, actuators were placed on the base and linkages are used as a transmission system to direct the actuator motions to

driven joints. Provided that the torque on the motor shaft is known, the torque on the link shaft can be computed by

$$\tau = \tau_m N \eta \quad (4.1)$$

where  $N$  and  $\eta$  are the reduction ratio and efficiency of the speed reducer. It is important to note that although the efficiency of the speed reducer does not alter the kinematic relations such as position, velocity, and acceleration, it significantly affects any torque related property. Reduction ratios and efficiencies of the speed reducers were presented in table 3.7 together with the actuator characteristics.

Assuming the dynamics of the motor simply described by a rigid load rotating about the shaft axis, the equation describing the system is:

$$\tau_m = J_m \ddot{\theta}_m \quad (4.2)$$

where  $J_m$  is the motor shaft's mass moment of inertia about the axis of rotation and  $\ddot{\theta}_m$  is its angular acceleration. When a load is attached to the output of the motor coupled with speed reducer, and then the total torque developed at the motor shaft,  $\tau_T$  is equal to the sum of the torque dissipated by the motor  $\tau_m$  and its load seen by the motor shaft  $\tau_L$ .

$$\tau_T = \tau_m + \tau_L \quad (4.3)$$

Load torque  $\tau_L$  can be computed according to Eq. (4.4).

$$\tau_L = \frac{\tau}{N\eta} \quad (4.4)$$

where  $\tau$  represents the torque of each joint as given by the equations of motion, Equation (3.8). Combining the equations of motion in matrix form, eq. (3.9), with

eq. (4.1), (4.2), (4.3), (4.4), manipulator equations of motion in matrix form can be obtained as:

$$\bar{\tau}_T = \tilde{J}_m \ddot{\theta}_m + (\tilde{N} \tilde{\eta})^{-1} \left\{ \tilde{J} \ddot{\theta} + \tilde{C}(\theta, \dot{\theta}) + G(\theta) \right\}. \quad (4.5)$$

$\tilde{J}_m, \tilde{N}$  and  $\tilde{\eta}$  are now diagonal matrices for proper matrix operation. Further manipulating this equation, the following expression for the manipulator equations of motion results:

$$\bar{\tau}_T = \left[ \tilde{J}_m + (\tilde{N}^2 \eta)^{-1} \tilde{J} \right] \ddot{\theta}_m + (\tilde{N} \tilde{\eta})^{-1} \left\{ \tilde{C}(\theta, \dot{\theta}) + G(\theta) \right\} \quad (4.6)$$

The first term in the right side of the equation can be referred to as the effective inertia matrix. It is evident from the equation that the rotor inertia can have significant effect on the overall dynamics of a manipulator. Therefore, as stated in previous chapter, the manipulator was designed with high gear ratios that cause rotor inertia to match link inertia, so that non-linear rigid body dynamics can be neglected altogether in the controller design and the system can be controlled by linear control techniques.

### 4.3 Electro-Mechanical Modeling

A schematic linear circuit model of a transmission system composed of a motor, a speed reducer, and a mechanical load is shown in figure 4.1. Electro-mechanical characteristics of the motor and the speed reducer are presented in table 4.1. As stated in chapter 3, identical motors were used for both driven joints.

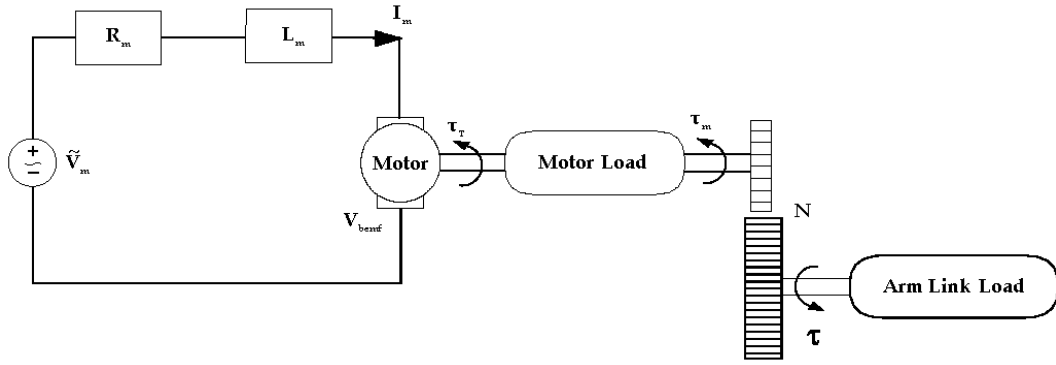


Figure 4.1 Schematic diagram of the motor, speed reducer, and mechanical load

In order to develop a dynamic model for the motor, Kirchhoff's voltage law was applied around the armature windings which yields:

$$V_m = L_m \dot{I}_m + I_m R_m + V_{bemf} \cdot \quad (4.7)$$

Table 4.1 Motors and speed reducers' electro-mechanical characteristics

Parameter	Description	Value	Units
$J_m$	Motor inertia	$43 \times 10^{-4}$	$\text{kg m}^2$
$K_m$	Motor torque constant	1.73	$\text{Nm A}^{-1}$
$K_e$	Motor voltage constant	1.06	$\text{V s rad}^{-1}$
$R_a$	Winding resistance	1.88	$\Omega$
$L_a$	Winding inductance	$15.5 \times 10^{-3}$	H
$T_s$	Continuous stall torque	12	Nm
$T_p$	Theoretical maximum torque	43.5	Nm
N	Speed reducer reduction ratio	119	-
$\eta$	Speed reducer efficiency	0.8	-

$V_{\text{bemf}}$  in eq. (4.7) represents the back electro-motive force. It is an internal voltage that counteracts motor voltage supply, and is produced when the rotor rotates in a magnetic field. It is linearly proportional to the motor shaft angular speed. That is,

$$V_{\text{bemf}} = K_e \dot{\theta}_m \quad (4.8)$$

where  $K_e$  is referred as the motor voltage constant.

After electro-mechanical modeling, the relationship between the electrical and mechanical components of the system was established in order to relate the control torque action to the underlying physical control variables which actually excite the actuator. Electrical and mechanical systems were coupled to the one other through an algebraic torque equation. In general, torque developed at the motor shaft is assumed to increase linearly with the effective current, independent of the speed and position, according to:

$$\tau_T = K_m I_{\text{eff}} \quad (4.9)$$

The overall block diagram for a single joint, obtained from equation (4.6), (4.7), (4.8) and (4.9), combined with the drive system, can be depicted as shown in figure 4.2.

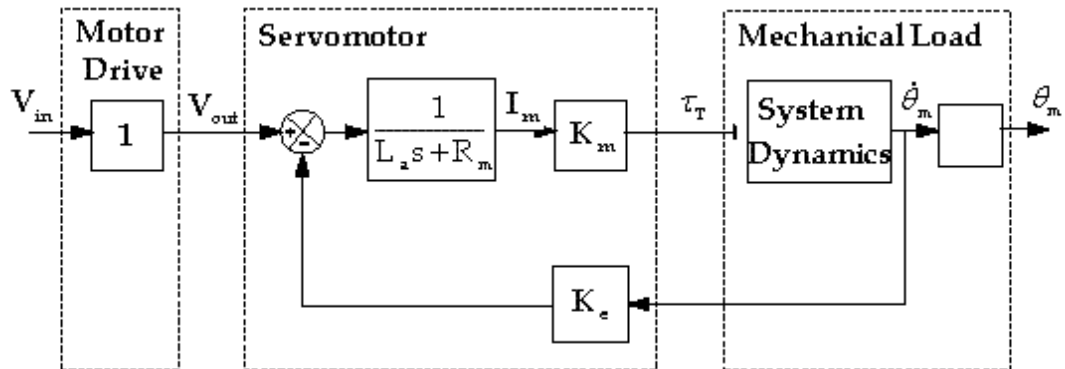


Figure 4.2 Block diagram of electro-mechanical system and mechanical load

As a first step to design control system based on linear methods, a simplified load was assumed for each actuator. Namely, all the non-linear terms in eq. (4.6) such as centrifugal forces, gravity and friction were neglected. Equations of motion of the manipulator in matrix form is then:

$$\bar{\tau}_T = \tilde{J}_{\text{eff}} \ddot{\theta}_m \quad (4.10)$$

$$\text{where } J_{\text{eff}} = \tilde{J}_m + (\tilde{N}^2 \eta)^{-1} \tilde{J}(\theta) \quad (4.11)$$

In order to reduce the control problem to single axis control with fixed inertia, effective inertia seen by each actuator was assumed as the sum of the inertia of the driven joint and coupling inertia between joints. System dynamics of each joint is then given by

$$\tau_{Ti} = [J_{mi} + (N_i^2 \eta)^{-1} (J_{ii} + J_{ij})] \ddot{\theta}_i \quad (4.12)$$

#### 4.4 Control System Hardware

As stated in chapter 2, VisualMotion control system from Bosch-Rexroth Indramat was used in the SPRS control system. VisualMotion is a programmable multi-axis motion control system capable of controlling up to 32 digital intelligent motor drives. PC software used for motion control management is named as VisualMotion Toolkit (VMT). VisualMotion Toolkit (VMT) is software for motion control programming, parameterization, system diagnostics and motion control management. VMT also includes a DDE server which is a communication protocol between Microsoft Windows programs and motion control system. The hardware used with VisualMotion Toolkit is the PPC-R motion control card.

The SPRS motion control system consists of the following components:

- PPC-R motion control card
- RECO02 I/O modules
- VisualMotion Toolkit program
- ECODRIVE03-SGP01 motor drives
- Permanent magnet synchronous servomotors

ECODRIVE03-SGP01 digital motor drives have built in motion control system. The control loop structure is made up of a cascaded (nested) position, velocity and torque/force loop. Depending on the operating mode of the drive, only the torque control loop or the torque and velocity control loops or the position, velocity and torque control loops can become operative. The control structure is depicted in figure 4.3.

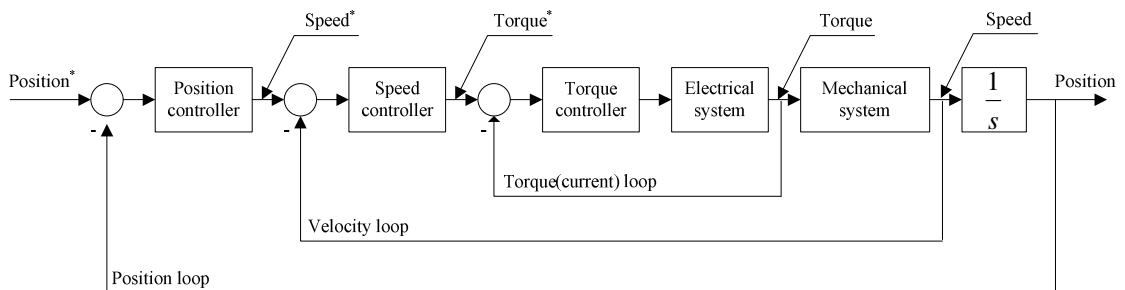


Figure 4.3 Cascaded control of a single joint

As shown in the figure above, built-in motion control system uses PI controller in the torque and velocity loops and proportional controller in position loop. In motion control systems, integral compensation is generally not used in the position loop. This is referred to as “naked” position servo loop.

PI controllers in the torque and velocity loops were adjusted by the following procedure.

1. Open loop gain,  $K$ , that will meet the phase margin requirement without compensation was determined.
2. Bode plot of the uncompensated system with crossover frequency from step 1 was plotted and the low-frequency gain evaluated.
3. The corner frequency,  $\omega_c$ , was chosen as to be decade below the new crossover frequency.
4. Design was iterated until the controller parameters are adjusted to meet adequate closed loop bandwidth and phase margin requirements.

PI controller has the transfer function:

$$G_C(s) = K_p + \frac{K_I}{s} = \frac{Ki(\frac{K_p}{K_I}s + 1)}{s} = K \frac{(\tau s + 1)}{s}$$

where the corner frequency is given by

$$\tau = \frac{K_p}{K_I} = \omega_c.$$

Since the same procedure is followed for both driven axis of the robotic arm, the controller parameters only for joint 1 will be described in the following sections.

#### 4.4.1 Tuning of Current Loop Controller Parameters

Figure 4.4 shows the current loop structure. Since the block diagram in this figure is not solvable, block diagram reduction techniques were applied to separate the servo loops to an inner and outer servo loops as shown in figure 4.5 and 4.6.

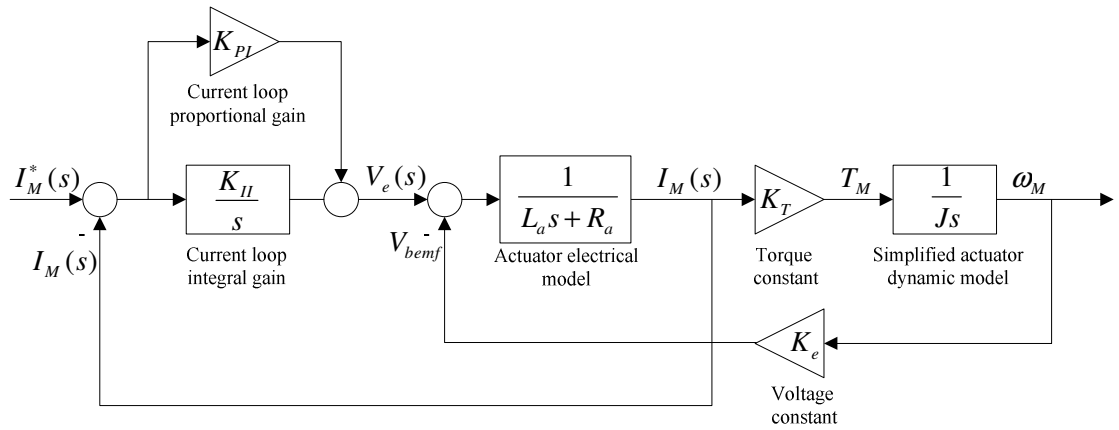


Figure 4.4 Block diagram of torque control loop

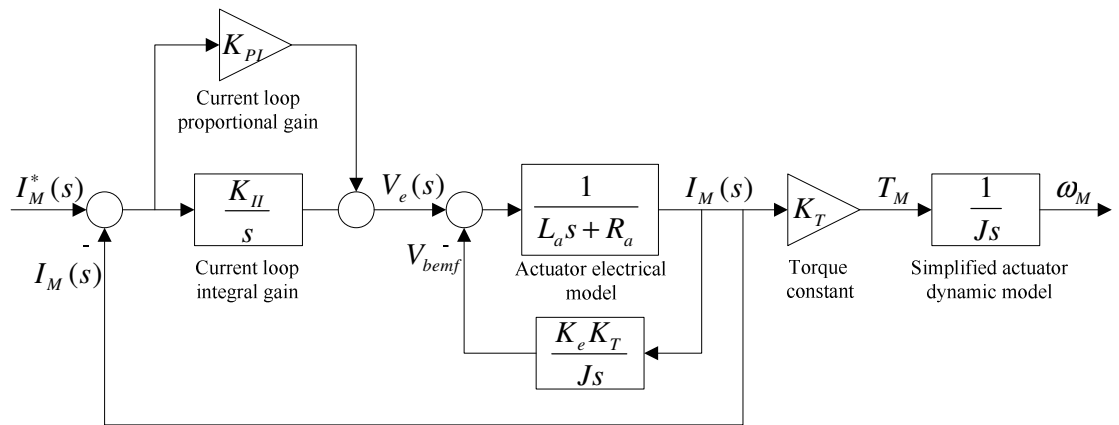


Figure 4.5 Interleaved loops redrawn as nested loops

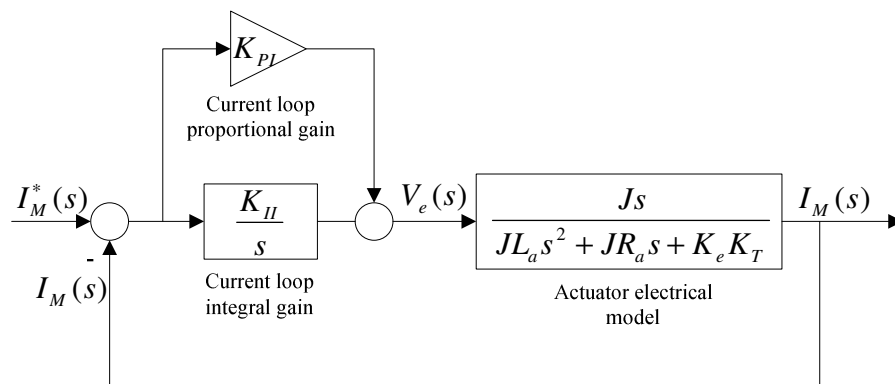


Figure 4.6 Simplified current loop block diagram

Parameters of PI controller in current loop have been set by the drive manufacturer and can not be adjusted for specific applications. Open loop and closed loop bode plots obtained from the current loop controller block diagram of figure 4.6 are shown in figure 4.7 and 4.8. In these figures, magnitude plots represent the ratio of commanded current signal and the response of the current controller to this command, [Ampere/Ampere] Figure 4.10 shows the step response of the current controller to 1 Ampere current command.

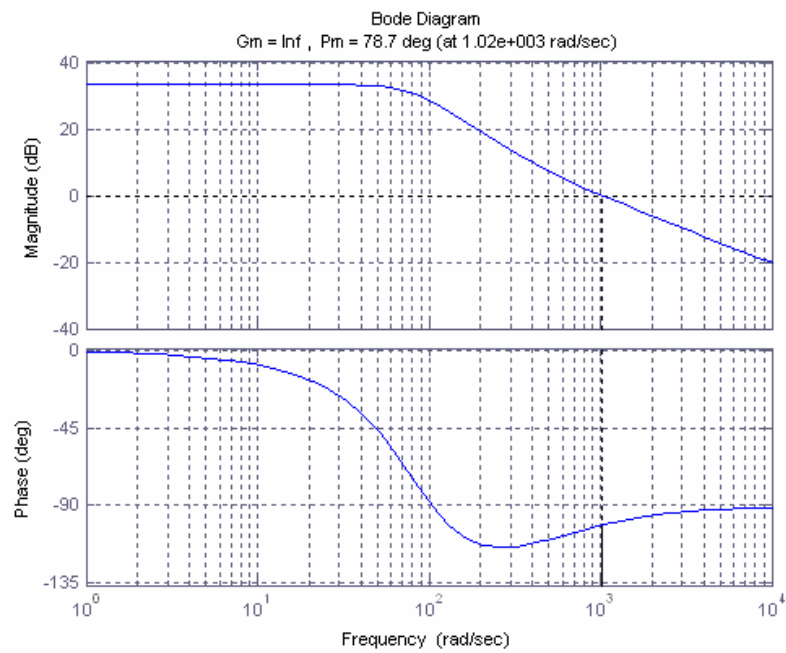


Figure 4.8 Open loop bode diagram of the current loop

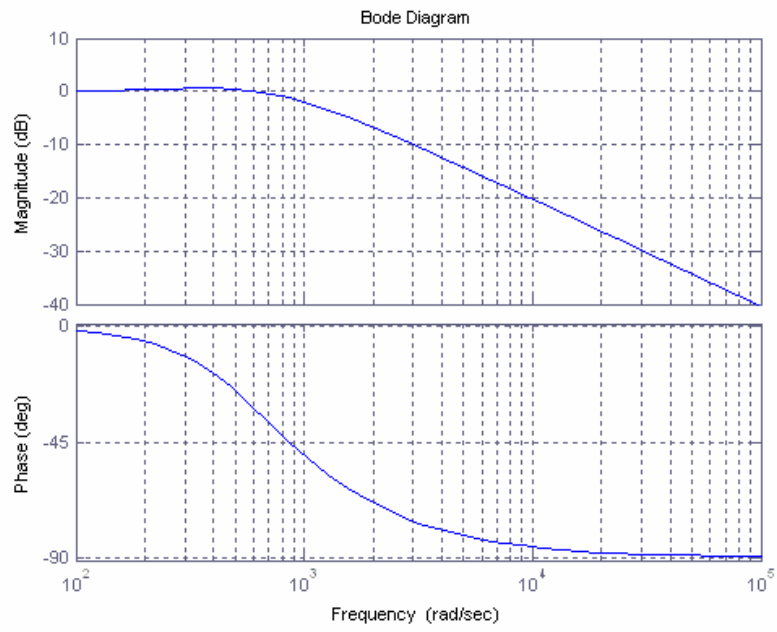


Figure 4.9 Closed loop bode diagram of the current loop

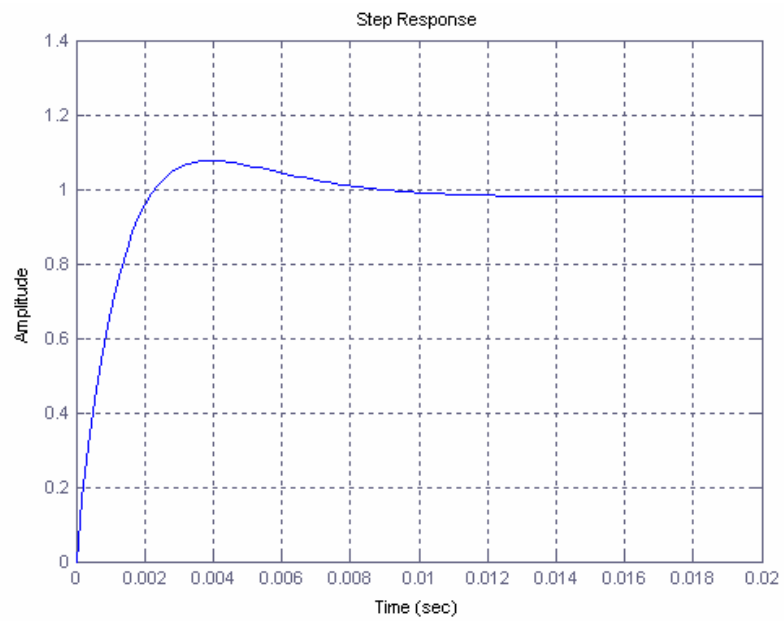


Figure 4.10 Step response of the current loop

#### 4.4.2 Tuning of Velocity Loop Controller Parameters

In order to adjust the parameters of PI controller in velocity loop, current loop was assumed as ideal and represented by unity. Figure 4.11 shows velocity loop block diagram.

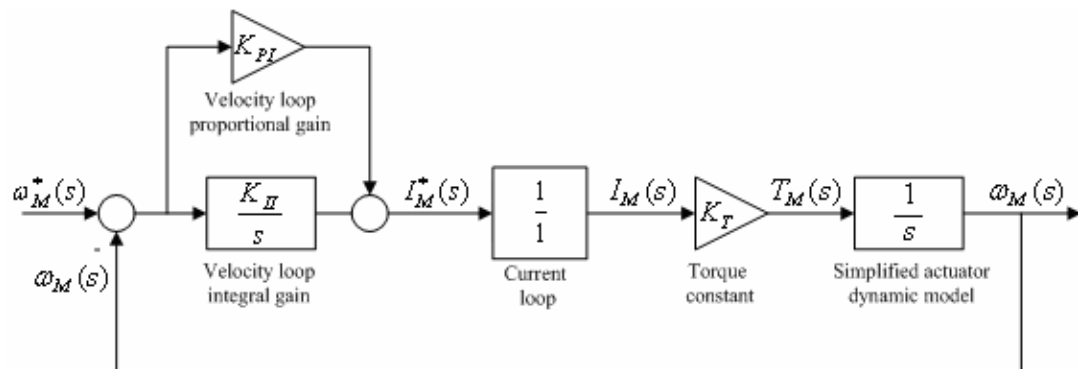


Figure 4.11 Block diagram of velocity loop

In general, the accepted rule for setting the servo compensation begins by removing the integral gain. The proportional gain is then adjusted to a level where the velocity servo response is just stable. The proportional gain is then reduced slightly further for a margin of safety. Then the corner frequency was adjusted to be a decade lower than the crossover frequency in open loop bode plot

Open loop and closed loop bode plots obtained from the velocity loop controller block diagram of figure 4.11 are shown in figure 4.12 and 4.13. In these figures, magnitude plots represent the ratio of commanded velocity signal and the response of the velocity controller to this command, [(rad/sec) / (rad/sec)]. Figure 4.14 shows the step response of the velocity controller to 1 rad/sec velocity command.

As seen in the figures, velocity loop has  $60^\circ$  phase margin and 125 rad/sec ( $\sim 20$  Hz) closed loop bandwidth, which are typical for industrial robots.

Table 4.2 Velocity loop controller parameters

Parameter	Description	Value	Units
$K_{II}$	Integral gain	0.8	$A \cdot \text{sec} / \text{rad}$
$K_{PI}$	Proportional gain	45	$A \cdot \text{sec} / \text{rad}$

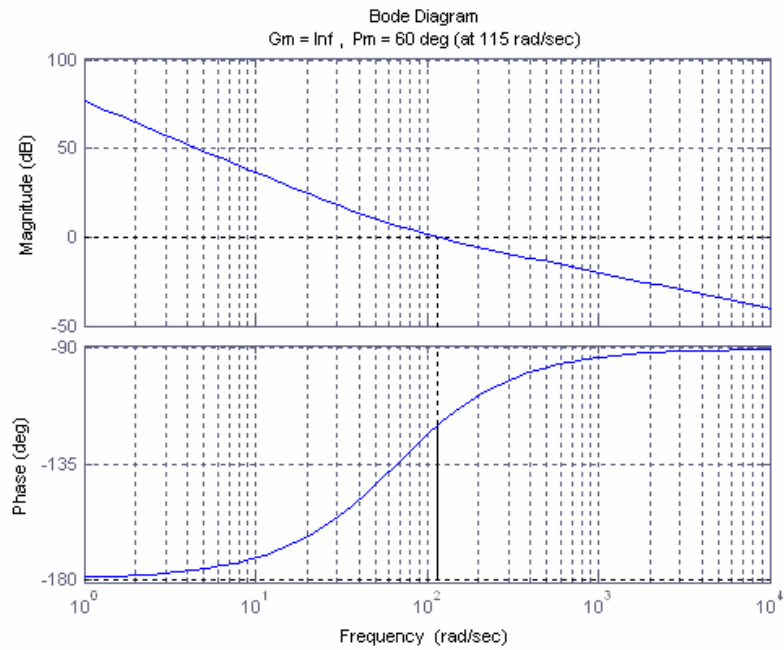


Figure 4.12 Open loop bode diagram of the velocity loop

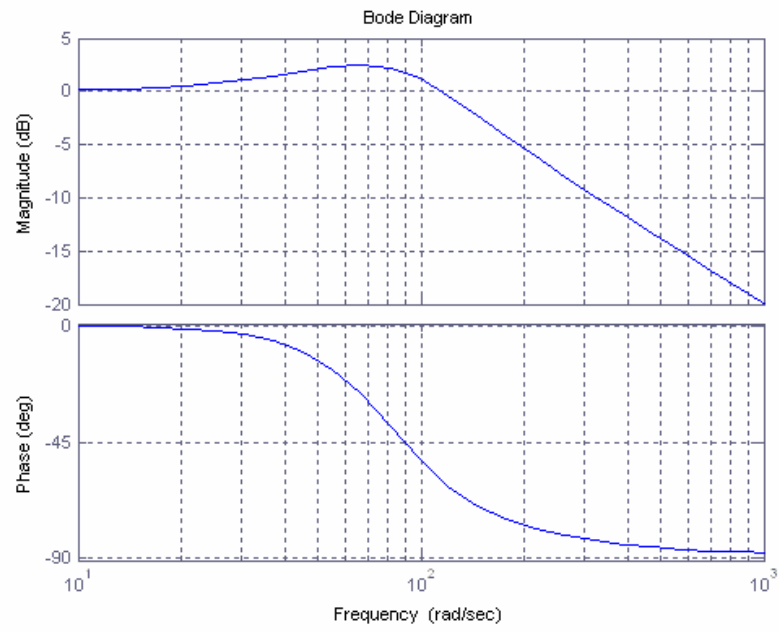


Figure 4.13 Closed loop bode diagram of the velocity loop

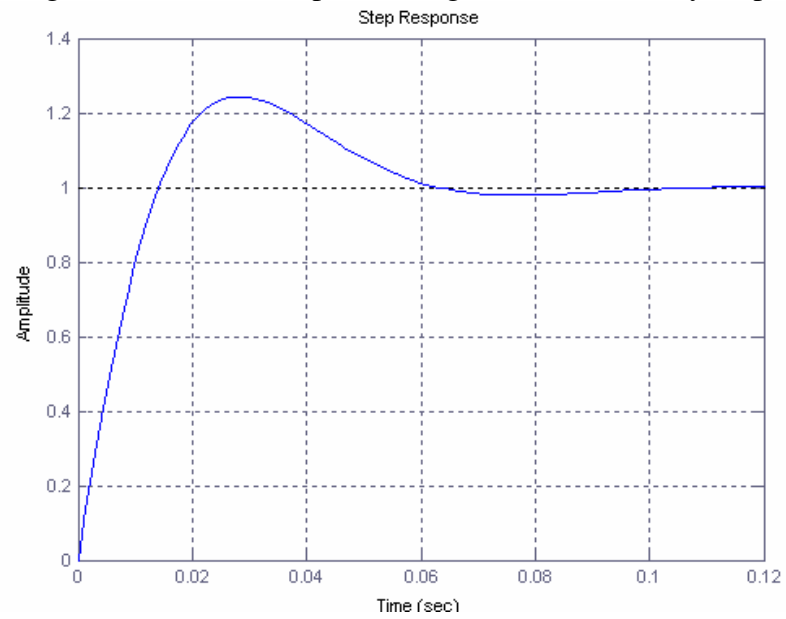


Figure 4.14 Step response of the velocity loop

### 4.4.3 Tuning of Position Loop Controller Parameters

Having adjusted the velocity controller parameters, position loop around the velocity loop was closed by assuming ideal velocity loop as shown in figure 4.15.

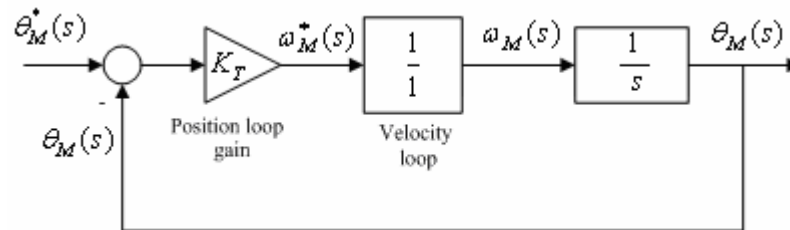


Figure 4.15 Block diagram of position loop

Open loop and closed loop bode plots obtained from the position loop control block diagram of figure 4.15 are shown in figure 4.16 and 4.17. In these figures, magnitude plots represent the ratio of commanded position signal and the response of the position controller to this command, [rad / rad]. Figure 4.18 shows the step response of the position controller to 1 rad position command. As seen in the figures, position loop has  $90^\circ$  phase margin and 25.2 rad/sec ( $\sim 4$  Hz) closed loop bandwidth.

Table 4.2 Position loop controller parameters

Parameter	Description	Value	Units
$K_{PP}$	Integral gain	25	$\text{sec}^{-1}$

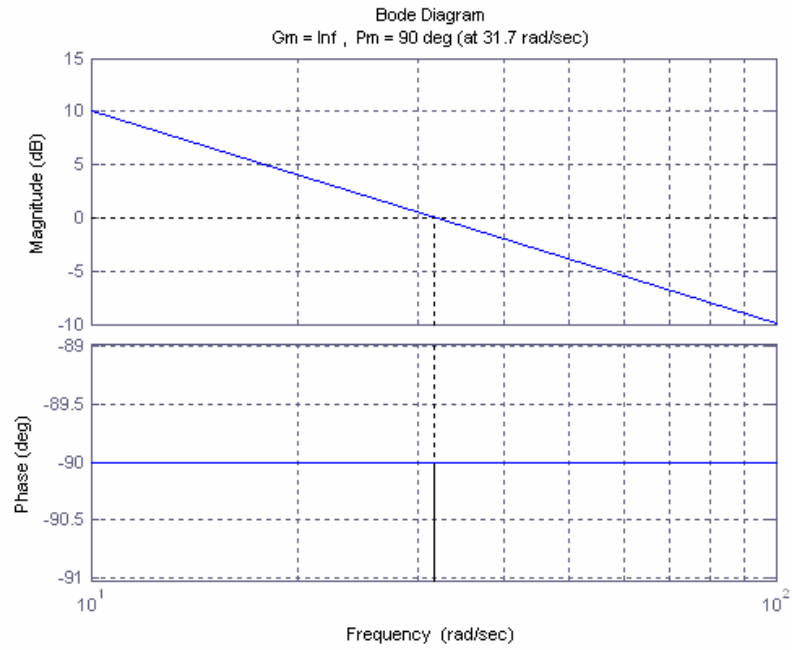


Figure 4.16 Open loop bode diagram of the position loop

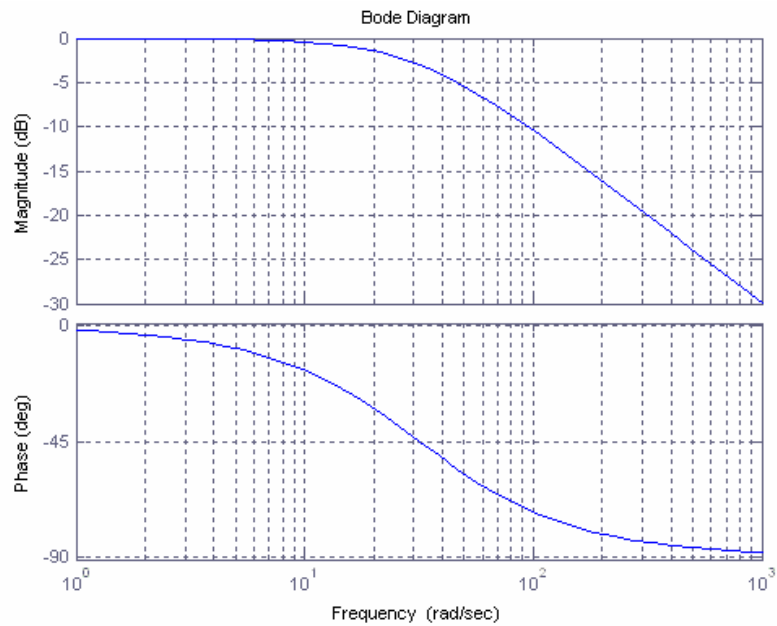


Figure 4.17 Closed loop bode diagram of the position loop

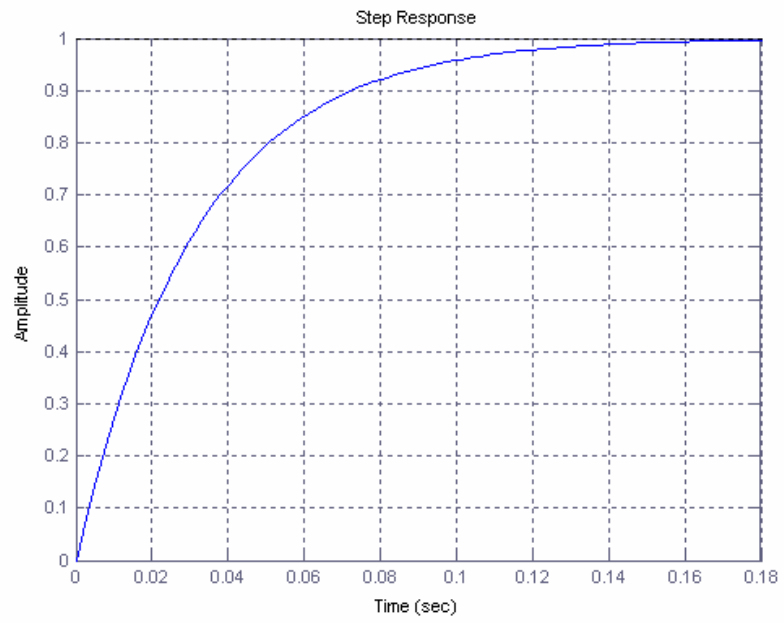


Figure 4.18 Step response of the position loop

## CHAPTER 5

### SYSTEM SIMULATION

#### 5.1 Introduction

Robotics is a multidisciplinary technology that requires strong integration of classical engineering fields as shown in figure 5.1. While mechanical engineering contributes to the topic for the study of static, dynamic and constructional situations, mathematics provides necessary tools for synthesis and analysis of robotic systems. Control theory supplies means of moving the system in a desired manner and computer science constitutes a development environment for motion control algorithms. Hardware where the motion control algorithms run is designed according to the principals of Electrical and Electronics engineering.

During the early years of robotics, neither an exact theory nor hardware and software tools were present to assist engineers in designing these technologically sophisticated systems. Designers from distinct disciplines were using their reach experience of machine building and control. These experiences represented sufficient background for the design of many successful systems. However, the necessity for more complex, precise, and high-speed robotic systems required to strengthen connections between distinct principles by appropriate software and hardware engineering tools.

In classical machine design methodology, mechanical designers and software developers come face to face with difficult challenges in robotics projects. Separate hardware and software development groups work simultaneously and independently in this methodology. Both groups have to wait until the realization of target hardware

in order to measure the performance of the system. When prototype hardware and substantial portion of the software which controls the hardware becomes available, two designs are combined in a phase called system integration and testing begins. Often the modification of decisions taken in the early stages of design could be unavoidable to achieve desired performance. This situation cause higher cost by increasing development cycles and waste of time for the overall project.

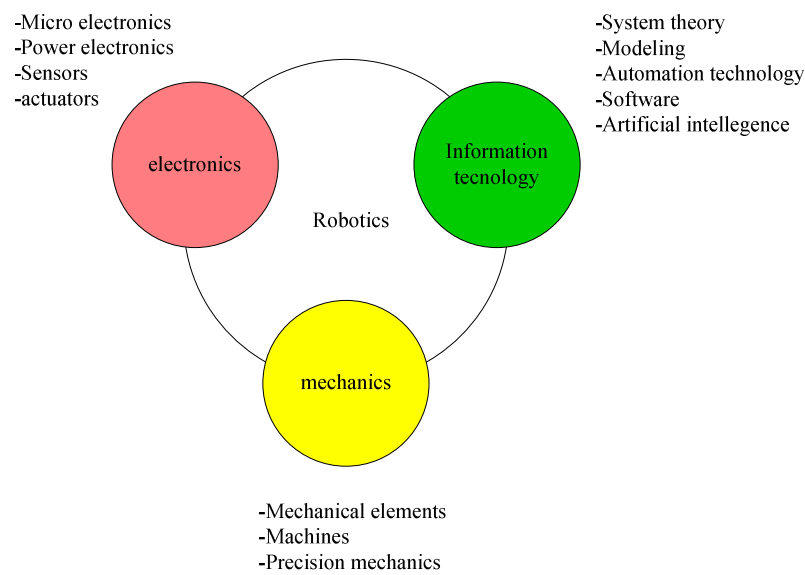


Figure 5.1 Distinct principles in robotics

Parallel to rapid developments in digital processor technology, many hardware and software engineering tools have been developed. These tools significantly influenced the design methods of robotics systems like all other engineering domains. By utilizing these new tools, design of such complex systems requiring strong integration of distinct disciplines is no longer difficult compared to the past. Presently, such tools offer advanced methods for system simulation of robotic systems and user-friendly calculation of design parameters. By enabling system

simulation, they allow observing system behaviors before expensive hardware setups actually built.

Following sections briefly introduce the concept of system simulation. Since the simulation is becoming an invaluable tool for robotic design by allowing designers to study the interaction of components and the variations of the design parameters before manufacturing, special attention is paid for different simulation techniques.

## 5.2 System Simulation Techniques

System simulation techniques applied to the design of robotic systems are drawing attentions because of the potential they offer. These techniques are especially invaluable if the hardware and software are developed simultaneously in order to minimize iterative development cycles and to meet short time to market schedules.

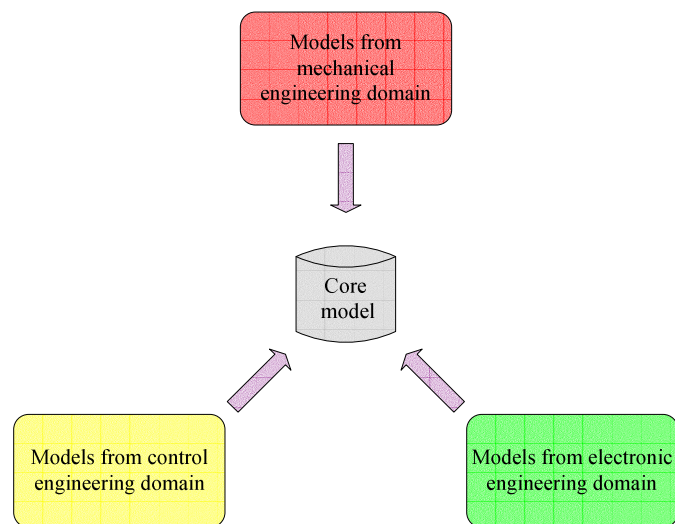


Figure 5.2 Distinct models in core model of a robotic system

As stated in previous sections, development process of robotic systems is different from other development processes in the sense that it spans over many closely coupled engineering domains. However, some problems arise from the fact that different engineering domains use different models and modeling environments during the design work. For example, control engineers are used to model in the form of transfer functions or state space descriptions which do not have direct relations to the physical parameters of the robotic system that the mechanical engineers deal with. Therefore, for the purpose of system simulation, it is very important to represent all models from different engineering domains in a core model of the entire system. This core model should be able to hold models from different engineering domains in its body. Concept is schematically depicted in figure 5.2.

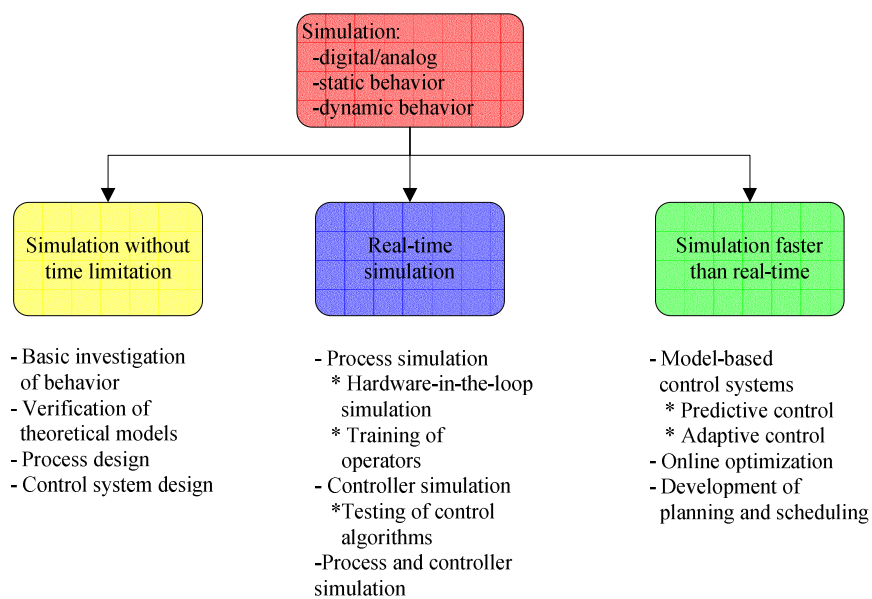


Figure 5.3 Three methods of system simulation

System simulation methods can be divided into three based on their speed of computation:

- Simulation without time limitation,
- Real-time simulation, and
- Simulation faster than real-time.

Figure 5.3 shows these methods with specific examples.

### 5.2.1 Simulation without Time Limitation

System simulation without time limitation allows not only observing the effect of design parameter changes on overall system but also correcting fatal errors made in the early stages of conceptual design before expensive system realization. In this method, both the controller and process are simulated without regarding the time. This non-real-time simulation can serve as a basis for real-time simulation. It is sometimes necessary to perform simplifications and optimizations on the model contained in the simulation in order to make it suitable to run in real-time. Figure 5.4 depicts the concept.

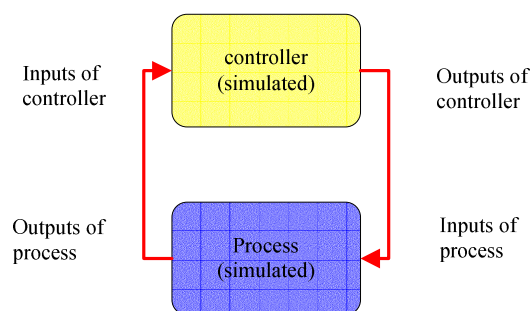


Figure 5.4 Simulation without time limitation

### 5.2.2 Real-Time Simulation

Real-time simulation is performed such that the input and output signals show the same time-dependent values as the real, dynamically operating component. A computational speed can be a problem for highly dynamic systems compared to the required algorithms and calculation speed. Figure 5.5 shows different kind of real-time simulation methods.

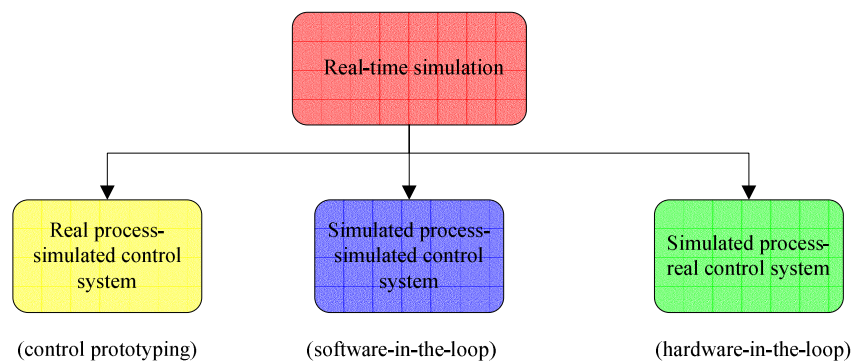


Figure 5.5 Three methods of real-time simulation

The reason for the real-time requirement is coming from the fact that one part of the investigated system is not simulated but real. There are three cases:

- Real process can be operated together with simulated control system. This approach is called control prototyping simulation.
- Simulated processes can be operated with the real control system hardware, which is called hardware-in-the-loop simulation.
- Simulated process can be run with the simulated control system in real time.

### 5.2.2.1 Control Prototyping Simulation

Real time control system simulation with hardware other than final production hardware may be performed for the design and testing of complex control systems and their algorithms under real-time conditions. The process, actuators and sensors can be real as schematically shown in figure 5.6. This is called control prototyping.

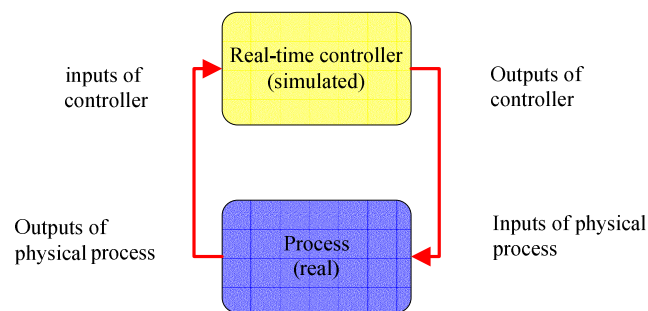


Figure 5.6 Control prototyping

Main advantages of this method are,

- Accelerated design stages of signal processing methods, process models, and control system structure,
- Testing of signal processing and control systems, together with other design of actuators, process parts, and sensor technology,
- Creating simpler models and algorithms to meet requirements of lower cost, and
- Determining of specifications for final hardware and software.

### 5.2.2.2 Hardware-in-the-loop Simulation

Real components are operated in connection with real-time simulated components in hardware-in-the-loop simulation. Generally, the real control system hardware and software are used together with the process simulated by HIL simulator as shown in figure 5.7. Sometimes the controlled process can involve both real and simulated components. Sometimes, real actuators are used and the process and sensors are simulated. The main reason behind using real actuators is that some actuators are difficult to model. Also, they can be integrated to control system.

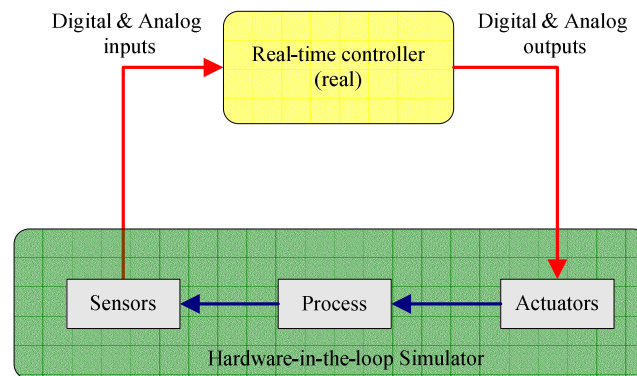


Figure 5.7 Hardware-in-the-loop simulation

Main advantages of this method are,

- Design and testing of the control hardware and software without operating a real process,
- Testing of the control hardware and software under extreme environmental conditions in the laboratory
- Testing of the effects of faults and failures of actuators, sensors, and computers of on the overall system,
- Reproducible experiments, frequently repeatable,

- Easy operation with different man-machine interfaces,
- Saving of cost and development time.

### **5.2.3 System Simulation Software Tools**

System simulation of complex robotic systems may require sophisticated numerical algorithms. As stated in previous sections, wide span of robotics design over distinct engineering fields revealed the need of new design tools having the ability of representing models from different fields. Package software MATLAB/SIMULINK and LABVIEW offer powerful tools for overcoming this problem. Dynamic system modeling and control system design can be performed and required codes for simulation can be automatically generated by using these tools. They provide also tight integration with I/O hardware for rapid control prototyping, hardware-in-the-loop testing (HIL), and production. Following sections give more detailed description of these simulation tools.

MATLAB from Mathworks is a high-performance language for technical computing. It integrates computation, visualization, and programming in an easy-to-use environment where problems and solutions are expressed in familiar mathematical notation.

SIMULINK is an add-on to MATLAB that enables dynamic system simulation in a block diagram oriented graphical environment. SIMULINK can be used to explore the behavior of real-world dynamic systems from different engineering domains. Developing a simulation in SIMULINK involves dragging blocks from a palette onto a drawing area and connecting the blocks with lines that represents signal flows.

SimMechanics extends the capabilities of SIMULINK with tools for modeling and simulating mechanical systems. SimMechanics is a set of block libraries and special simulation features for use in the SIMULINK environment. Mechanical systems

consisting of any number of rigid bodies, connected by joints representing degrees of freedom of the mechanical structure can be modeled by the blocks in these libraries.

SimPowerSystems provides easy and rapid means of modeling and simulating power systems. The libraries contain models of typical power equipment such as transformers, lines, machines, and power electronics.

Stateflow is another add-on to SIMULINK that offers graphical design and development tool for control and supervisory logic used in conjunction with SIMULINK. Modeling and simulation of complex reactive systems based on finite state machine theory can be performed by using Stateflow.

The Real-Time Windows Target is a PC solution for prototyping and testing real-time systems. It is an environment a single computer is used as a host and target system. After creating a model and performing a non-real-time simulation with SIMULINK, executable code can be generated by using either with Real-Time Workshop or Stateflow Coder and a C compiler. Then, the application can be run in real time.

xPC Target is another solution for prototyping, testing, and deploying real-time systems using standard PC hardware. It is an environment that uses a target PC, separate from a host PC, for running real-time applications. In this environment a desktop computer can be used as a host PC with MATLAB, SIMULINK, and Stateflow to create a model using SIMULINK blocks and Stateflow charts. After creating the model, a non-real-time simulation can be run. Then, I/O blocks in xPC target libraries can be added to model, and then the host PC with Real-Time Workshop or Stateflow Coder and a C/C++ compiler can be used to create executable code. The executable code is downloaded from the host PC to the target PC running the xPC Target real-time kernel. After downloading the executable code, you can run and test your target application in real time.

Real-Time Workshop and Stateflow Coder are two extensions of capabilities found in SIMULINK and MATLAB to enable rapid prototyping of real-time software applications on a variety of systems. They constitute a rapid and direct path from system design to implementation by generating C code from SIMULINK block diagrams and Stateflow charts. This code can be used by other tools providing compilation and execution targets.

Another software tool for system simulation tasks is LABVIEW from National Instruments. It is a powerful development environment for signal acquisition, measurement, data presentation. LABVIEW is also a high level approach to technical computing like MATLAB/SIMULINK and gives flexibility of a programming language without the complexity of traditional low-level development tools. The tight integration of the LABVIEW with I/O hardware facilitates the development of control prototyping and hardware-in-the-loop simulation applications. It contains built-in measurement analysis capabilities and a graphical compiler for optimum performance.

Real-Time Module is an add-on to LABVIEW that provides necessary tools in order to develop real-time applications. It works pretty much similar to xPC Target add-on of the SIMULINK. After developing real time application on a host computer, the program can be downloaded to independent hardware target with a real-time operating system by using Real-Time module.

FPGA Module supplies a graphical development environment for Field-Programmable Gate Array (FPGA) chips on National Instruments reconfigurable I/O hardware. With this module, a custom application can be created on a host computer running Windows, and then it can be implemented in hardware. It allows direct access to I/O hardware with user-defined LABVIEW logic to define custom hardware for rapid control prototyping, device simulation and closed loop control applications.

Another add-on to LABVIEW, State Diagram Toolkit allows the simulation of finite-state machines. LABVIEW code that implements finite-state machine logic can be interactively created and simulated by using this toolkit.

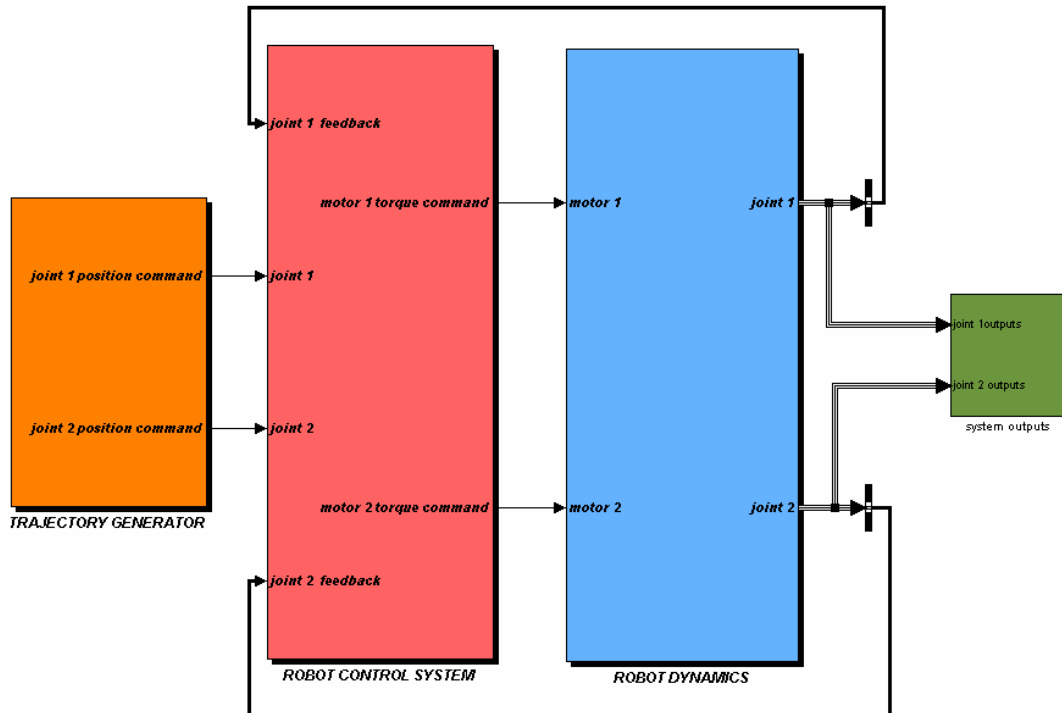
## **5.3 System Simulation of the Robotic Arm**

### **5.3.1 Simulation in Non-real-time**

System simulation of the robotic arm without time consideration was performed by using MATLAB/Simulink and related toolboxes and blocksets. It consisted of 8 distinct stages:

- Building a trajectory generator
- Modeling of the physical system
- Modeling of the control system
- Merging distinct models
- Running the simulation in non-real time
- Creating the real-time application
- Running the application in real-time
- Analyzing and visualizing results

Resulting system simulation block diagram is shown in figure 5.8. As seen in the figure, system simulation consists of three main subsystems: trajectory generator, control system, and robot dynamics.



5.8 System simulation block diagram

Main consideration in trajectory generator was the smoothness of the motion since rough, jerky motions tend to increase wear on the mechanism and cause vibrations by exciting resonances of the mechanical structure. Linear interpolation method is used in trajectory generation. However, in order to remove discontinuities, parabolic blend regions are added at the path points. During the blend portion of the trajectory, constant acceleration equal to the allowable workpart acceleration is used to change velocity smoothly. Outputs of the trajectory generator were buffered in a look-up table to improve the speed of the simulation. Figure 5.9 shows trajectory generator subsystem.

Control system design was described in chapter 4. Modeling of the robot control system was performed by using standard Simulink blocks. Figure 5.10 shows the resulting graphical model.

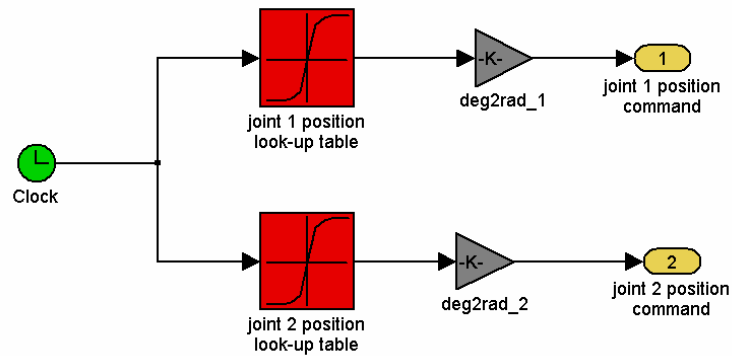


Figure 5.9 Trajectory generator subsystem

In figure 5.8, system simulation block diagram, robot dynamics subsystem contains the physical modeling of the manipulator. It was described in chapter 3. As stated section 3.5.5 of chapter 3, dynamics of the manipulator was modeled by using MATLAB/Simulink together with SimMechanics blockset. SimMechanics is a blockset that extends the capabilities of MATLAB/Simulink with tools for modeling and simulating mechanical systems. SimMechanics is a set of block libraries and special simulation features for use in the Simulink environment. Figure 3.49 shows the resulting physical model of the manipulator by using SimMechanics blockset.

After merging the subsystems, system simulation was performed. Position, velocity and acceleration responses of the driven joints are presented in figure 5.15 through 5.20. From the results, it was concluded that theoretically the system tracks the motion commands with a maximum time delay of 0.150 [sec].

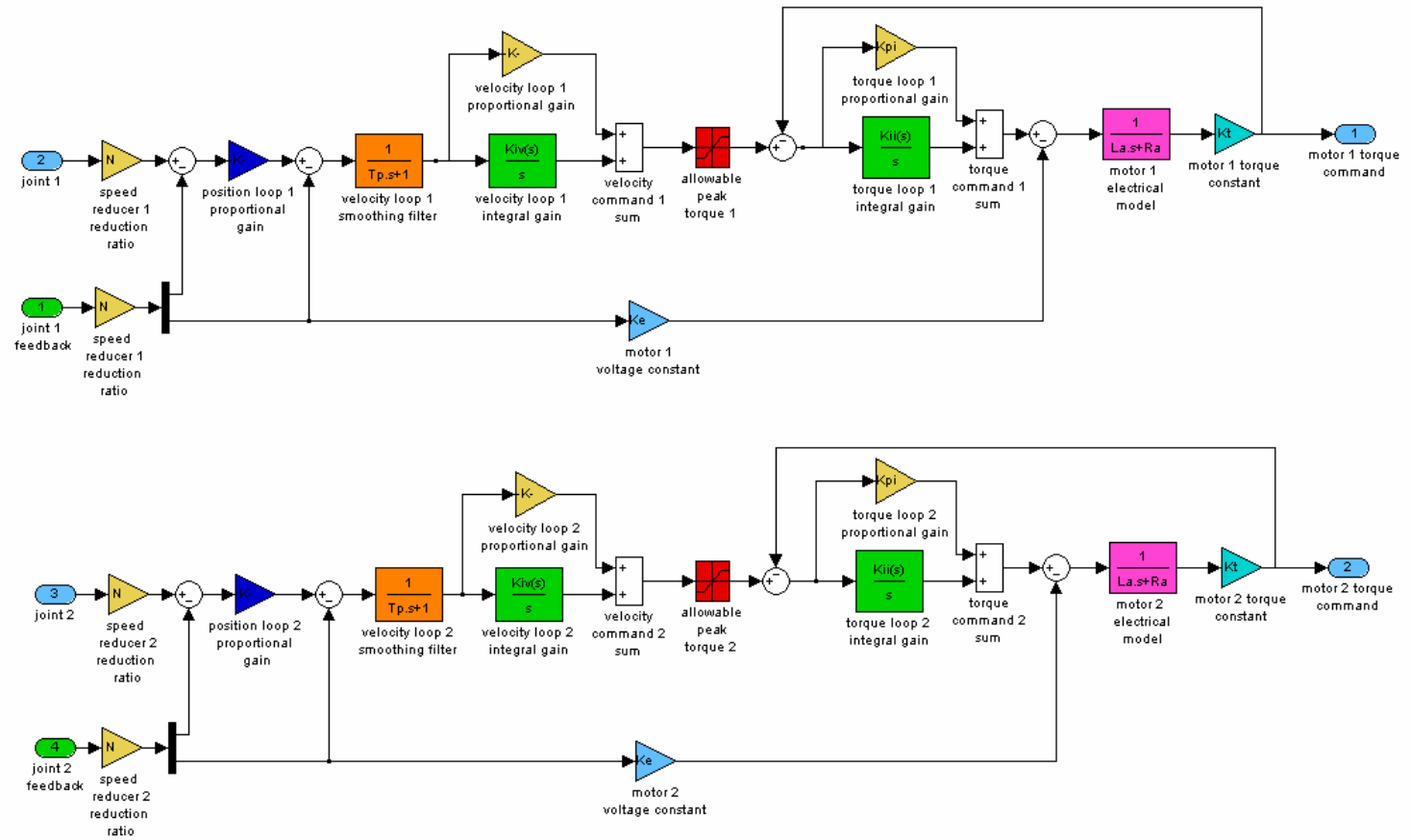
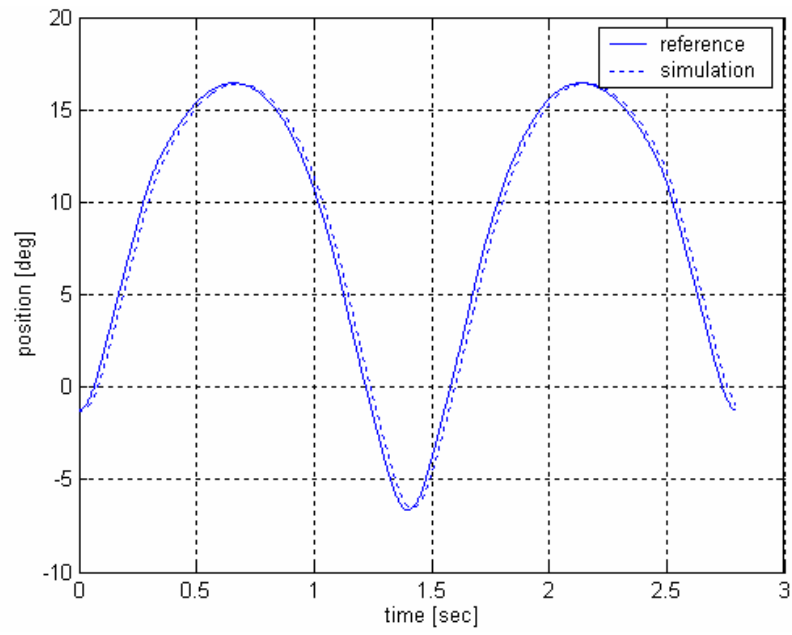
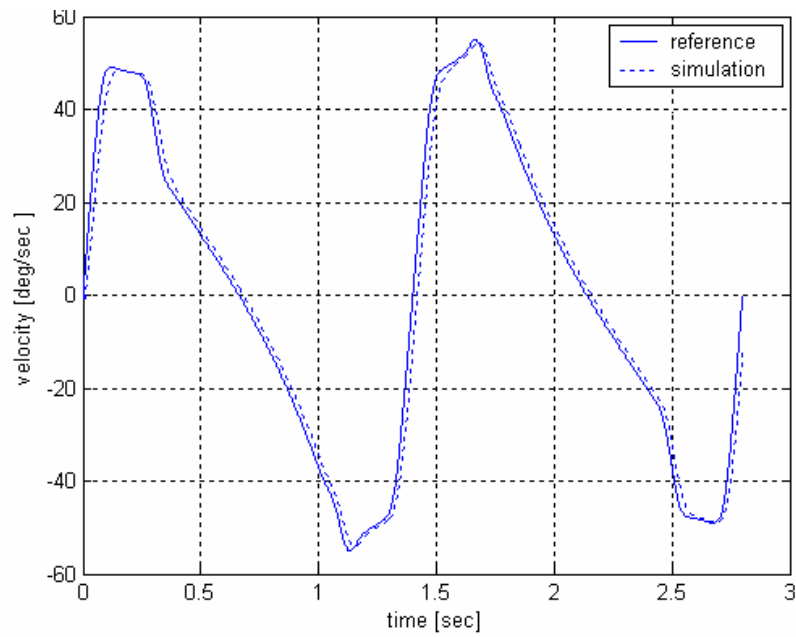


Figure 5.10 Robot control subsystem



5.15 Joint 1 position response



5.16 Joint 1 velocity response

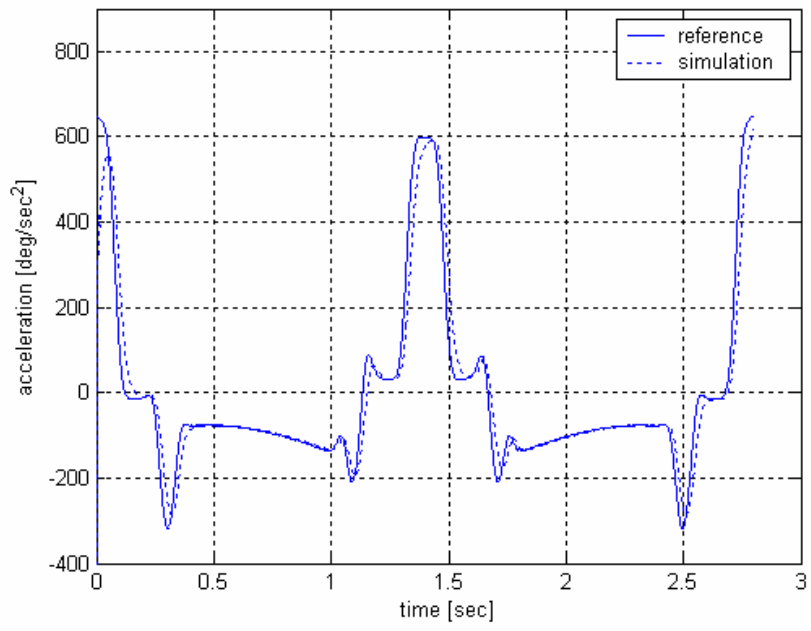


Figure 5.17 Joint 1 acceleration response

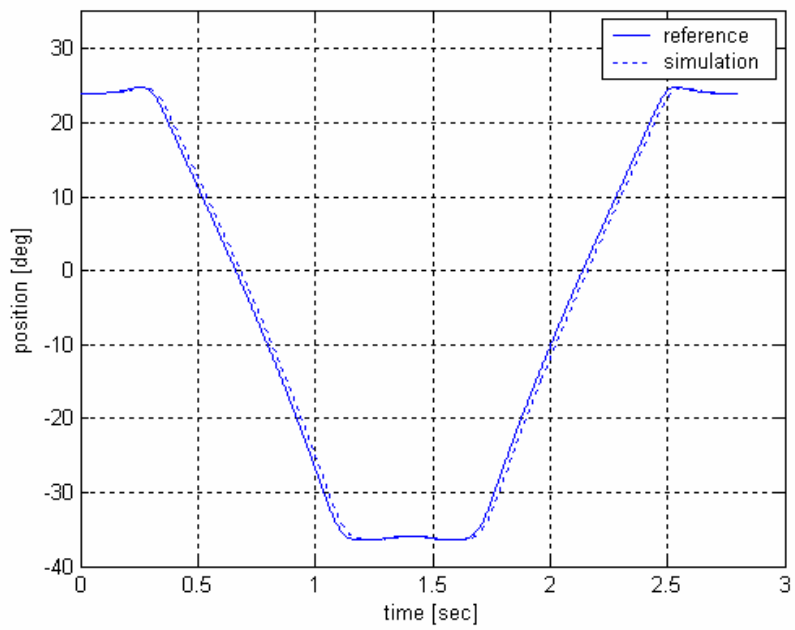


Figure 5.18 Joint 2 position response

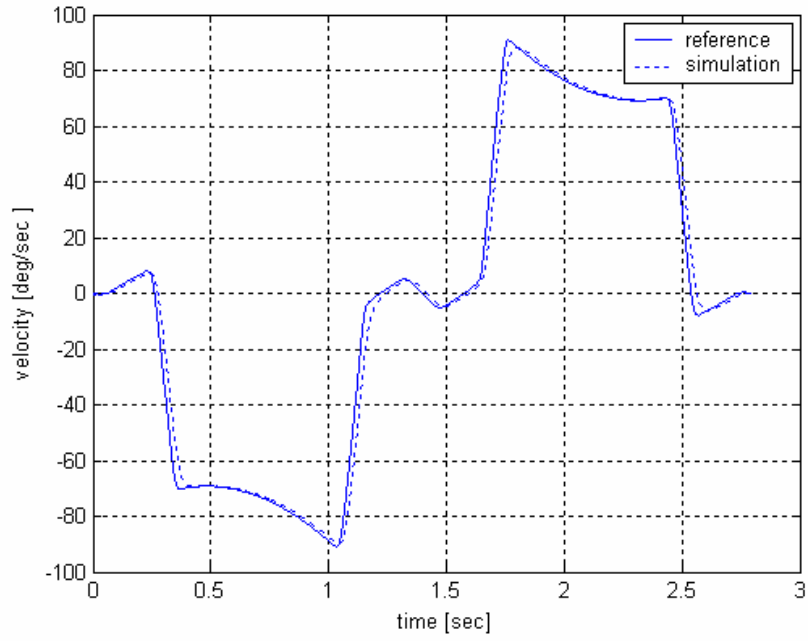


Figure 5.19 Joint 2 velocity response

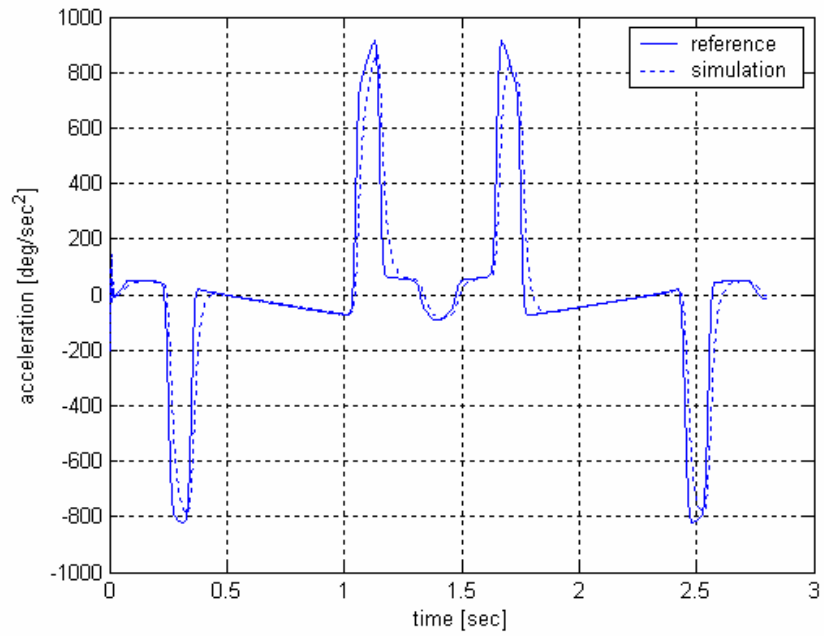


Figure 5.20 Joint 2 acceleration response

### 5.3.2 Simulation in Real-time

After checking the behavior of the system by running simulation in non-real time, real-time application was generated. Real-time simulation was performed by using MATLAB/Simulink and related toolboxes and blocksets.

The Real-Time Windows Target is a blockset in Simulink that can be used to prototype and test real-time systems. It is a self-targeting system where the host and target is the same computer. After creating a model by using MATLAB/Simulink, an executable code can be generated with Real Time Workshop and a third party C compiler. Then the application can be run in real-time with Simulink external mode in order to evaluate the performance of the system under development. Figure 5.21 shows Real-Time Windows Target library.

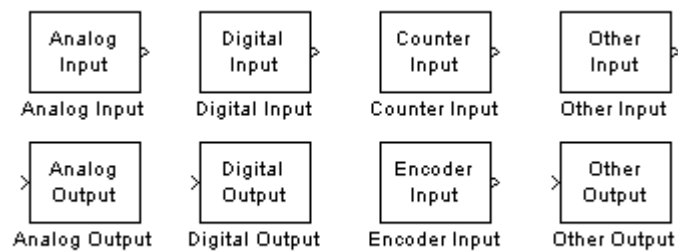


Figure 5.21 Real-Time Windows Target Library

Real-Time Windows Target uses a small kernel to ensure that real-time application runs in real time. The real-time kernel runs at CPU ring zero and uses built in PC clock as its primary source of time. The kernel uses the interrupt to trigger the execution of the compiled model in order to give the real-time application the highest priority available. For price sampling, the kernel reprograms the PC clock to higher frequency. Since the Windows operating system uses the same PC clock as a primary

source of time, the kernel sends a timer interrupt to the operating system at the original interrupt rate. The kernel interfaces and communicates with I/O hardware using I/O driver blocks, and it checks for the proper installation of the I/O board. If the board has been properly installed, drivers allow the real-time application to run.

In this study, Real Time Windows Target blocks were used to interface the Simulink block diagrams with the external world. Actually the overall block diagram of the real time simulation was the same as in non-real-time simulation as shown in figure 5.8. The only difference was that robot dynamics initially modeled by SimMechanics blocks was replaced with the Real Time Windows Target blocks. Figure 5.22 shows new robot dynamics subsystem.

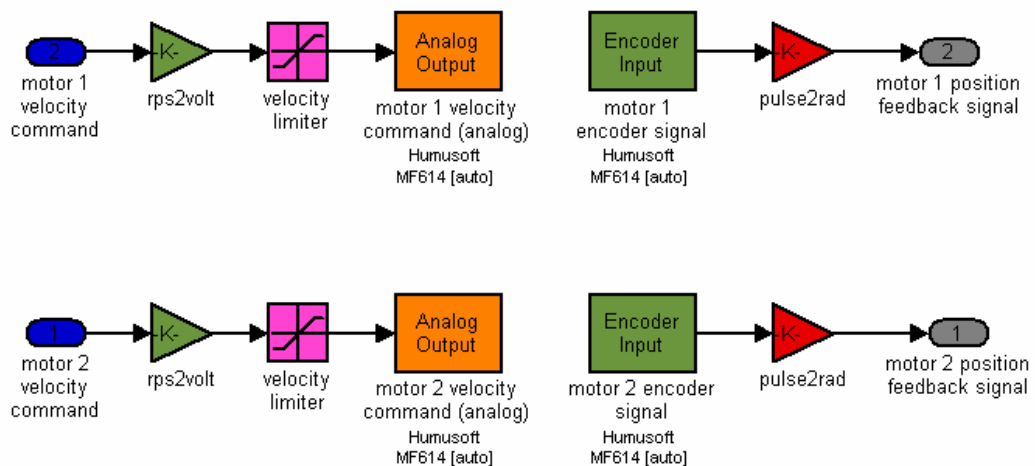


Figure 5.22 Robot Dynamics subsystem

In order to run the application in real-time, Real Time Workshop and a third-party C compiler were used to generate an executable code that runs with the Real-Time Windows Target Kernel. Then, the host PC is used as a target PC at the same time and application was run in real time. The physical setup is shown in figure 5.23. Communication between Simulink and the real-time application was through the

Simulink external mode interface module. This module talks directly to the real-time kernel, and is used to start the real-time application, change parameters, and retrieve scope data.

Communication between Real-Time Windows Target and the external world was established by using a data acquisition (DAQ) card. While the application is running, Real Time Windows Target signals sampled signals from the input channels of DAQ card and used the data as inputs to block diagram. After processing, outputs sent it back to the output channels of the DAQ card.

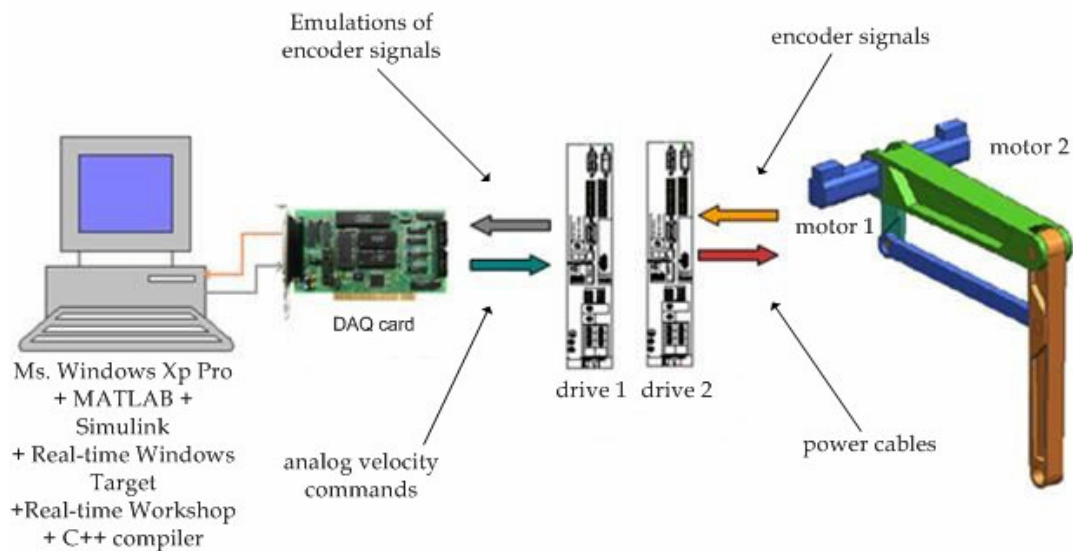


Figure 5.23 Setup for real time simulation

Real-time system simulation results are shown in figure 5.24 through 5.29.

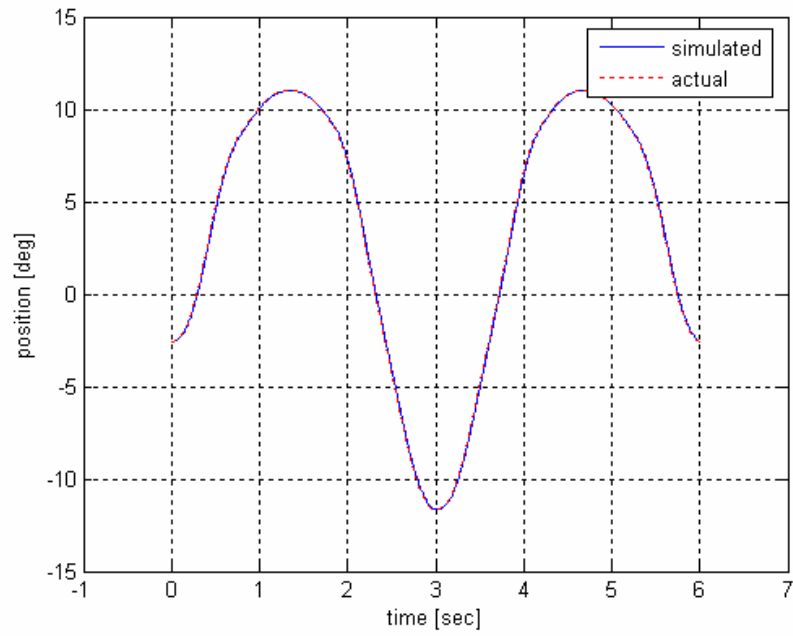


Figure 5.24 Joint 1 position response

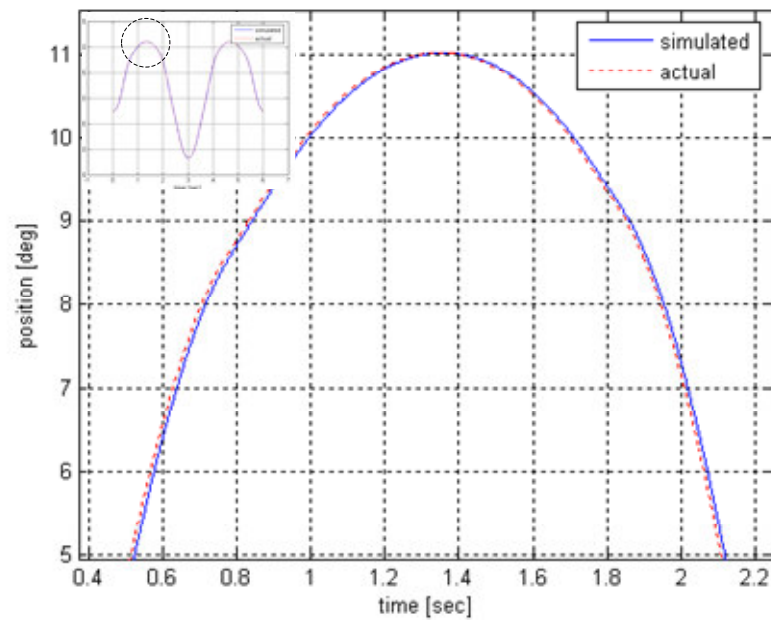


Figure 5.25 A close-up view at Joint 1 position response

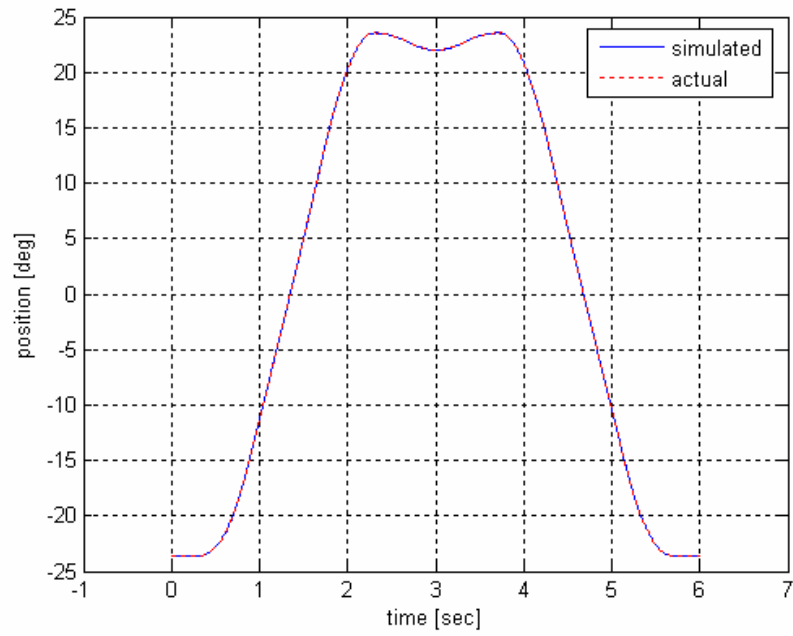


Figure 5.26 Joint 2 position response

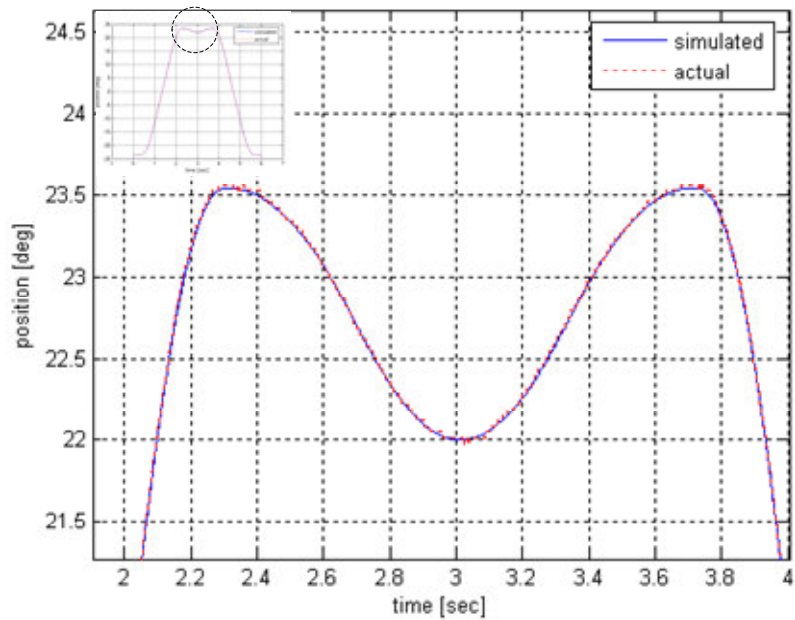


Figure 5.27 A close-up view at joint 2 position response

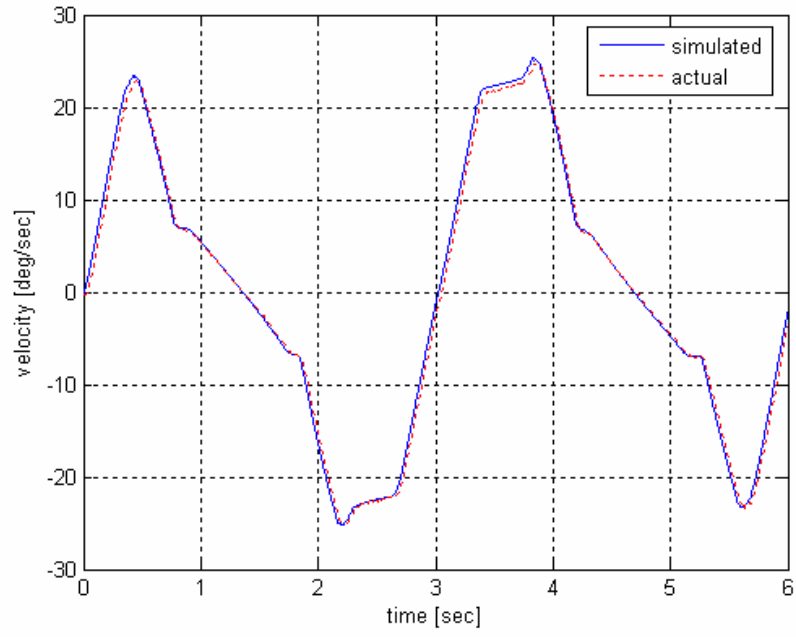


Figure 5.28 Joint 1 velocity response

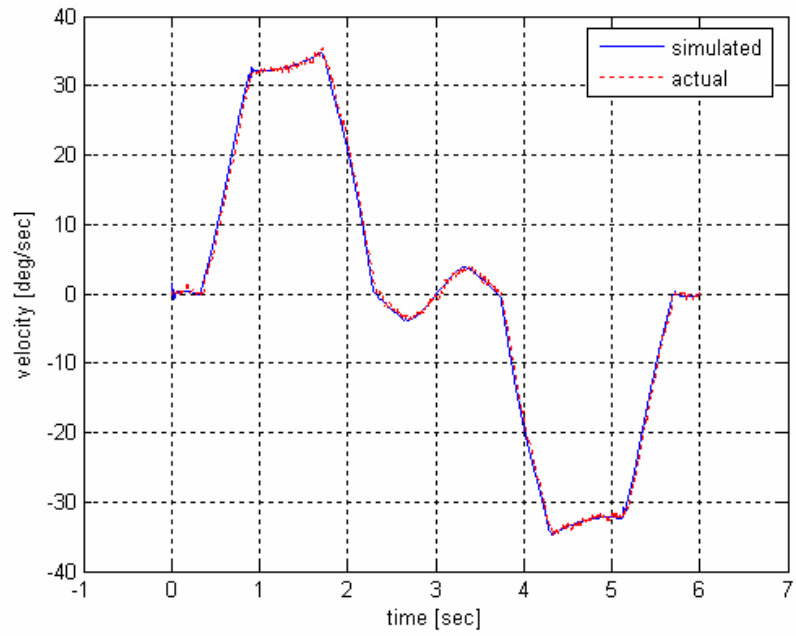


Figure 5.29 Joint 2 velocity response

## CHAPTER 6

### DESIGN OF THE GRIPPER SYSTEM

#### 6.1 Introduction

All robotic systems performing secondary packaging operation require an end effector in order to fulfill the intended task. An end effector for a robotic system is an interface between the robot and the product to be handled. More clearly, this is the part of the system that physically interacts with the environment. Therefore, Design of the gripper should reflect this extremely important role, matching the capabilities of the robot to the requirements of the intended task.

Robotic handling of food products presents sophisticated problems compared to rigid materials because they can be very fragile and deformable. They can be also easily bruised and marked when they come into contact with hard and/or rough surfaces. During handling, once the food products have been picked up they must be held securely in such a way that the position and orientation remain accurately known with respect to the robotic arm. While the pick and place operation is being performed, static and dynamic forces that can damage to products arise. Therefore, motion of the robot is constraint by these contact forces and the actions of the robot and the gripper determine whether the operation will be successfully completed or not. As a conclusion, the ideal gripper design should be performed by producing independent solutions to the three considerations shown in figure 6.1.

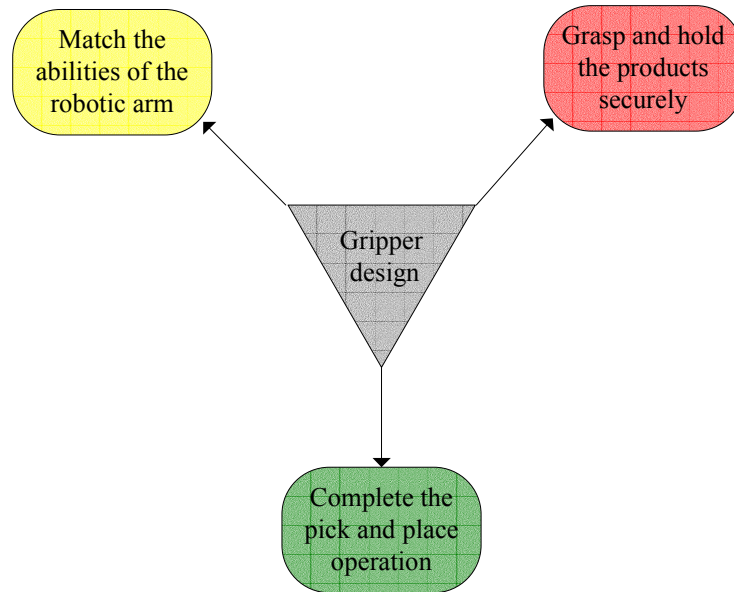


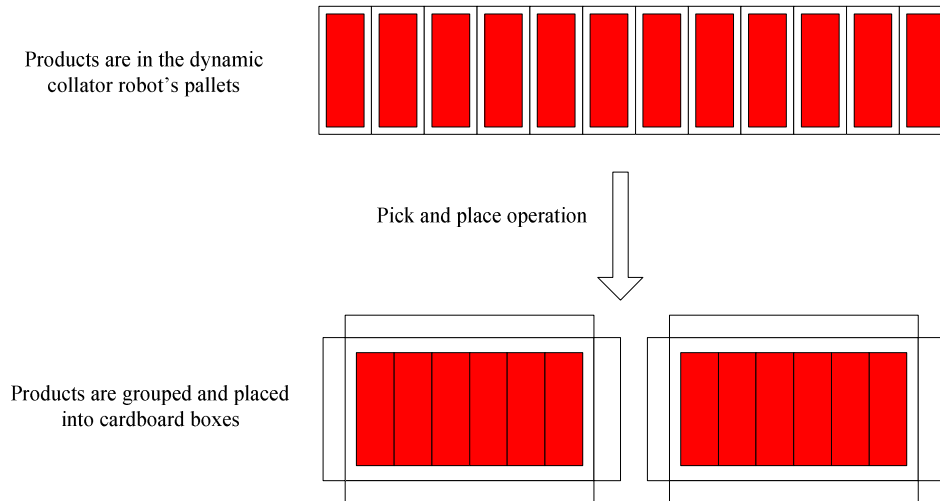
Figure 6.1 Main considerations of a gripper

## 6.2 The SPRS Gripper Benchmark Goals

In the study, the first benchmark goal of the gripper was the handling of 12 products in each pick and place cycle without causing any distortion to the packages. Because deformed or folded products reduce the attraction of customers and shorten the shelf life in the market. Besides price, consumers look at the shape, color, and appearance before checking the taste and flavor. Even a small distortion on the package may cause rejection by the customer even it does not violate the hygiene and food safety regulations.

The second benchmark goal was the grouping of the products. As stated in chapter 2, SPRS was designed to fill two separate cardboard boxes concurrently. Therefore, in addition to pick and place action, the gripper should also divide sorted products in the dynamic sorter machine's pallets into two separate groups. Furthermore, interval

between the products within the same group must also be reduced in order to place the products into the cardboard boxes. Figure 6.2 depicts the situation.



6.2 Grouping of the products (TOP VIEW)

As a summary, following benchmark goals are set for the SPRS gripper system:

- Ability to pick and place 12 products in each cycle without causing any distortion to the packages
- Ability to group products properly
- Ability to function at a rate of 20 cycles per minute
- Ability to integrate with the robotic arm
- Reliability of around 99.9%
- Ability to detect the presence of the products
- Ability to function properly up to 1 g [m/sec<sup>2</sup>] acceleration

Taking these goals into consideration, design of the gripper system was performed in two steps:

- Design of the pick-up mechanism
- Design of the grouping mechanism

Figure 6.3 and 6.4 show 3-D isometric and actual view of the gripper system integrated with the robotic arm.

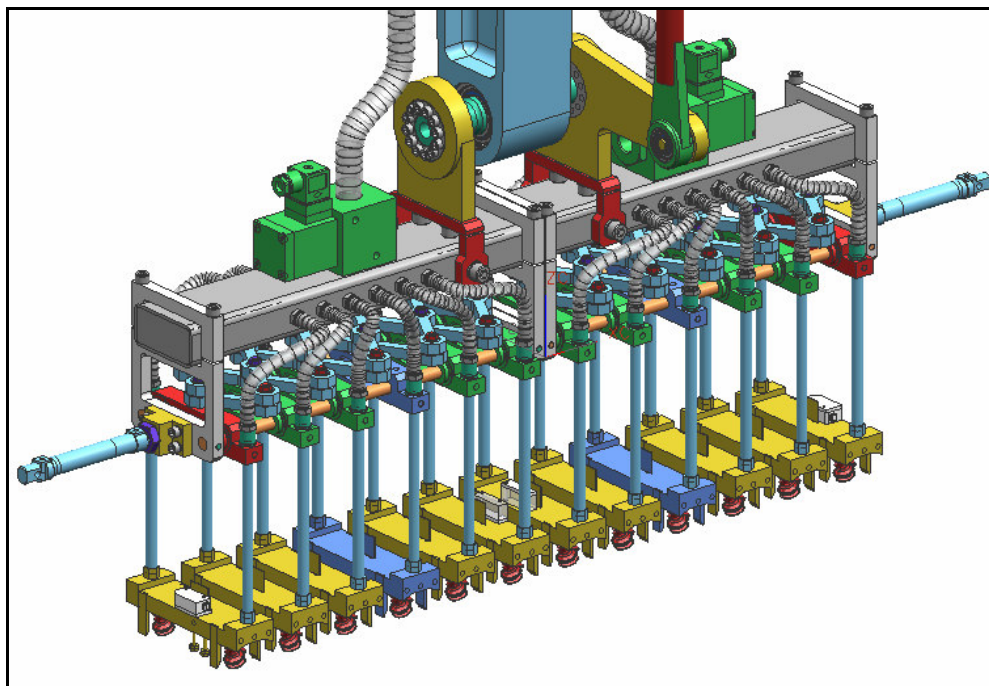


Figure 6.3 3-D Isometric view of the gripper system

### 6.3 Design of the Pick-up Mechanism

Standard methods for gripping a workpiece in the industry falls under two general categories: clamping and attracting methods. Clamping methods utilize jaw-type devices which exert pressing forces on two or more opposing surfaces of the work piece. The work piece is held between the jaws of the gripper by the resulting

frictional force. Pneumatic, hydraulic and electrical actuators are general sources of power for these systems. By far, most of the grippers on the market are powered by pneumatic actuators. Because they have no motor or gears and it is simple to translate the power of a piston /cylinder system into gripping force and they put out a high amount of gripping force in a small space. In addition, most manufacturing facilities already have compressed air, so little effort is required to bring it to a gripper in a cost efficient manner.



Figure 6.4 Actual gripper integrated with the robotic arm

When there is a need for high gripping force, hydraulic actuators are generally used. However, there are drawbacks associated with hydraulics. They are costly and

generally less accurate than pneumatic and electric. More importantly, hydraulic grippers are not suitable for clean room applications in food manufacturing.

Electric grippers are suitable for applications that require high speeds and light or moderate gripping forces. Electric grippers are cleaner than either pneumatic or hydraulic grippers because they do not put out any dirt or particulate, so they are more suitable for clean room applications. The major advantage of electrically powered grippers is control. A microprocessor can be added to an electric gripping system which can be made to vary the executed force or torque. Such a sensor can be added at little additional cost to make the gripper more able to cope with a variety of sizes and shapes. This diminishes the need of changing gripper to accommodate different types of parts. The major drawback of electric grippers is their weight. They tend to be heavier and produce less force than pneumatic and hydraulic grippers.

The second category, which is attracting methods, utilize vacuum, magnetic, electrostatic adhesion, magneto-adhesion, thermal adhesion, chemical adhesion and all other methods characterized by other attracting forces. Electro-adhesion utilizes techniques requiring high voltages and insulated surfaces for manipulation while magneto-adhesion is suitable for ferromagnetic materials only. Thermal adhesion can not be used for grasping of food packages because they involve attainment of freezing temperatures and thoroughly wet the material being picked up. Chemical adhesion is not suitable because the effectiveness of chemical adhesives reduces over time, unless replaced.

Selection of the grasping method was made based on special requirements of the manufacturing environment and physical properties of the product to be handled. After some investigation, vacuum suction was found most appropriate for use as a mechanism for grasping. In the following sections, design of the pick-up mechanism was described. Main steps in the design were:

- Selection of suction cups

- Force analysis
- Design of the suction cups mounting element
- Design of the vacuum distributor
- Selection of the type and size of the vacuum generator
- Selection of solenoid valves

### 6.3.1 Selection of Suction Cups

As stated in introductory chapters, robotic handling of ETİ TUTKU product presents important challenges because, as being a food product, it is very fragile and deformable. It can be also easily bruised and marked when they come into contact with hard and/or rough surfaces. During the pick and place operation, static and dynamic forces that can damage to products can arise. Therefore, geometric properties, particular trajectory of the product and arising forces were carefully investigated in the selection of suction cups. Figure 6.5 shows different views of ETİ TUTKU product.



Figure 6.5 Different views of ETİ TUTKU

Analysis of the ETİ TUTKU product geometry suggested that because of the slight variations, suction cups should be able to function with slightly curved surfaces with varying heights. Taking into account these requirements, bellows type suction cups with 1.5 corrugations made from silicon, manufactured by PIAB, were selected. In

application, it was observed that the high elasticity of the silicon suction cups compensated for any unevenness on the surface level of the product. Bellows offered adequate damping when the suction cup positioned on the product. Figure 6.6 shows the 3-D CAD view of the selected suction cup. Technical specifications are presented in table 6.2.



Figure 6.6 3-D cad view of the selected suction cup

Table 6.1 Technical specifications of the selected suction cup (B15-2)

Parameter	Description	Value	Units
$m$	Mass	1.5	$g$
$A_s$	Effective suction cup area	$1.13 \cdot 10^{-4}$	$m^2$
$v_i$	Internal volume	$0.225 \cdot 10^{-6}$	$m^3$
$h_s$	Hardness	$50^{\circ}$	$shore$
$x_v$	Max. vertical movement	6.5	$mm$

### 6.3.2 Force Analysis

Aim of the force analysis was to find the required level of vacuum in order to perform the intended pick and place operation. After computing the forces acting on

a single product for different types of motion of the robotic arm with the gripper system, vacuum level was calculated and the vacuum pump, which must be able to supply the vacuum level found in calculations, was selected from the corresponding manufacturer catalog.

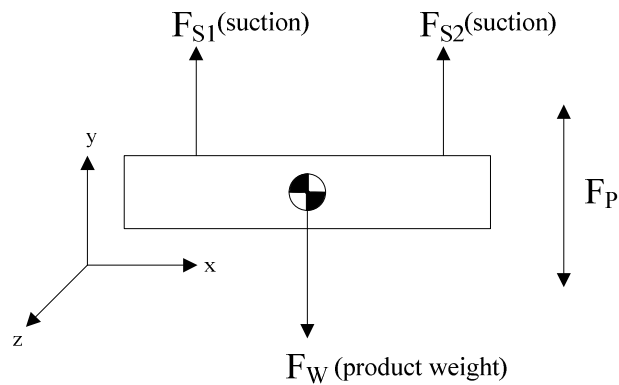


Figure 6.9 Forces on the product during prehension

Movement of the system can broadly be classified as prehension and retention. Prehension of an object involves vertical motion of the gripper toward the products and grasping the products using suction through the suction cups. The forces that come into existence on a single product during this process are the forces due to suction through the suction cups,  $F_s$ , the weight of the product,  $F_w$ , and the force generated due to the prehension movement of the robotic arm,  $F_p$ . A grasp is stable if the suction generated during pick-up is large enough to overcome the effect of the weight of the product and the forces due to the acceleration of the gripper, toward or away from the object. Figure 6.9 depicts these forces during prehension. Numerical values are presented in table 6.1.

As seen in the figure, at the worst case condition in prehension where the product is subjected to acceleration of 1 g in y direction, forces created by the suction cups should be able to hold the product securely. This means that all static and dynamic forces must be balanced.

Table 6.2 Technical Specifications

Parameter	Description	Value	Units
M	Mass of the product	0.132	kg
$A_S$	Effective suction cup area	$1.13 \cdot 10^{-4}$	$m^2$
$\mu$	Coefficient of friction	0.5	-
N	Factor of safety	2.5	-
g	Gravitational acceleration	9.81	$m/sec^2$

For vertical direction, force balance can be written as:

$$+\uparrow \sum F_Y = 0 \Rightarrow F_{S1} + F_{S2} - F_W - F_R = 0 \quad (6.1)$$

where  $F_p = m \cdot g$ . Considering also the factor of safety, suction forces  $F_{S1}$  and  $F_{S2}$  can be written as follows:

$$F_{S1} = F_{S2} = D_p \cdot A_S / n \quad (6.2)$$

where  $D_p$  is the difference between ambient and vacuum pressure. Then,

$$2 \cdot (D_p \cdot A_S / n) - 2 \cdot m \cdot g = 0 \Rightarrow D_p = \frac{m \cdot g \cdot n}{A_S} \quad (6.3)$$

Replacing the symbolic variables with numerical values given in table 6.1,  $D_p$  can be calculated as 358 [mbar].

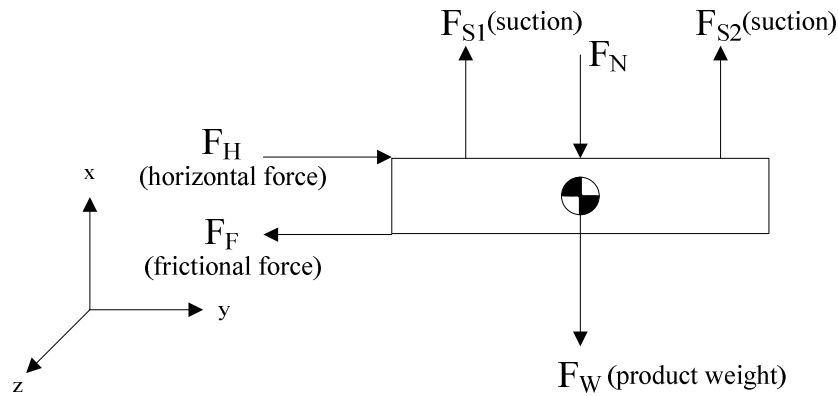


Figure 6.10 Forces on the product during prehension

Retention of the product during pick and place cycle involves a force due to the acceleration of the gripper when translating from the pick-up position to place down position. In this type of motion, an opposing shear force acts against the direction of motion of the gripper, as represented in figure 6.10.

During retention, the force generated due to the movement of the robot in horizontal direction  $F_H$ , tends to cause the material to slip. The frictional force  $F_F$ , must be at least large enough to prevent this slippage. Therefore, writing force balance equation in horizontal direction:

$$+ \rightarrow \sum F_x = 0 \Rightarrow F_H - F_F = 0. \quad (6.4)$$

It is known that  $F_F = \mu \cdot F_N$ , where  $\mu$  is the coefficient of friction between the product package and the suction cup material. Normal force  $F_N$  can be calculated by vertical force balance equation:

$$+\uparrow \sum F_Y = 0 \Rightarrow F_{S1} + F_{S2} - F_W - F_N = 0 \Rightarrow F_N = F_{S1} + F_{S2} - F_W. \quad (6.5)$$

Above equation can be rewritten by using pressure differential and factor of safety terms as:

$$F_N = (D_p \cdot A_s / n) + (D_p \cdot A_s / n) - m \cdot g = F_N = 2 \cdot (D_p \cdot A_s / n) - m \cdot g. \quad (6.6)$$

Then, horizontal force balance equation become:

$$\mu \cdot [2 \cdot (D_p \cdot A_s / n) - m \cdot g] = m \cdot g \quad (6.7)$$

Above equation can be rearranged to compute required vacuum level in order to stabilize the movement of the product during retention as follows:

$$D_p = \frac{n \cdot m \cdot g}{2 \cdot A_s} \left(1 + \frac{1}{\mu}\right) \quad (6.8)$$

Replacing the symbolic variables with numerical values given in table 6.1,  $D_p$  can be calculated as 430 [mbar].

### 6.3.3 Design of the Suction Cups Mounting Element

The key parameters in the design of the grasp geometry were the shape and size of the pick up surface. Considering the grasping stability, it was decided to use four suction cups for each mounting element and suction cups were inclined in order to adjust the suction cup orientation perpendicular to product. This design was greatly increased the stability of the grasping operation. Figure 6.7 shows the 3-D cad view of suction cups mounting element and grasp geometry.

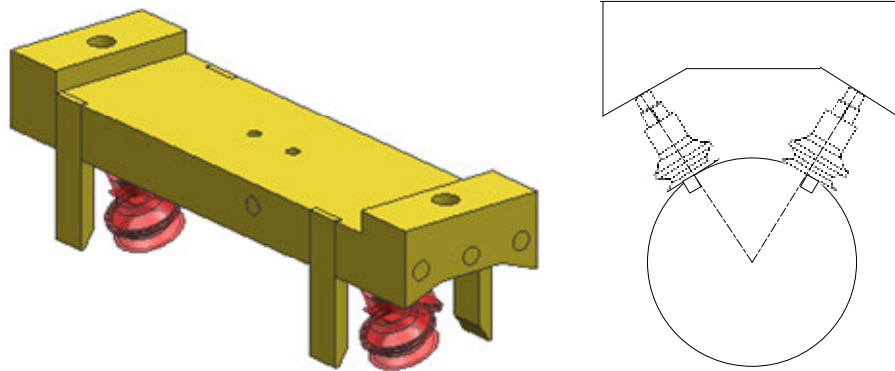


Figure 6.7 3-D CAD view of the suction cups holder

It was concluded that the gripper must be able to be in function even two of the suction cups miss the product in grasping operation. Therefore, as shown in the cross-sectional view of the suction cups mounting element in figure 6.8, 2 distinct air channels were created to feed the vacuum to suction cups to increase the grasping stability further.

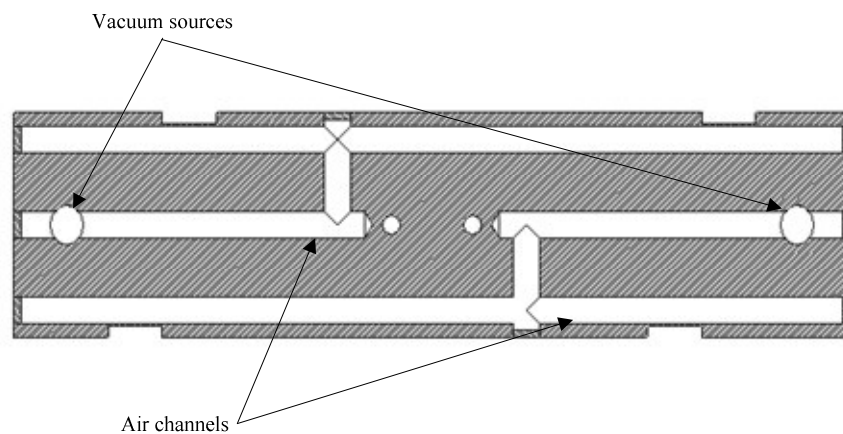


Figure 6.8 Cross-sectional view of the suction cups mounting element

### 6.3.4 Design of the Vacuum Distributor

Inside volume of the aluminum profile in the gripper was used as the vacuum distributor and the vacuum is transmitted to the suction cups by using specifically designed vacuum hoses. Figure 6.9 shows the vacuum distributor and hoses.

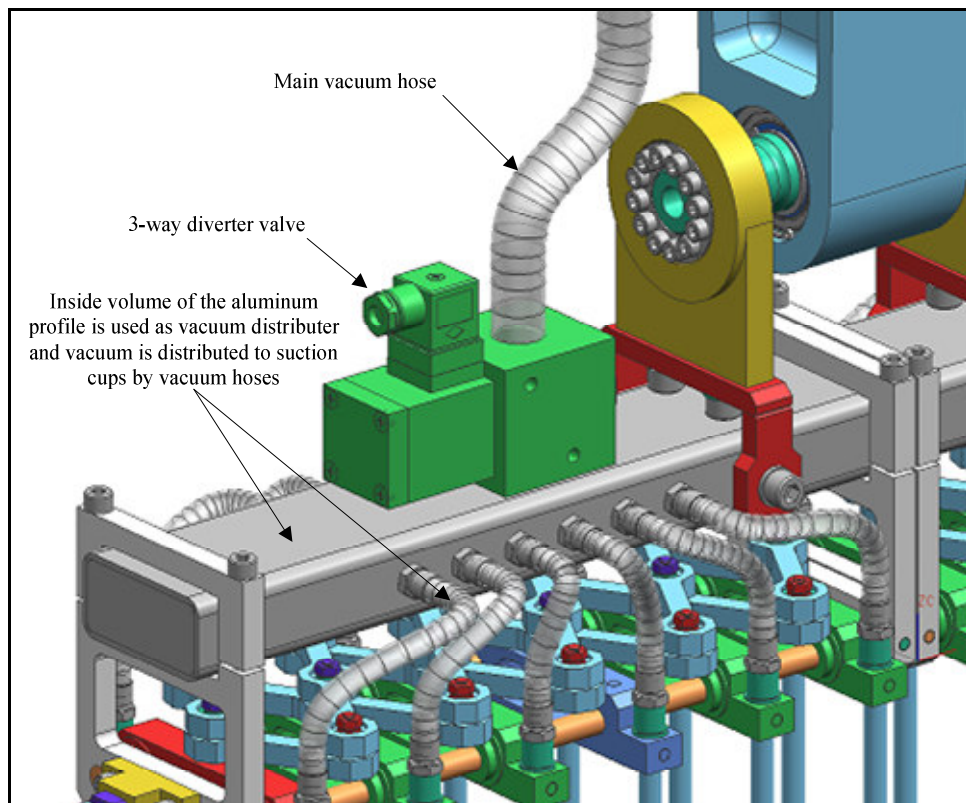


Figure 6.9 Vacuum distributor and hoses

### 6.3.5 Selection of the Type and Size of The Vacuum Generator

Various types of vacuum generators can be used to generate the vacuum. Basically, there are three types of vacuum generators commonly used in vacuum systems:

- ejectors
- vacuum pumps
- vacuum blowers

Main distinction between these vacuum generators is their suction capacity under different vacuum level as shown in figure 6.10. Each of these generators has its specific advantages, but one principle is common to all types: high suction capacity together with high vacuum always incurs high energy consumption and thus high operating costs.

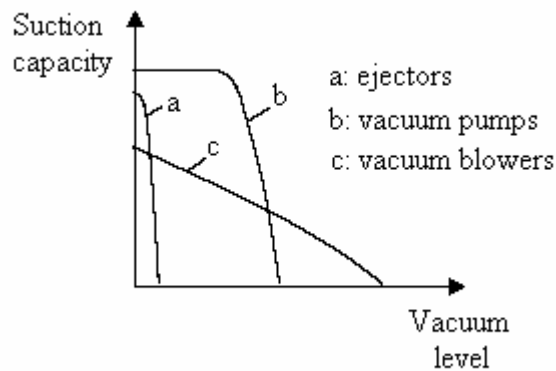


Figure 6.10 Suction capacities of different vacuum generators

As seen in figure 6.10, vacuum pumps provide high vacuums at low volume flow rates, i.e. low suction capacity. They are particularly suitable where non-porous workpieces are to be handled. There are various types of pumps, namely dry-running pumps, oil-lubricated pumps and water-ring pumps. Dry-running and water-ring pumps require very little maintenance. In addition, dry-running pumps can be installed in any desired orientation, while oil-lubricated and water-ring pumps can be installed and operated only in a horizontal position. Oil-lubricated pumps require maintenance, but are capable of generating very high vacuums of up to  $-0.98$  bar.

In contrast to vacuum pumps, vacuum blowers generate low vacuums at a high volume flow rate, i.e. high suction capacity. They are the right choice wherever porous workpieces, through which can diffuse relatively easily, are to be handled.

Ejectors generate a high vacuum at a relatively low volume flow rate. However, they differ from the pumps and blowers in that they generate the vacuum pneumatically, using the so-called "Venturi" principle. In an ejector, a stream of compressed air flows through a drive nozzle. At this "artificial bottleneck", the velocity of the air stream is far higher than in the supply line, resulting in a reduced pressure at the cone-shaped outlet. This draws the air out of the vacuum connection, generating the desired vacuum. The major advantage of ejectors is that they have no moving parts and therefore require absolutely no maintenance and never wear out. Ejectors generate no heat, can be very small, and permit the implementation of very short cycle times.

Table 6.3 Technical specifications of the selected vacuum pump (VT 4.40)

Parameter	Description	Value	Units
$V$	Suction air rate	40	$m^3 / h$
$P_{\max}$	Max. absolute vacuum	150	$mbar$
$P_m$	Installed motor power	1.25	$kW$
$n$	Noise level	67	$dB$
$m$	Mass	38.5	$kg$

Taking the requirements of evacuation time, possibility of air leakage, possible power supply and cycle times and after consulting to the past experience of the vacuum component suppliers, oil-free, air-cooled rotary vane vacuum pump

manufactured by BECKER was selected. Technical specifications of the vacuum pump are presented in table 6.3.

### 6.3.5.1 Calculation of the Evacuation Time

Vacuum system requires a time period in order to evacuate the air volume so that the picking action takes place. The air volume to be evacuated,  $V_E$ , can be calculated as:

$$V_E = V_1 + V_2 + V_3 + V_4 \quad (6.9)$$

where

$V_1$  = volume of the suction pads =  $11.04 \cdot 10^{-6} [m^3]$ ,

$V_2$  = volume of the suction cups mounting element =  $95.40 \cdot 10^{-6} [m^3]$ ,

$V_3$  = volume of the vacuum hoses =  $732.87 \cdot 10^{-6} [m^3]$ ,

$V_4$  = volume of the vacuum distributor =  $1369.12 \cdot 10^{-6} [m^3]$ .

By using the numerical values,  $V_E$  can be calculated as  $2208.43 \cdot 10^{-6} [m^3]$ . Then the evacuation time can be calculated by using following empirical formula:

$$t = \frac{1.3 \cdot V_E \cdot \ln\left(\frac{P_a}{P_e}\right)}{V} \quad (6.10)$$

where

$P_a$  = initial absolute pressure =  $1013 [mbar]$ ,

$P_e$  = final absolute pressure =  $583 [mbar]$ .

Together with the numerical values, evacuation time,  $t$ , can be calculated as 0.143 [sec], which is acceptable considering the cycle time requirements of the overall system. Note that the pressure differential was calculated as 430 [mbar] in section 6.3.1. Final absolute pressure,  $P_e$ , was calculated by subtracting this value from the initial absolute pressure.

### 6.3.6 Selection of the Solenoid Valves

For a complete vacuum circuit, solenoid valves are required for the function of controlling the air flow in the vacuum system. The valves were selected on the basis of the following criteria:

- Suction capacity of the vacuum generator
- Control Voltage
- Function of the solenoid valve (NO/NC)

Based on these requirements, normally closed, directly controlled 3/2-way solenoid valve manufactured by SCHMALZ was selected. Considering the suction capacity of the vacuum generator, two identical valves were utilized. Technical specifications of the valve are presented in table 6.4.

Table 6.4 Technical specifications of the selected valve (EMVO-12)

Parameter	Description	Value	Units
$d_n$	Nominal diameter	12	<i>mm</i>
$q_n$	Nominal flow rate	21	$m^3 / h$
$P_c$	Power consumption	18.3	<i>W</i>
$V$	Operating voltage	24	<i>volt</i>
$m$	Mass	38.5	<i>kg</i>

## 6.4 Design of the Grouping Mechanism

As stated in introductory section at the beginning of the chapter, in addition to pick and place action, the gripper should also divide sorted products in the dynamic sorter machine's pallets into two separate groups. Furthermore, interval between the products within the same group must also be reduced in order to place the products into the cardboard boxes. These challenging requirements for grouping action were successfully fulfilled by utilizing two distinct accordion mechanisms. Figure 6.11 shows the grouping mechanism and its corresponding bearing arrangements.

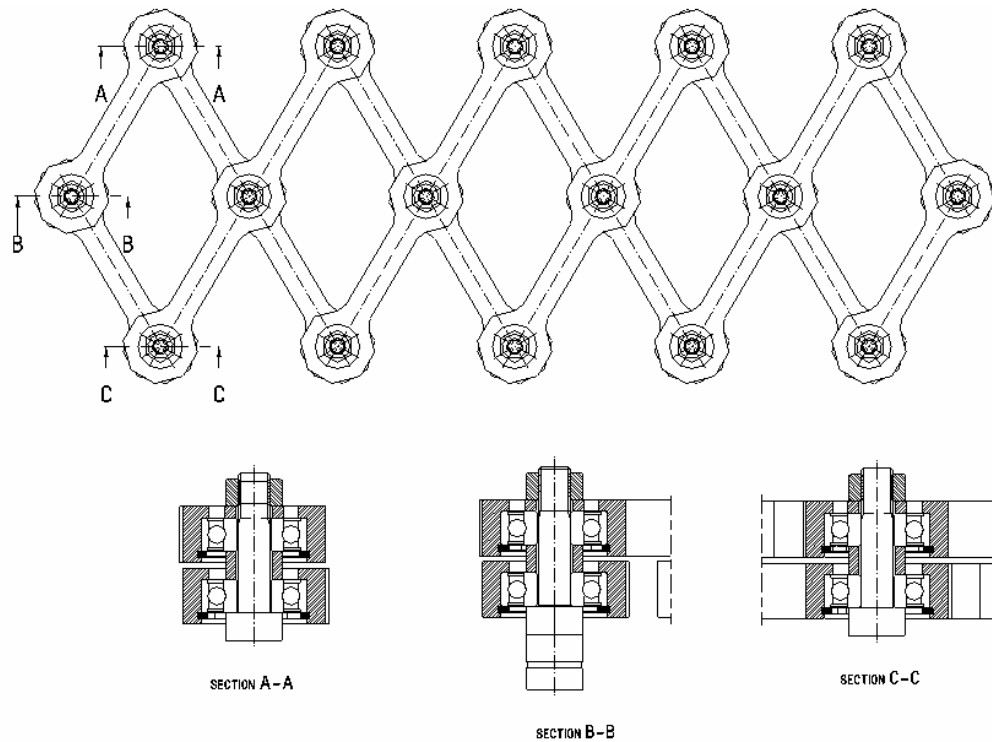


Figure 6.11 Bearing Arrangements of grouping mechanism

Considering the loading conditions of the grouping mechanism, deep groove ball bearings, manufactured by SKF, are used. All bearings are identical to each other.

Main dimensions and technical specifications are presented in figure 6.12 and table 6.5, respectively.

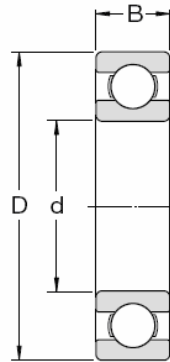


Figure 6.12 Main dimensions of a deep groove ball bearing

Table 6.5 Technical specifications of the bearing in accordion mechanism

Principal Dimensions			Basic load ratings		Mass	Bearing Designation
d	D	B	Dynamic, C	Static, C <sub>0</sub>		
mm			kN		kg	-
55	90	18	29.60	21.20	0.39	626

Because of the advantages mentioned in previous sections, each mechanism was energized by two standard pneumatic actuators, manufactured by FESTO Industry and Trade Inc., having adjustable cushion at both ends. These cushions were adjusted in order to prevent jerky motion of the actuators that can result in dropping products during robotic handling. Figure 6.13 depicts how the pneumatic cylinders connected to the system. Technical specifications of the pneumatic cylinder are presented in table 6.6.

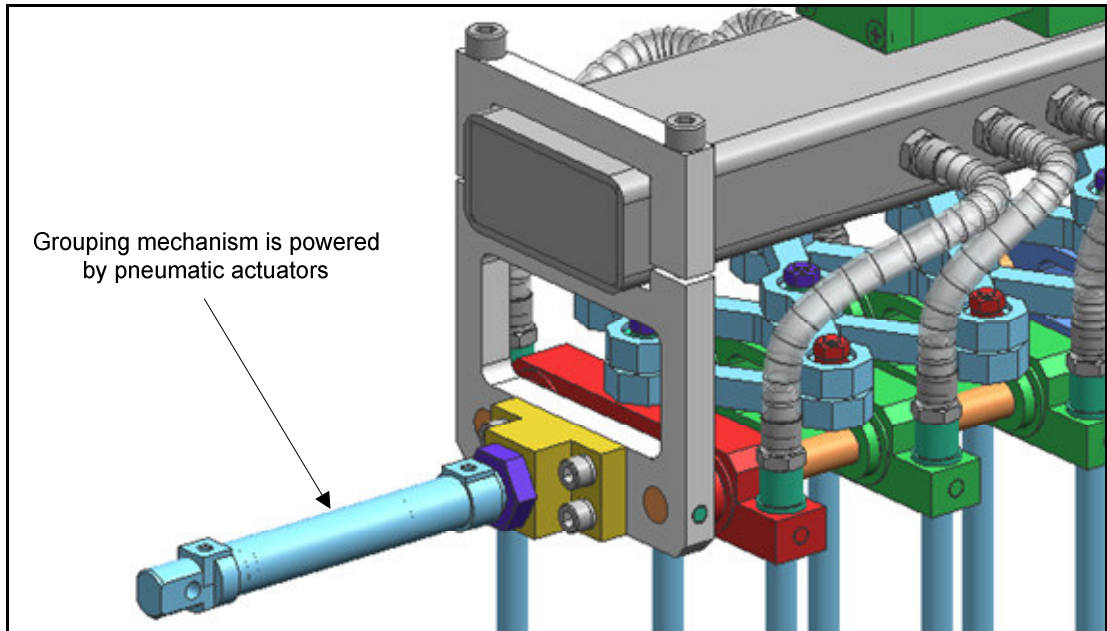


Figure 6.13 Pneumatic actuators of the grouping mechanism

Table 6.6 Technical specifications of pneumatic actuators (DSNU-16-80-PPVA)

Parameter	Description	Value	Units
$d$	Piston diameter	16	$mm$
$E_{max}$	Extension force at 6 bar	121	$N$
$R_m$	Retraction force at 6 bar	104	$N$
$S_{max}$	Maximum stroke	63	$mm$
$m$	Mass	0.134	$kg$

## CHAPTER 7

### SUMMARY AND CONCLUSION

#### 7.1 Summary

The use of robotic systems in consumer goods industry has increased over recent years. However, food industry has not taken to the robotics technology with the same desire as in other industries due to technical and commercial reasons. Difficulties in matching human speed and flexibility, variable nature of food products, high production volume rates, lack of appropriate end-effectors, high initial investment rate of the so-called systems and low margins in food products are still blocking the range of use of robotics in food industry. In this thesis study, as a contribution to the use of robotic systems in food industry, a secondary packaging robotic system for ETİ TUTKU manufacturing line was designed. Objectives of the study were:

- Increasing the manufacturing capacity,
- Increasing the labor productivity by the redistribution of laborers,
- Reducing the product cost and manufacturing time,
- Eliminating the manual and boring tasks.

The system is composed of two basic subsystems:

- A dual-axis controlled pick and place robotic arm with the manipulation rate of 20 cycles per minute.
- A gripper unit with the ability of picking 12 workparts at one cycle and performing grouping action during the pick and place operation.

Mechanical and control systems design of basic subsystems are performed within the scope of the study. During the designing process, instead of using classical design methods, modern computer-aided design and engineering tools are utilized. System performance was precisely predicted by detailed system simulations in both real and non-real-time and inevitable design modifications were performed before expensive system realization.

## **7.2 Conclusion**

Robotic handling of food products presents sophisticated problems compared to rigid materials because they can be very fragile and deformable. They can be also easily bruised and marked when they come into contact with hard and/or rough surfaces. Therefore, the most important design constraint was to perform the secondary packaging operation of ETİ TUTKU product automatically at a rate of 200 products/minute without causing any distortion to product. After performing experiments on the secondary packaging robotic system designed within the scope of the thesis study, it was concluded that the system is able to respond to the capacity of the secondary packaging process of ETİ TUTKU manufacturing line. During experiments, it was observed that the system can be able to perform the secondary packaging operation at a rate of 240 products per minute, which is 25 percent higher than the current manufacturing capacity of ETİ TUTKU manufacturing line.

## REFERENCES

- [1] British Robot Association, “BRA Robot Facts”, Aston Science Park Inc., (no date given).
- [2] International Standards Organization, ISO/TR8373.
- [3] Groover, M. P., “Automation, Production Systems, and Computer-Integrated Manufacturing”, Prentice Hall International Inc., 2001.
- [4] Craig, J. J., “Introduction to Robotics”, Addison-Wesley Publishing Company Inc., 1989.
- [5] Fu, K. S., Gonzales, R. C., Lee, C. S. G., “Robotics: Control, Sensing, Vision, and Intelligence”, McGraw-Hill, 1987.
- [6] Sciavicco, L., Siciliano, B., “Modeling and Control of Robot Manipulators”, McGraw-Hill, 1996.
- [7] Niku, S. B., “Introduction to Robotics Analysis, Systems Applications”, Prentice Hall International Inc., 2001.
- [8] Koren, Y., “Robotics for Engineers”, McGraw-Hill, 1985.
- [9] Asada, H., Slotine, J.J.E, “Robot Analysis and Control”, John Wiley and Sons, 1986.

- [10] Paul, R.P., "Robot Manipulators, Mathematics, Programming, and Control", the MIT Press, 1981.
- [11] Gopalswamy, A., Gupta, P., Vidyasar, M., "A New Parallelogram Linkage Configuration for Gravity Compensation Using Torsional Springs", International Conference on Robotics and Automation, 1992.
- [12] Miro, J.V., White, A.S., "Modeling an Industrial Manipulator a Case Study", Simulation Practice and Theory, Vol. 9, pp. 293-319, 2002.
- [13] Erzincanli, F., Sharp J.M., "Meeting the need for robotic handling of food products", Food Control, Vol. 8, No.4 pp. 185-190, 1997.
- [14] Wallin, P. J., "Robotics in the food industry: An update", Trends in Food Science & Technology, Vol. 8, 1997.
- [15] Lee, H.S., Chang, S.L. "Development of a CAD/CAE/CAM system for a robot manipulator", Journal of Materials Processing Technology, Vol. 140, pp. 100-104, 2003.
- [16] Pons, J. L., Ceres, R., and Jiménez, A. R., "Mechanical Design of a Fruit Picking Manipulator: Improvement of Dynamic Behavior", International Conference on Robotics and Automation Minneapolis, Minnesota, 1996.
- [17] Dulger L.C., Uyan, S., "Modeling Simulation and Control of a Four Bar Mechanism with a Brushless Servo Motor", Mechatronics, Vol. 7, No. +, pp. 369-383, 1997.
- [18] Sobh, T.M., Dekhil, M., H., T.V., and Sabbavarapu, A., "Prototyping a Three-Link Robot Manipulator", International Journal of Robotics and Automation, Vol. 14, No. 2, 1999.

- [19] Amerongen J. V., Breedveld B., “Modeling of Physical Systems for the Design and Control of Mechatronic Systems”, *Annual Reviews in Control*, vol. 27, pp. 87-117, 2003.
- [20] Fukuda, T., Arakawa, T., “Intelligent Systems: Robotics versus Mechatronics”, *Annual Reviews in Control*, vol. 22, pp. 13-22, 1998.
- [21] Pagilla, P.R., Yu, B., “Mechatronic Design and Control of a Robot System Interacting with an External Environment”, *Mechatronics*, Vol.12, pp. 791-811, 2002.
- [22] Ingio, R.M., “Simulation of the Dynamics of an Industrial Robot”, *IEEE Transactions on Education*, Vol. 34, 1991.
- [23] Krasner, J., “Model-Based Design and Beyond: Solutions for Today’s Embedded Systems Requirements”, *Embedded Market Forecasters*, 2004.
- [24] Sanvido, M. A. A., Schaufelberger, V. C. W., “Testing Embedded Control Systems Using Hardware-in-the-Loop Simulation and Temporal Logic”, 15th Triennial World Congress, 2002.
- [25] Kolluru, R., Valavanis, K. P., Steward, A., and Sonnier, M. J., “A Flat-Surface Robotic Gripper for Handling Limp Material”, *IEEE Robotics & Automation Magazine*, 1995.
- [26] Setiwan, A., I., Furukawa, T., Preston, A., “A Low-Cost Gripper for Apple Picking Robot”, *Proceedings of the 2004 IEEE International Conference on Robotics & Automation*, 2004.

- [27] Causey, G. C., and Quinn, R. D., "Gripper Design Guidelines for Modular Manufacturing", Proceedings of the 1998 IEEE International Conference on Robotics & Automation, 1998.
- [28] Younkin G., W., "Industrial Servo Control Systems Fundamentals and Applications", Marcel Dekker Inc., 2003.
- [29] Franklin G. F., Powell, J. D., Workman, M., "Digital Control of Dynamic Systems", Addison Wesley Longman Inc., 1998.
- [30] Ogatha K., "Modern Control Engineering", Prentice Hall International Inc., 1997.
- [31] Rzevski, G., "Designing Intelligent Machines", Butterworth-Heinemann Ltd, 1995.
- [32] Franklin G. F., Powell, J. D., Naeini, A. E., "Feedback Control of Dynamic Systems", Prentice Hall International Inc., 2002.
- [33] Shigley, J. E., Mischke, C. R., Budynas, R. G., "Mechanical Engineering Design", McGraw-Hill, 2004.
- [34] Kuo, B. J., "Automatic Control Systems", John Wiley & Sons Inc., 1995.
- [35] Bolton, W., "Electronic Control Systems in Mechanical and Electrical Engineering", Prentice Hall International Inc., 2003.
- [36] Mott, R. L., "Machine Elements in Mechanical Design", Prentice Hall International Inc., 2004.
- [37] Asada, H., Kamal, Y. T., "Direct Drive Robotics, Theory and Practice", Massachusetts Institute of Technology, 1987.

- [38] Lilly K. W., “Efficient dynamic Simulation of Robotic Mechanisms”, Kluwer Academic Publishers, 1993.
- [39] Bishop, R.H. (editor), “The Mechatronics Handbook”, CRC Press, 2002.
- [40] Ljung, L., “Issues in system identification”, IEEE Control Systems Magazine, January 1991.
- [41] Sanvido, M.A.A., Cechticky, V., Schaufelberger, W., “Testing embedded control systems using hardware-in-the-loop simulation and temporal logic”, Proceedings of 15<sup>th</sup> IFAC Triennial World Congress, 2002, Barcelona, Spain.
- [42] Ledin, J., “Simulation takes off with hardware”, CMP Books, 2002.
- [43] The Mathworks, “The Mathworks – MATLAB and SIMULINK for Technical Computing”, [www.mathworks.com](http://www.mathworks.com), 12.08.2005.
- [44] National Instruments, “National Instruments – Test and Measurement”, [www.ni.com](http://www.ni.com), 15.08.2005.
- [45] Oykun, E., “Production, Assembly, and Application of an Industrial Robot”, METU Mechanical Engineering Master of Science Thesis, 2001.
- [46] Ünver T., “The Computer Aided Design of an Industrial Robot”, METU Mechanical Engineering Master of Science Thesis, 1997.

## APPENDIX A

### TRAJECTORY PLANNING ALGORITHM

```
function C_path=rpath(tf);

%Path planer for the generic pick and place robot.
%Trajectory generation was computed in Cartesian space.
%The rpath function returns position, velocity and acceleration
%of the end effector with respect to "x" and "y" coordinates
%at time "tf" seconds. In order to compute all of the trajectory,
%this function must be called continuously in
%a loop while incrementing tf 0 to 2.8
%Points of the path are defined by four points, two of them are start
%and end points, other of two are via points.

%first part of the function is calculations along the y-axis

y1=0;y4=0; % [mm], start and end points;
y2=200;y3=200; % [mm], via points;

%durations for the three motion segments;
td12=.25; td23=.8; td34=0.25; % [sec]

%default acceleration at the blend points;
acc_d=9810; %mm/sec^2;

%calculations for the first motion segment;
y1ddot=sign(y2-y1)*acc_d;

    if y1ddot==0

        t1=0;

    else

        t1=td12-sqrt(td12.^2-(2*(y2-y1)/y1ddot));
```

```

end

y12dot=(y2-y1)/(td12-.5*t1);

%calculations for the second motion segment;
y23dot=(y3-y2)/td23;
y2ddot=sign(y23dot-y12dot)*acc_d;

if y2ddot==0

    t2=0

else

    t2=(y23dot-y12dot)/y2ddot;

end

%returning to the linear portion of first motion segment;
t12=td12-t1-.5*t2;

%calculations for the last motion segment;
y4ddot=sign(y3-y4)*acc_d;
t4=td34-sqrt(td34.^2+(2*(y4-y3)/y4ddot));
y34dot=(y4-y3)/(td34-.5*t4);

%calculations for the second via point y3;
y3ddot=sign(y34dot-y23dot)*acc_d;
t3=(y34dot-y23dot)/y3ddot;
t23=td23-.5*t2-.5*t3;
t34=td34-.5*t3-t4;

for t=0:0.001:tf;

if t<t1

    tinb=t;
    y=y1+.5*y1ddot*tinb.^2;
    ydot=y1ddot*tinb;
    yddot=y1ddot;
    y_new_1=y;

elseif t>t1 & t<t1+t12

    tinl=t-t1;
    y=y_new_1+y12dot*tinl;
    ydot=y12dot;

```

```
yddot=0;  
y_new_2=y;
```

```
elseif t>t1+t12 & t<t1+t12+t2
```

```
tinb=t-(t1+t12);  
y=y_new_2+y12dot*tinb+.5*y2ddot*tinb^2;  
ydot=y12dot+y2ddot*tinb;  
yddot=y2ddot;  
y_new_3=y;
```

```
elseif t>t1+t12+t2 & t<t1+t12+t2+t23
```

```
tinl=t-(t1+t12+t2);  
y=y_new_3+y23dot*tinl;  
ydot=y23dot;  
yddot=0;  
y_new_4=y;
```

```
elseif t>t1+t12+t2+t23 & t<t1+t12+t2+t23+t3
```

```
tinb=t-(t1+t12+t2+t23);  
y=y_new_4+y23dot*tinb+.5*y3ddot*tinb^2;  
ydot=y23dot+y3ddot*tinb;  
yddot=y3ddot;  
y_new_5=y;
```

```
elseif t>t1+t12+t2+t23+t3 & t<t1+t12+t2+t23+t3+t34
```

```
tinl=t-(t1+t12+t2+t23+t3);  
y=y_new_5+y34dot*tinl;  
ydot=y34dot;  
yddot=0;  
y_new_6=y;
```

```
elseif t>t1+t12+t2+t23+t3+t34
```

```
tinb=t-(t1+t12+t2+t23+t3+t34);  
y=y_new_6+y34dot*tinb+.5*y4ddot*tinb^2;  
ydot=y34dot+y4ddot*tinb;  
yddot=y4ddot;  
y_new_7=y;
```

```

end

end

%second part of the function is calculations along the x-axis

x1=0;x4=-800; % [mm], start and end points;
x2=0;x3=-800; % [mm], via points;

%durations for the three motion segments;
td12=.25; td23=0.8; td34=0.25; % [sec]

%default acceleration at the blend points;
acc_d=9810; %mm/sec^2;

%calculations for the first motion segment;
x1ddot=sign(x2-x1)*acc_d;

    if x1ddot==0;

        t1=0;

    else

        t1=td12-sqrt(td12.^2-(2*(x2-x1)/x1ddot));

    end

x12dot=(x2-x1)/(td12-.5*t1);

%calculations for the second motion segment;
x23dot=(x3-x2)/td23;
x2ddot=sign(x23dot-x12dot)*acc_d;
t2=(x23dot-x12dot)/x2ddot;

%returning to the linear portion of first motion segment;
t12=td12-t1-.5*t2;

%calculations for the last motion segment;
x4ddot=sign(x3-x4)*acc_d;

    if x4ddot==0;

        t4=0;

    else

```

```

t4=td34-sqrt(td34.^2+(2*(x4-x3)/x4ddot));

end

x34dot=(x4-x3)/(td34-.5*t4);

%calculations for the second via point x3;
x3ddot=sign(x34dot-x23dot)*acc_d;
t3=(x34dot-x23dot)/x3ddot;
t23=td23-.5*t2-.5*t3;
t34=td34-.5*t3-t4;

for t=0:0.001:tf;

if t<t12

    tinl=t-t1;
    x=x1+x12dot*tinl;
    xdot=x12dot;
    xddot=0;
    x_new_2=x;

elseif t>t1+t12 & t<t1+t12+t2

    tinb=t-(t1+t12);
    x=x_new_2+x12dot*tinb+.5*x2ddot*tinb^2;
    xdot=x12dot+x2ddot*tinb;
    xddot=x2ddot;
    x_new_3=x;

elseif t>t1+t12+t2 & t<t1+t12+t2+t23

    tinl=t-(t1+t12+t2);
    x=x_new_3+x23dot*tinl;
    xdot=x23dot;
    xddot=0;
    x_new_4=x;

elseif t>t1+t12+t2+t23 & t<t1+t12+t2+t23+t3

    tinb=t-(t1+t12+t2+t23);
    x=x_new_4+x23dot*tinb+.5*x3ddot*tinb^2;
    xdot=x23dot+x3ddot*tinb;

```

```

xddot=x3ddot;
x_new_5=x;

elseif t>t1+t12+t2+t23+t3 & t<t1+t12+t2+t23+t3+t34

    tinl=t-(t1+t12+t2+t23+t3);
    x=x_new_5+x34dot*tinl;
    xdot=x34dot;
    xddot=0;
    x_new_6=x;

elseif t>t1+t12+t2+t23+t3+t34

    tinb=t-(t1+t12+t2+t23+t3+t34);
    x=x_new_6+x34dot*tinb+.5*x4ddot*tinb^2;
    xdot=x34dot+x4ddot*tinb;
    xddot=x4ddot;
    x_new_7=x;

end

end

Px=x;Pxdot=xdot;Pxddot=xddot;
Py=y;Pydot=ydot;Pyddot=yddot;

C_path=[Px;Pxdot;Pxddot;Py;Pydot;Pyddot];

%Trajectory generation of the second half of the movement.
%In this portion the manipulator returns back
%this algorithm is same as the first half, except tf has
%1.3 second offset.
if (tf>=1.3)
    tf=tf-1.3;

%calculations along the y-axis
y1=0;y4=0; % [mm], start and end points;
y2=200;y3=200; % [mm], via points;

%durations for the three motion segments;

```

```

td12=.25; td23=0.8; td34=0.25; % [sec]

%default acceleration at the blend points;
acc_d=9810; %mm/sec^2;

%calculations for the first motion segment;
y1ddot=sign(y2-y1)*acc_d;

    if y1ddot==0

        t1=0;

    else

        t1=td12-sqrt(td12.^2-(2*(y2-y1)/y1ddot));

    end

y12dot=(y2-y1)/(td12-.5*t1);

%calculations for the second motion segment;
y23dot=(y3-y2)/td23;
y2ddot=sign(y23dot-y12dot)*acc_d;

    if y2ddot==0

        t2=0

    else

        t2=(y23dot-y12dot)/y2ddot;

    end

%returning to the linear portion of first motion segment;
t12=td12-t1-.5*t2;

%calculations for the last motion segment;
y4ddot=sign(y3-y4)*acc_d;
t4=td34-sqrt(td34.^2+(2*(y4-y3)/y4ddot));
y34dot=(y4-y3)/(td34-.5*t4);

%calculations for the second via point y3;
y3ddot=sign(y34dot-y23dot)*acc_d;
t3=(y34dot-y23dot)/y3ddot;
t23=td23-.5*t2-.5*t3;
t34=td34-.5*t3-t4;

```

```

for t=0:0.001:tf;

    if t<t1

        tinb=t;
        y=y1+.5*y1ddot*tinb.^2;
        ydot=y1ddot*tinb;
        yddot=y1ddot;
        y_new_1=y;

    elseif t>t1 & t<t1+t12

        tinl=t-t1;
        y=y_new_1+y12dot*tinl;
        ydot=y12dot;
        yddot=0;
        y_new_2=y;

    elseif t>t1+t12 & t<t1+t12+t2

        tinb=t-(t1+t12);
        y=y_new_2+y12dot*tinb+.5*y2ddot*tinb^2;
        ydot=y12dot+y2ddot*tinb;
        yddot=y2ddot;
        y_new_3=y;

    elseif t>t1+t12+t2 & t<t1+t12+t2+t23

        tinl=t-(t1+t12+t2);
        y=y_new_3+y23dot*tinl;
        ydot=y23dot;
        yddot=0;
        y_new_4=y;

    elseif t>t1+t12+t2+t23 & t<t1+t12+t2+t23+t3

        tinb=t-(t1+t12+t2+t23);
        y=y_new_4+y23dot*tinb+.5*y3ddot*tinb^2;
        ydot=y23dot+y3ddot*tinb;
        yddot=y3ddot;
        y_new_5=y;

    elseif t>t1+t12+t2+t23+t3 & t<t1+t12+t2+t23+t3+t34

```

```
tinl=t-(t1+t12+t2+t23+t3);  
y=y_new_5+y34dot*tinl;  
ydot=y34dot;  
yddot=0;  
y_new_6=y;
```

```
elseif t>t1+t12+t2+t23+t3+t34
```

```
tinb=t-(t1+t12+t2+t23+t3+t34);  
y=y_new_6+y34dot*tinb+.5*y4ddot*tinb^2;  
ydot=y34dot+y4ddot*tinb;  
yddot=y4ddot;  
y_new_7=y;
```

```
end
```

```
end
```

```
end
```

```
Px=x;Pxdot=xdot;Pxddot=xddot;  
Py=y;Pydot=ydot;Pyddot=yddot;
```

```
C_path=[Px;Pxdot;Pxddot;Py;Pydot;Pyddot];
```

```
end
```

## APPENDIX B

### INVERSE KINEMATICS ALGORITHM

*%program purpose : the program "inv\_kin" calculates the angles of joints for the  
%given coordinates defined in the stationary coordinate  
%system*

```
function A_space=inverse_kinematics(pplan);
```

```
%decomposing the input argument;  
x=pplan(1)+1200;x_dot=pplan(2);x_ddot=pplan(3);y=pplan(4)-  
700;y_dot=pplan(5);y_ddot=pplan(6);
```

```
%defining the length of the links;  
L1=875;L2=800;  
%tool offset 0 mm;  
x_coor=x;y_coor=y;
```

```
%cartesian position vector;  
X=[x_coor;y_coor];
```

```
%cartesian velocity vector;  
X_dot=[x_dot;y_dot];
```

```
%cartesian acceleration vector;  
X_ddot=[x_ddot;y_ddot];
```

```
%the angle for the second link;  
theta_2=-acos((x_coor.^2+y_coor.^2-L1.^2-L2.^2)./(2*L1*L2));
```

```
%the angle for the second link;  
A=[-L2*sin(theta_2) L2*cos(theta_2)+L1;L2*cos(theta_2)+L1 L2*sin(theta_2)];  
Load=[ x_coor ; y_coor ];  
sol=inv(A)*Load;  
theta_1=atan2(sol(1),sol(2));
```

```

%calculation of the inverse of the JACOBIAN matrix;
J_inv=[cos(theta_1+theta_2)/(L1*sin(theta_2))
sin(theta_1+theta_2)/(L1*sin(theta_2)) ; (-L1*cos(theta_1)-
L2*cos(theta_1+theta_2))/(L1*L2*sin(theta_2)) (-L1*sin(theta_1)-
L2*sin(theta_1+theta_2))/(L1*L2*sin(theta_2))];

%calculation of the joint velocities;
theta_dot=J_inv*X_dot;

theta_1_dot=theta_dot(1);
theta_2_dot=theta_dot(2);

%calculation of the derivative of the inverse of the JACOBIAN matrix;
J_inv_dot_1_1=(-sin(theta_1+theta_2)*(theta_1_dot+theta_2_dot)*L1*sin(theta_2)-
L1*cos(theta_2)*theta_2_dot*cos(theta_1+theta_2))/(L1*sin(theta_2)).^2;

J_inv_dot_1_2=(cos(theta_1+theta_2)*(theta_1_dot+theta_2_dot)*L1*sin(theta_2)-
L1*cos(theta_2)*theta_2_dot*sin(theta_1+theta_2))/(L1*sin(theta_2)).^2;

J_inv_dot_2_1=((L1*sin(theta_1)*theta_1_dot+L2*sin(theta_1+theta_2)*(theta_1_dot
+theta_2_dot))*L1*L2*sin(theta_2)-L1*L2*cos(theta_2)*theta_2_dot*(-
L1*cos(theta_1)-L2*cos(theta_1+theta_2)))/(L1*L2*sin(theta_2)).^2;

J_inv_dot_2_2=(-L1*cos(theta_1)*theta_1_dot-
L2*cos(theta_1+theta_2)*(theta_1_dot+theta_2_dot))*L1*L2*sin(theta_2)-
L1*L2*cos(theta_2)*theta_2_dot*(-L1*sin(theta_1)-
L2*sin(theta_1+theta_2))/(L1*L2*sin(theta_2)).^2;

J_inv_dot=[J_inv_dot_1_1 J_inv_dot_1_2;J_inv_dot_2_1 J_inv_dot_2_2];

%calculation of the joint accelerations;

theta_ddot=J_inv_dot*X_dot+J_inv*X_ddot;

theta_1_ddot=theta_ddot(1);
theta_2_ddot=theta_ddot(2);

%calculation of the variables in actuator space
alpha_1=theta_1; alpha_1_dot=theta_1_dot; alpha_1_ddot=theta_1_ddot;
alpha_2=pi/2+theta_2+theta_1; alpha_2_dot=theta_2_dot+theta_1_dot;
alpha_2_ddot=theta_2_ddot+theta_1_ddot;

A_space=[alpha_1;alpha_1_dot;alpha_1_ddot;alpha_2;alpha_2_dot;alpha_2_ddot];

```